The Role of RNA Binding Proteins in Regulating Infection and Double-stranded RNA Sensing

By

William Dunker

Dissertation

Submitted to the Faculty of the

Graduate School of Vanderbilt University

in partial fulfillment of the requirements

for the degree of

DOCTOR OF PHILOSOPHY

in

Microbe-Host Interactions

August 31, 2021

Nashville, Tennessee

Approved:

Jeffrey Rathmell, Ph.D.

Mark Denison, M.D.

Heather Pua, M.D., Ph.D.

Vivian Gama, Ph.D.

John Karijolich, Ph.D.

Acknowledgements

I would like to thank my thesis advisor, Dr. John Karijolich, for his encouragement and assistance throughout my thesis work. John did an incredible job training me especially as I was his first graduate student. He encouraged me to think of the big picture questions in science, to think creatively on my projects, and to work on a project that highly interested me. His leadership and mentorship have continually inspired me and have made me a better scientist. He always understood when I needed to take some time off to visit my wife in Minnesota and yet still promoted an excellent work ethic that I will take with me throughout my life and career.

I also want to thank the Karijolich lab members, both past and present, for their training, support, thoughtful scientific insight, and advise over my graduate school career. I would particularly like to thank Dr. Yang Zhao, Dr. Xiang Ye, Dr. Yu Song, Nancy Li, and Antiana Richardson. Furthermore, I want to thank my thesis committee members, Drs. Jeff Rathmell, Mark Denison, Heather Pua, and Vivian Gama for their help and guidance throughout the years.

The friends that I have made at Vanderbilt and prior to coming here, as well as my family, also deserve thanks for providing support and relief throughout the years. Finally, I especially want to thank my wife, Dr. Brianna Dunker, for her support and understanding of my graduate school schedule and I would not have gotten through it without her.

Table of Contents

List of Tables

Introduction:

Chapter 2:

List of Figures

Introduction:

Chapter 1:

Chapter 2:

Appendix:

Introduction

My thesis investigates how RNA binding proteins (RBPs) regulate viral infection and a dsRNA sensing immune response. The goal of the Karijolich laboratory is to study how RNA metabolism and processing are regulated during viral infection and immune activation, and my thesis work includes projects on both topics. My thesis research focuses on two ubiquitous RBPs: FUS and TDP-43. I demonstrate that FUS restricts KSHV reactivation by regulating RNA polymerase II transcription of viral genes, and that TDP-43 prevents RIG-I activation and a lethal interferon response by regulating endogenous RNA polymerase III transcript abundance and localization. This introduction will describe the 1) KSHV life cycle and host regulation, 2) a description of FUS and its role in RNA metabolism, 3) the double-stranded RNA sensing pathway and interferon signaling, and 4) background on TDP-43 and its associated diseases.

Section I: Kaposi's Sarcoma-associated Herpesvirus (KSHV)

Human Herpesvirus and γ-herpesviruses

Herpesviruses have been discovered throughout the animal kingdom and most vertebrates have at least one life-long herpesviral infection [1]. These viruses are enveloped and have large, double-stranded DNA genomes. One of the universal characteristics of this virus family is that they exhibit two distinct life cycle phases. Following infection, the viruses establish latency that is defined by genome persistence, limited viral transcription, zero viral particle production, and the ability to reactivate into its

lytic phase following specific stimuli to produce and release infectious virions that will infect other cells [2].

Eight different herpesviruses frequently infect humans and most adults are infected with at least one virus [3]. They are divided into three subfamilies based on associated diseases, tropism, speed and duration of its lytic cycle, and the cell types in which they primarily establish latency. α-herpesviruses comprise herpes simplex virus (HSV)-1 (HHV-1), HSV-2 (HHV-2), and varicella zoster virus (VZV) (HHV-3) (Table 0.1). They have a broad cellular tropism, a rapid infection cycle, and primarily establish latency in neurons. β-herpesviruses include human cytomegalovirus (HCMV) (HHV-5), herpesvirus 6A and 6B (HHV-6A and B), and herpesvirus 7 (HHV-7), infect a smaller number of cell types than the α-herpesviruses, and primarily persist in CD34+ hematopoietic stem cells, CD14+ monocytes, T cells, and neuronal cells. Finally, γ-herpesviruses are comprised of Epstein-Barr virus (EBV) (HHV-4) and Kaposi's sarcoma-associated herpesvirus (KSHV) (HHV-8), infect the fewest number of cell types, have a long replication cycle, and primarily establish latency in B cells and endothelial cells. γ-herpesviruses are unique as they are oncogenic, with chronic infection leading to lymphoproliferative diseases, sarcomas, and lymphomas [4].

Name	Sub-family	Primary Persistent Cell Types	Associated Diseases
Herpes Simplex Virus (HSV-1)	α	Sensory and cranial nerve ganglia	Cold sores, skin lesions, keratitis, encephalitis, genital ulcers
Herpes Simplex Virus (HSV-2)	α	Sensory and cranial nerve ganglia	Genital ulcers
Varicella Zoster Virus (VZV)	α	Sensory and cranial nerve ganglia	Chicken pox, shingles
Epstein-Barr Virus (EBV)	γ	B lymphocyte	Mononucleosis, lymphoma
Human Cytomegalovirus (HCMV)	β	Monocyte, lymphocyte	Congenital defects
Herpesvirus 6A/6B	β	Leukocyte	Roseola

Herpesvirus 7	β	T cells	Roseola
Kaposi's sarcoma-associated herpesvirus (KSHV)	γ	B lymphocyte, endothelial cell	Kaposi's sarcoma, primary effusion lymphoma, multicentric Castleman's disease

Table 0.1: Human Herpesviruses

KSHV Prevalence and Associated Diseases

Unlike most of the other human herpesviruses, KSHV infection is not common throughout the human population and has varying seroprevalence rates around the globe. There is a high rate of infection in sub-Saharan Africa where >50% of adults are infected, while ~20-30% of adults in the Mediterranean region have KSHV antibodies [5]. Europe, Asia, and the USA have much lower infection percentages at typically <10%, although specific groups have higher positive percentage rates such as homosexual men.

KSHV is associated with several different diseases that typically depend upon the means of transmission, age, and underlying conditions. Kaposi sarcoma (KS) is the most prevalent KSHV associated cancer and is classified as classic, transplant-associated, endemic, or AIDS-related [6]. KS is one of the most common AIDS-associated cancers. It presents as inflammatory, multi-focal cutaneous lesions that frequently occur in the lower extremities and is diagnosed with a KSHV-infected spindle cell biopsy. KSHV is also associated with primary effusion lymphoma (PEL), a rare and highly aggressive B cell lymphoma that has a less than 6 month survival rate [7]. Most PEL patients are co-infected with HIV and ~50% have or will develop KS. Finally, KSHV is also associated with Multicentric Castleman Disease (MCD), a B cell lymphoproliferative disorder frequently diagnosed in HIV patients [6]. If left untreated, this pro-inflammatory disease is typically fatal within 2 years.

KSHV Life Cycle

As with all human herpesviruses, KSHV has two life cycle phases, latency and lytic reactivation (Figure 0.1). KSHV infects endothelial and fibroblast cells via macropinocytosis or clathrin-mediated endocytosis, respectively, although the mechanism of entry into B cells and other cell types has not yet been determined [8]. The virus primarily establishes latency upon infection of B cells and endothelial cells, where the viral episome is tethered to the host chromosome to be maintained during host replication by the primary latent transcript latency-associated nuclear antigen (LANA). [9] Latency is defined as the expression of few and specific latent viral genes and a lack of virion production [10]. The latent viral products maintain latency by promoting host survival, enhancing cell cycle progression, and preventing immune activation, and are essential for KSHV-associated disease development as most associated cancers are KSHV positive.

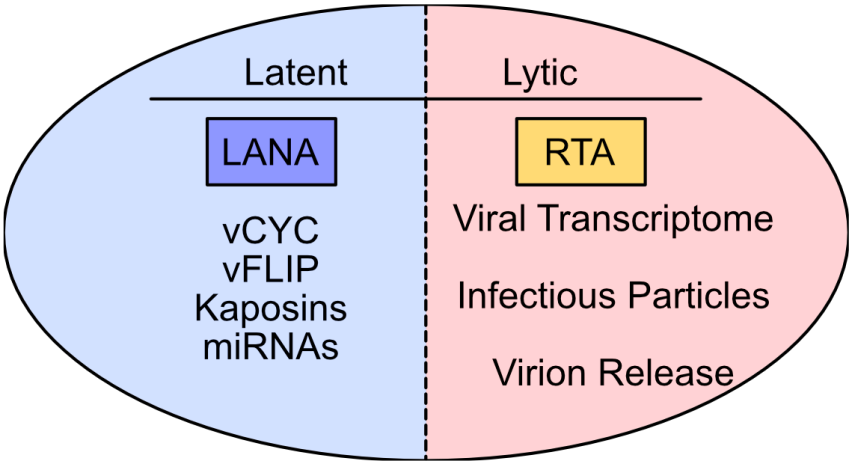

Figure 0.1: KSHV life cycle

Latent KSHV infection can transition to lytic reactivation by specific stimuli. Reactivation can be initiated by artificial treatments, such as TPA and sodium butyrate, as well as physiological conditions like viral co-infection, hypoxia, and oxidative stress [10]. Lytic reactivation is characterized by the expression of the entire viral transcriptome, assembly of infectious particles, and release of virions to seed further infection. The viral transactivator replication and transcription activator (RTA) is the main driver of reactivation and its expression alone is sufficient to induce the lytic cycle. The RTA promoter is repressed by several host and viral proteins in latency to prevent reactivation, including NF-kB, the transcriptional repressor protein Hey1, and the viral latency protein LANA [11]. RTA activity initiates lytic gene expression in a temporally-defined transcriptional viral gene expression cascade [12]. Immediate early genes encode transcriptional regulators, early genes primarily function in viral DNA replication and translation, and late genes encode viral structure and egress associated proteins. Lytic products have a range of pro-viral functions, including facilitating an inflammatory, angiogenic, and proliferative state that contributes to KSHV associated disease progression [13]. Virion assembly commences in the nucleus where newly replicated genomes are packages into capsids, followed by tegument protein addition, and subsequent budding to acquire an envelope and release of infectious particles.

KSHV Co-option and Regulation of Host Transcription Machinery

KSHV regulates and co-opts several host processes to promote and enhance its lytic reactivation. Examples include RNA localization, decay, export, and proline metabolism [14,15]. Importantly, the virus uses the host transcription machinery during

reactivation and regulates the process at several stages. KSHV recruits RNA polymerase II (RNAPII) to viral episomes to facilitate its reactivation and form spontaneously aggregating “transcriptional factories” that localize to the genomic viral DNA [16]. This recruitment also reduces the total amount of RNAPII available to the host, resulting in decreased global gene expression. KSHV also hijacks host co-transcriptional RNA modification machinery to enhance reactivation. For example, N^6-methyladenosine (m^6A), the most abundant RNA modification, is present on the *ORF50* (RTA) transcript to both stabilize and direct pre-mRNA splicing to generate a functional RTA protein [17,18]. KSHV further regulates enhancer and super-enhancer activities during latency to maintain viral persistence, oncogene expression, and cellular survival, and also during lytic reactivation to drive viral replication [19,20].

RNA Binding Protein Restriction of KSHV

Numerous host proteins have been identified as KSHV restriction factors that target various latency, viral reactivation, and *de novo* infection processes. These include DNA sensors such as IFI16 and cGAS, epigenetic factors like the NuRD complex and the histone demethylase KDM2B, and the genomic structure regulators CTCF and cohesin [21–24]. In addition, several other restriction factors are RNA binding proteins (RBPs) that restrict different stages of RNA metabolism. Nonsense-mediated decay (NMD) is an RNA decay mechanism that degrades incorrectly processed RNAs prior to translational completion. The pathway has recently been demonstrated to restrict the KSHV lytic cycle by targeting cellular and viral mRNAs, including the transactivator RTA transcript, to repress the virus [25].

The interferon inducible proteins IFIT1, 2, and 3 bind and detect a variety of non-host RNA substrates to inhibit translation of viral transcripts. Recent studies have demonstrated that IFIT1, 2, and 3 are induced during the KSHV lytic cycle, restrict the virus, and that IFIT1 binds viral mRNAs [26]. Double-stranded RNA (dsRNA) sensors also restrict KSHV reactivation, specifically the RIG-I-like receptors (RLRs). The two signaling receptors RIG-I and MDA5 bind specific dsRNA ligands to induce an antimicrobial response. KSHV lytic reactivation induces RIG-I and MDA5 activation to restrict KSHV by binding distinct classes of RNAs [27,28]. Specifically, RIG-I binds host-derived triphosphorylated RNA polymerase III transcripts, revealing an interaction between RNA processing and RLR activation, and demonstrating that defects in RNA biogenesis can result in a robust immune response.

Section I Summary

KSHV is an oncogenic γ-herpesvirus that is the causative agent of KSHV, PEL, and MCD, and tightly regulates and co-opts host machinery to enhance its lytic cycle. Although several RNA binding proteins have been identified as KSHV restriction factors, additional investigation is necessary to identify other proteins and how they restrict the virus. This thesis presents a study that demonstrates that the RNA binding protein FUS restricts KSHV reactivation and identifies FUS as a new antiviral protein that prevents RNA polymerase II activity on viral genes.

Section II: The RNA Binding Protein FUS

FUS is a Ubiquitous RNA Binding Protein

There are hundreds of RNA binding proteins (RBPs) expressed in human cells. Many RBPs are expressed in a cell type-specific manner to regulate gene expression depending on cellular and tissue function. Conversely, other RBPs are ubiquitously expressed in most cell types and tissues. One such protein family is the TET/FET family, which is comprised of Translocated in Liposarcoma/ Fused in Sarcoma (TLS/FUS), Ewing's sarcoma (EWS), and TATA-binding protein-associated factor 15 (TAF15). The three proteins are predominately nuclear localized, highly expressed in all tissues and cell types, and impact gene expression [29]. Like all TET/FET proteins, the 526 amino acid TLS/FUS protein has a N-terminal Gln, Gly, Ser, Tyr (QGSY)-rich domain, internal RNA recognition motif (RRM), zinc finger domain (ZFD), and three RGG domains that also bind RNA (Figure 0.2). Furthermore, FUS is highly conserved as similar FUS sequences have been identified in over 84 species including mammals [30].

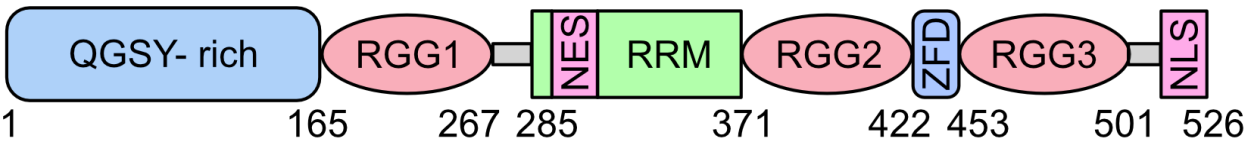

Figure 0.2: FUS structural domains

FUS Associated Diseases

FUS is associated with several diseases. The N-terminal transcriptional activation domain can fuse with the CHOP transcription factor to generate the onco-fusion protein FUS-CHOP that causes >90% of myxoid liposarcoma cases [31]. FUS-CHOP activates SRC-FAK signaling, and FAK expression correlates with sarcoma tumor aggressiveness, revealing how FUS-CHOP drives this cancer [32]. Indeed, expression of this onco-fusion protein is associated with a higher potential for metastasis. Furthermore, FUS can fuse with the transcription factors ERG or FEV in EWS cancers, ATF1 in angiomatoid fibrous histiocytoma, and CREB3 L1 or L2 in low-grade fibromyxoid sarcoma. FUS also impacts cellular growth as loss of this protein reduces proliferation and enhances mitotic arrest. Finally, FUS and other FET onco-fusion proteins interact with the SWI/SNF chromatin remodeling complex more readily than wild-type FET proteins [33]. Expression of the onco-fusion proteins results in changes in global H3K27 trimethylation levels and gene expression, demonstrating that FET proteins deregulate SWI/SNF activity in several different types of cancers.

FUS is highly associated with a variety of neurodegenerative diseases, including amyotrophic lateral sclerosis (ALS), frontotemporal lobar degeneration (FTLD), and the polyglutamine diseases, which include spinocerebellar ataxia, dentatorubropallidoluysian atrophy, and Huntington disease [34]. Although ALS and FTLD impact different regions of the nervous system, ALS and FTLD are both late-onset diseases that have similar genetic, clinical, and neuropathological features. ALS is defined by a fatal and progressive degeneration of upper and lower motor neurons, leading to muscular atrophy and paralysis. Respiratory failure and pneumonia cause death within 3-5 years on average.

~90-95% of cases are from unknown causes and are termed sporadic ALS (sALS), while the remaining ~5-10% arise from inherited familial gene mutations known as familial ALS (fALS). FUS is a primary disease-associated gene for familial and sporadic ALS, and FUS mutations comprise about ~4% of fALS cases making it one of the most mutated proteins in the disease. Other mutated proteins include TDP-43 (see section III), SOD1, and C9ORF72. Furthermore, FUS mutations in ALS can drive cytoplasmic relocalization of the protein to form aggregates in neuronal and glial cells. Over 50 different patient mutations have been identified with approximately two-thirds located in the ZFD, RGG2/3, and NLS domains. One example is the NLS mutation R521C. Patients with this mutation exhibits neuronal cytoplasmic inclusions, and glial and neuronal cell loss. FTLD a progressive disease associated with frontal and temporal lobe degeneration [35]. It is the second most common cause of dementia in patients older than 65 behind Alzheimer's disease. FTLD-FUS has three related clinicopathological subtypes: atypical FTLD-U, neuronal intermediate filament inclusion disease (NIFID), and basophilic inclusion body disease (BIBD) [34]. Furthermore, FUS is associated with neuronal intranuclear inclusion aggregates in polyglutamine disease, although its impact on disease progression requires further investigation.

FUS Regulates Gene Expression and Transcription

Similar to many other RBPs, FUS regulates various gene expression processes including splicing, microRNA biogenesis, transcription, as well as DNA repair. FUS impacts splicing at several stages, including coupling transcription and splicing by interacting with RNA polymerase II and the U1 snRNP, binding to and around alternative splice sites at GGU and related motifs, and by forming complexes with splicing factors

[36–39]. It also stimulates processing of specific microRNAs by binding the transcription start site, interacting with the pri-microRNA, and enhancing Drosha levels at the loci, while FUS depletion results in a reduction of microRNA levels [40]. Furthermore, FUS promotes DNA damage repair as it is recruited to sites of DNA damage in a PAR-dependent manner [41]. FUS mutations in the nuclear localization signal restrict a PARP-dependent DNA damage response that drives further cytoplasmic FUS localization and contributes to neurodegeneration in motor neurons.

FUS in also found in membrane-less organelles during certain conditions in the cell. Hyperosmolar stress induces FUS relocalization to the cytoplasm and assembly into stress granules to enhance cell survival [42]. FUS is also involved in paraspeckle formation, which is a membrane-less organelle that contains specific mRNAs and RNA binding proteins that regulate transcription [43]. FUS interacts with NONO, an essential paraspeckle protein, and regulates NEAT1 levels, the paraspeckle scaffold RNA. Loss of FUS reduces paraspeckle formation, while FUS mutations in fALS cases enhances their formation. FUS further impacts mRNA processing and biogenesis through stability and transport. ALS mutations in FUS increase mRNA abundance due to enhanced RNA stability, for example with the FUS target RNA MECP2 [44]. FUS also promotes mRNA transport of the actin-stabilizing protein Nd1-L to dendritic spines where translation occurs, demonstrating that FUS shuttles bound mRNAs throughout the cell [45].

Importantly, FUS regulates transcription at several stages. A significant percentage binds to active chromatin and ALS mutations reduce chromatin binding [46]. Furthermore, FUS binds the promoter of some RNA polymerase II and III-transcribed genes and accumulates at the transcription start site [47,48]. FUS also interacts with

several transcription factors including the TFIID RNA polymerase II subunit and the C-terminal domain of RNA polymerase II to block serine-2 hyperphosphorylation and regulate transcriptional elongation [49,50]. Furthermore, FUS binds the RNA polymerase II CTD to form phase-separated condensates that enhance transcriptional initiation after phase transition, demonstrating that FUS is associated with transcriptional and post-transcriptional regulation [51].

FUS Regulates B Cell Development

RBPs impact RNA biogenesis at numerous stages including stability, splicing, localization, transcription, modification, and translation. As such, they are essential for cellular and organism development. Importantly, FUS regulates B cell lymphocyte development and activation in mice [52]. FUS is essential for survival as a homozygous knockout (FUS -/-) results in death within 16 hours after birth. Strikingly, FUS -/- newborns have fewer lymphocytes with a specific reduction in IgM B cells but not precursor B cells, demonstrating a deficiency in pre-B cell to B cell development. FUS -/- mice also exhibit genomic instability as defined by increased aneuploidy, chromosome breakage, extrachromosomal elements, and centromeric fusions, demonstrating a role in genome maintenance.

Section II Summary

FUS is a ubiquitous RNA binding protein that regulates several aspects of RNA biogenesis. Although the role that FUS has on transcription is well defined, what impact it has on viral infection has not been investigated. This thesis demonstrates that FUS restricts KSHV reactivation from PEL and latently infected epithelial cells. It binds specific

viral promoters on the episome and binds RNA polymerase II during the viral lytic cycle to repress CTD Serine-2 hyperphosphorylation. Loss of FUS results in increased transcriptional elongation of several viral genes, including the main transactivator RTA, demonstrating that FUS restricts KSHV by regulating viral transcription.

Section III: Double-stranded RNA Sensing and Signaling

Nucleic Acid Sensors

The innate immune system is the first line of defense against pathogens and is paramount for the detection of infectious agents. Germ line encoded pattern recognition receptors (PRRs) detect conserved pathogen-associated molecular patterns (PAMPs) that are present on and in pathogens to activate an immune response. The different classes of PRRs include the Toll-Like receptors (TLRs) that detect a variety of PAMPS, the NOD-like receptors (NLRs) that can activate the inflammasome, the C-type lectin receptors (CLRs) that recognize different components of fungi, and the double-stranded RNA (dsRNA) and double-stranded DNA (dsDNA) nucleic acid sensors (Table 0.2) [53,54].

Receptor	Ligand
TLR3	dsRNA
TLR7/8	ssRNA
TLR9	CpG DNA
ZBP1/DAI	DNA
AIM2	DNA
cGAS	DNA
IFI16	DNA
DDX41	DNA
RIG-I	Short (<1000bp) 5’(p)pp dsRNA; 5’ppp ssRNA; circular RNA

MDA5	Long (>1000bp) dsRNA
NLRP3	RNA, other stimuli
PKR	dsRNA

Table 0.2: Innate immune nucleic acid receptors and associated ligands

The nucleic acid receptors are predominantly localized in the cytoplasm. The primary DNA sensor in most cell types is cGAS, which binds dsDNA in a sequence independent manner and signals through the adapter protein STING to induce an antimicrobial response. Other receptors such as DDX41 and IFI16 also signal through STING, while IFI16 and AIM2 can induce inflammasome activation [55]. Interestingly, cytoplasmic RNA polymerase III is considered a DNA sensor as it detects dsDNA and transcribes immunostimulatory RNA that activates the RNA signaling pathway [56,57]. Furthermore, RNA sensors include the OAS proteins that signal through the adapter protein RNase L to activate RIG-I, PKR whose activation prevents cap-dependent translation to restrict pathogens, and the RIG-I-like receptors (RLRs), which are the primary dsRNA receptors [55].

RIG-I-like Receptors

The RIG-I-like receptor (RLR) family includes three members: retinoic-acid-inducible protein 1 (RIG-I/DDX58), melanoma-differentiation-associated gene 5 (MDA5/IFIH1), and laboratory of genetics and physiology 2 (LGP2/DHX58) [58]. While all three proteins are primarily localized in the cytoplasm and can bind dsRNA, only RIG-I and MDA5 activate the downstream signaling cascade due to LGP2 lacking CARD domains that are necessary for binding the adapter protein mitochondrial antiviral-signaling protein (MAVS) (Figure 0.3). MAVS is primarily anchored in the mitochondrial

membrane but is also found on the peroxisome [59]. RIG-I or MDA5 interaction with MAVS recruits TANK-binding kinase 1 (TBK1) and IκB kinase (IKK) to activate IRF3/IRF7 and NF-κB, respectively. These transcription factors then induce the expression of antimicrobial interferon and pro-inflammatory gene expression responses.

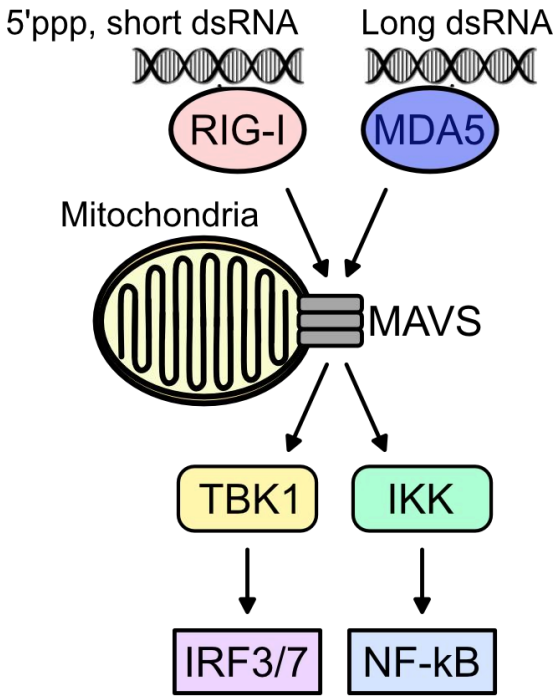

Figure 0.3: RIG-I-like receptor signaling pathway

RIG-I and MDA5 recognize distinct structural and chemical moieties on RNAs. For example, RIG-I preferentially recognizes short (<1000 bp) 5'-triphosphorylated (5'ppp) blunt dsRNAs, although it can also recognize 5'ppp single-stranded RNA (ssRNA) and circular RNAs at a lower affinity [60–66]. 2'-O-methylation of the 5' end of dsRNA also prevents RIG-I recognition [67]. Conversely, MDA5 binds long (>1000bp) dsRNAs independent of the 5'-end phosphorylation status [61,68]. Thus, the RLR pathway is

activated during a variety of infections and autoimmune diseases due to the wide range of RIG-I and MDA5-specific ligands.

Type I and III Interferon Signaling

The interferon regulatory factor (IRF) transcription factor family drives expression of interferons (IFNs), a family of pro-inflammatory cytokines that signal in an autocrine and paracrine fashion to induce an antimicrobial state. Type I IFNs include IFN α and β, type II is IFN γ, while type III includes IFN λ1 and λ2/3. Most cell types express the type I and III IFNs following activation of the innate immune system [69]. Type I IFNs signal through the interferon- α/β receptor (IFNAR) while type III IFNs bind the interferon- λ receptor (IFNLR). Activation of either receptor induces a shared signaling cascade to activate an antimicrobial response in the cell. While IFNAR is expressed in all cell types, IFNLR expression is cell-type specific. It is expressed in epithelial cells of the gastrointestinal lining and respiratory tract to induce a more robust IFN response to specific stimuli. IFNAR and IFNLR activation leads to JAK/STAT signaling, where STAT1/2 dimerize and interact with the transcription factor IRF9 to form the ISGF3 complex. ISGF3 is then translocated to the nucleus and binds ISRE elements to transcribe interferon stimulated genes (ISGs). There are hundreds of ISGs that restrict infection through a variety of mechanisms, including translational shutoff, blocking virion release, and further promoting an immune response.

Sensing of Endogenous dsRNA

Although nucleic acid sensors were originally described in the context of infection, recent investigations have demonstrated that endogenous RNAs can also activate them.

Immunostimulatory dsRNAs are generally not found within the host transcriptome as their presence would activate an interferon and pro-inflammatory gene expression response that would potentially result in lethality, thus they are tightly regulated through a variety of mechanisms. Recent studies have identified RBPs that regulate essential junctions of RNA biogenesis where their deletion results in dsRNA sensor activation. For example, depletion of heterogenous ribonucleoprotein (hnRNP) C, which regulates pre-mRNA splicing through the binding of proximal *Alu* elements, results in RIG-I-dependent cell death due to the generation of dsRNA hairpins formed between inverted *Alu* repeats [70–72]. Additionally, adenosine deaminase RNA specific (ADAR) enzymes recognize and deaminate adenosines to produce inosines within dsRNA hairpins to generate imperfect dsRNA structures. Loss of this activity results in RLR-dependent sensing of the perfectly complementary endogenous dsRNA hairpin [73–78]. Furthermore, the non-coding RNAs RN7SL and RNA5SP141 bind RIG-I following the loss of their protective RBPs, demonstrating that 'unshielded' RNA can be immunostimulatory [79,80].

Constitutive activation of dsRNA receptors by endogenous dsRNA can lead to several autoimmune diseases. These diseases are defined as interferonopathies due to the robust interferon response that contributes to the pathologies [81]. The MDA5 mutant A946T correlates with several autoimmune diseases such as multiple sclerosis (MS), rheumatoid arthritis, and systemic lupus erythematosus (SLE), and mice with the mutation develop lupus-like symptoms due to a systemic elevated interferon response. Aicardi-Goutieres syndrome (AGS) is a neuroinflammatory autoimmune disease that arises due to mutations in nucleotide processing proteins, such as ADAR1 and MDA5, that generate immunostimulatory dsRNA accumulation and hypersensitivity to ligands, respectively.

Finally, Singleton-Merten syndrome (SMS) is a multisystem disorder that is defined by an interferon profile, and MDA5 and RIG-I mutations have been identified in this disease that lead to the constitutive IFN expression.

Mechanisms of Interferon-driven Cell Death

Interferon signaling can induce cell death through a variety of mechanisms (Figure 0.4). First, interferon stimulation can activate apoptosis, a programmed form of cell death. Apoptosis is accomplished by either cell extrinsic signaling via a death receptor or cell intrinsic through the mitochondria releasing cytochrome C, and an interferon response drives cell death through the cell intrinsic pathway. There are a couple of mechanisms for this that require JAK/STAT signaling following IFNAR activation [82]. Interferon activates the ERK and JNK pathways to initiate apoptosis by promoting the activation of the anti-survival Bcl-2 members Bax and Bak. Interferons can also activate the pro-apoptotic protein Bim while downregulating the anti-apoptotic protein Bcl-xL when stimulated with TNF-α. Furthermore, several ISGs have pro-apoptotic activity including IFIT2, NOXA, and IFITM2. A type I interferon response can also activate necroptosis through a couple of mechanisms. The ISG DNA-dependent activator of IFN regulatory factors (ZBP1/DAI) is upregulated following interferon stimulation and forms a homodimer [83]. ZBP1 then interacts with the necroptotic kinases RIPK1 and RIPK3. Conversely, the ISG protein kinase R (PKR) can be induced following interferon signaling, which then interacts with RIPK1/3 similarly to ZBP1. [84] RIPK1/3 are then phosphorylated and activated, leading to the recruitment of the pseudokinase MLKL and its subsequent phosphorylation to promote its plasma membrane localization and pore formation.

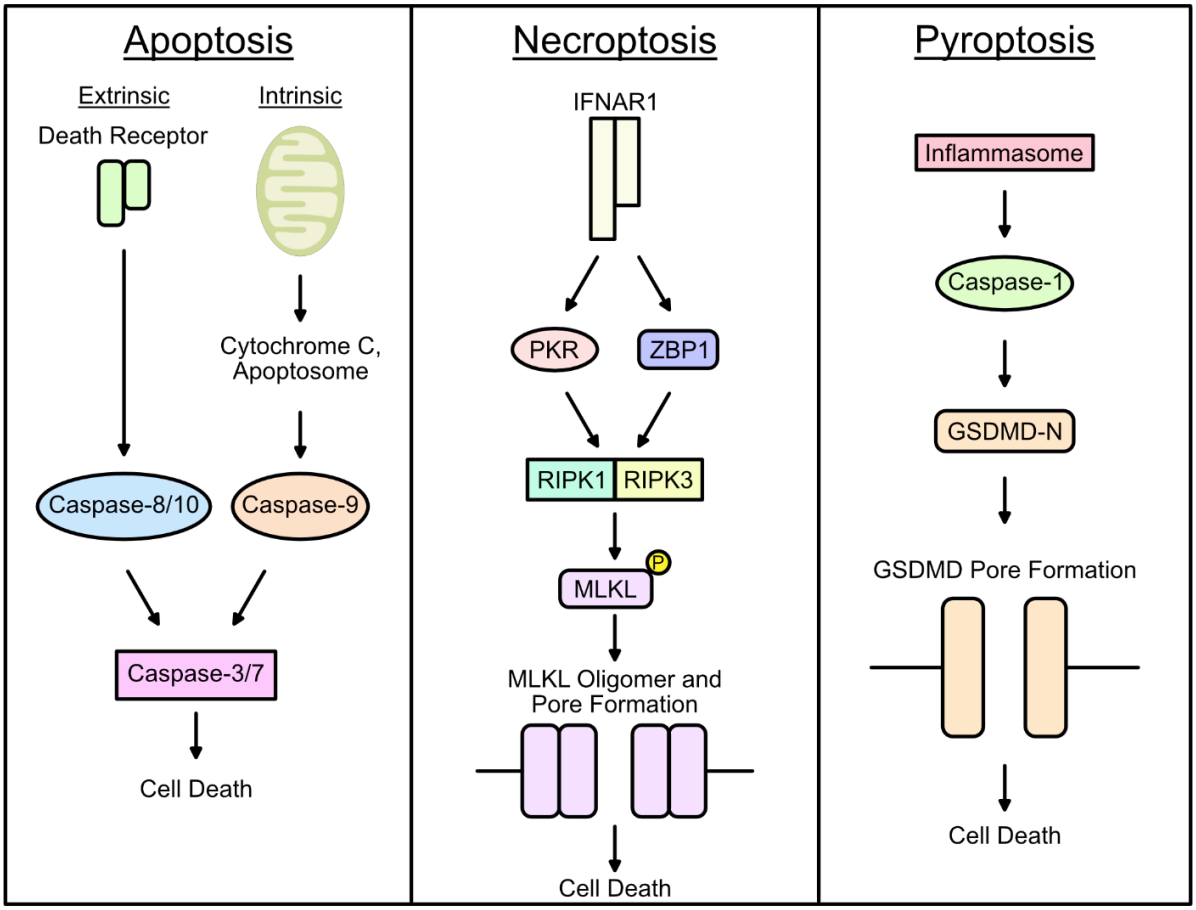

Figure 0.4: Interferon-stimulated cell death pathways

Finally, the inflammasome can also be activated by interferon signaling to induce pyroptotic cell death. Several different inflammasomes have been shown to activate pyroptosis in an interferon-dependent manner. These include NLRP3, AIM2, and RIG-I, which are upregulated following ISGF3 activation during infection [85]. Inflammasome activation is characterized by caspase-1 cleavage and activation, which cleaves gasdermin D (GSDMD) and the inflammatory cytokines IL-1β and IL-18, leading to GSDMD plasma membrane localization and pore formation to induce pyroptosis.

Section III Summary

Activation of the RIG-I-like receptors (RLRs) induces an antimicrobial interferon and pro-inflammatory cytokine response. As constitutive activation can cause autoimmune diseases, the regulation of the RLRs is essential for preventing an aberrant immune response to endogenous dsRNAs. Therefore, I sought to identify RNA binding proteins that prevent an interferon response and determine how they do so. This thesis presents a study that demonstrates that the RNA binding protein TDP-43 prevents endogenous dsRNA accumulation and an interferon response. Loss of TDP-43 activates RIG-I to induce a lethal type I interferon response due to accumulated and mislocalized RNA polymerase III-transcribed non-coding RNAs.

Section IV: The RNA Binding Protein TDP-43

TDP-43 is a Conserved, Ubiquitous RNA Binding Protein

Similar to FUS, TAR DNA binding protein 43 (TDP-43 (gene name *TARDBP*)) is a ubiquitous RNA binding protein that is expressed in most cell types and tissues. It is classified as a member of the heterogeneous nuclear ribonucleoprotein (hnRNP) family of RBPs as all members have at least one RNA binding domain [86]. The hnRNP family is involved in most stages of RNA biogenesis, such as alternative splicing, polyadenylation, transcription, and transport. Structurally, TDP-43 is comprised of a nuclear localization signal (NLS), two RNA recognition motifs (RRMs), a nuclear export signal (NES), and a prion-like glycine-rich C-terminal domain, and is primarily nuclear localized (Figure 0.5) [35]. In addition, TDP-43 is highly conserved as TDP-43 orthologs

have been identified in humans, mice, *Drosophila*, and *Caenorhabditis elegans* [87]. Furthermore, TDP-43 is essential for life as a knockout in mice is embryotic lethal at day 7.5, a knockout in zebrafish results in early death, and loss of TDP-43 in various cell types induces cell death [88,89].

Figure 0.5: TDP-43 structural domains

TDP-43 Associated Diseases

TDP-43 dysregulation and mutations are associated with several diseases including neurodegenerative diseases, which are the most studied. Amyotrophic lateral sclerosis (ALS) and frontotemporal lobar degeneration (FTLD) are highly associated with defects in TDP-43 function, expression, and localization, in addition to TDP-43 mutations [35]. TDP-43 mutations are found in ~5-10% of familial ALS cases, making it one of the most frequently mutated proteins in the disease. Most of these mutations occur in the C-terminal glycine-rich region. In addition to the fALS mutations, TDP-43 exhibits a proteinopathy in ~97% of all ALS cases which is characterized by the cytoplasmic re-localization of the predominantly nuclear protein. Cytoplasmic TDP-43 is further ubiquitinated and hyper-phosphorylated in inclusion bodies, and a portion is truncated into C-terminal fragments that form protein aggregates. TDP-43 mutations can promote cytoplasmic re-localization, aggregation, and resistance to proteases, as well as change protein stability and binding partners. Furthermore, TDP-43 overexpression, which can be found in ALS, drives cytoplasmic re-localization and aggregate formation while being

toxic in neurons [90]. Whether cytoplasmic re-localization contributes to ALS due to gain-of-toxic-function (enhanced cytoplasmic activity) or loss-of-function (reduced nuclear activity) has not been fully determined, although studies supporting both hypotheses have been published. In addition, ~45% of all FTLD cases have modified and truncated cytoplasmic TDP-43 aggregates similar to ALS patients and are termed FTLD-TDP [35]. TDP-43 mutations can also impact FTLD-TDP disease and there are several that overlap between ALS and FTLD.

Besides neurodegenerative diseases, TDP-43 is associated with other pathologies. Cytoplasmic and ubiquitinated TDP-43 inclusions have been identified in inclusion body myopathies, a disease that targets skeletal muscles and weakens them over time [91]. In addition, TDP-43 is highly upregulated in triple negative breast cancer (TNBC) while being associated with poor prognosis as it plays a role in tumor proliferation and metastasis due to changes in aberrant alternative splicing [92]. Furthermore, TDP-43 is involved in double-stranded DNA damage repair, demonstrating a link between TDP-43 and cancer as well as other genomic instability disorders [93].

TDP-43 defects are also associated with inflammatory conditions in disease. Elevated interferon levels and an activated immune system have been reported in the brains of ALS and FTLD patients as well as in animal models [94–97]. Furthermore, TDP-43 overexpression induces inflammation via mitochondrial DNA release and cGAS/STING activation [98]. TDP-43 overexpression also causes an inflammatory response in astrocytes that induces TDP-43 mislocalization to the cytoplasm and aggregation, suggesting a positive feedback loop between TDP-43 and inflammation [99,100].

TDP-43 Regulates Gene Expression

TDP-43 and FUS impact and regulate several stages of RNA metabolism by binding to target RNAs and proteins that regulate a variety of overlapping processes and are associated with similar diseases (Figure 0.6). Cross-linking and immunoprecipitation (CLIP)-seq demonstrates that TDP-43 preferentially binds long introns at UG-rich regions [101,102]. Some of its most well studied functions are in pre-RNA splicing and alternative splicing where TDP-43 binding near the 5' and 3' splice sites and can prevent or enhance splicing depending on the gene [103]. Interestingly, TDP-43 autoregulates its own RNA levels by binding its 3' UTR, resulting in suboptimal splice site usage and mRNA degradation. TDP-43 has further been shown to regulate splicing through spliceosomal RNA modifications. U1 and U2 snRNAs initiate splicing by binding the pre-RNA and recruiting the spliceosome. These RNAs are 2'-O-methylated at specific sites and the modification is facilitated by small Cajal body-specific RNAs (scaRNA) in Cajal bodies. TDP-43 binds to certain scaRNAs to localize them to Cajal bodies to enhance U1 and U2 modifications, and loss of TDP-43 reduces U1 and U2 snRNA modifications that may impact splicing [104].

TDP-43 has also been implicated in regulating RNA and protein export from the nucleus by interacting with the nuclear pore complex and nucleocytoplasmic transport machinery, as well as in transporting mRNA cytoplasmic granules [105,106]. TDP-43 further forms complexes in membrane-less organelles that regulate RNA export, transcription, and translation. Stress conditions promote cytoplasmic re-localization to form stress granules and loss of TDP-43 reduces stress granule assembly. Interestingly, TDP-43 stress granules have been identified in cell types associated with ALS/FTD,

suggesting its role in stress granule formation may contribute to neurodegenerative diseases [107]. TDP-43 is also essential for paraspeckle formation in the nucleus [108]. It prevents paraspeckle formation by binding the short isoform of the non-coding RNA NEAT1, the RNA scaffold of paraspeckles, which blocks paraspeckle formation in pluripotent cells. Differentiation induces paraspeckle formation as it reduces TDP-43 expression, resulting in the transition from short to long NEAT1 isoform accumulation and subsequent TDP-43 sequestration into paraspeckle due to NEAT1 binding.

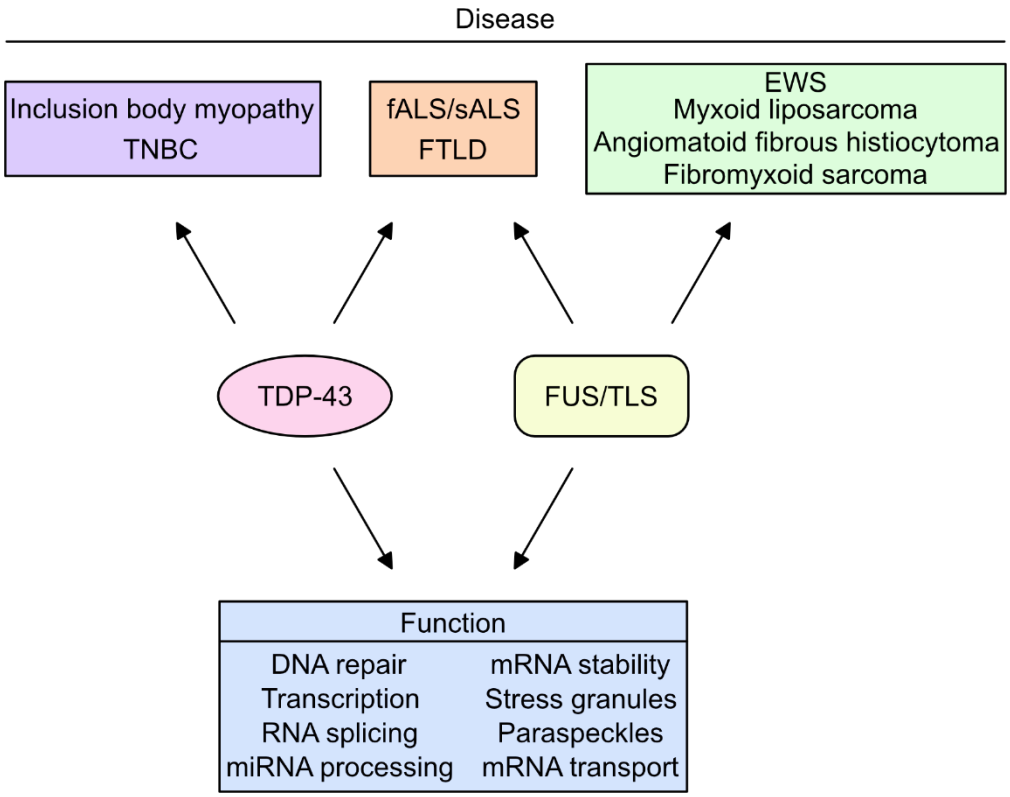

Figure 0.6: Overlap between FUS and TDP-43 function and disease

Finally, TDP-43 regulates RNA abundance at both the transcriptional and RNA degradation level by microRNA (miRNA) activity. The transcription elongation factor ELL, a protein in both the little elongation complex (LEC) and super elongation complex (SEC),

interacts with TDP-43 in human cells [109]. LEC regulates RNA polymerase II transcription of snRNAs at the initiation and elongation stages in *Drosophila*, while the SEC contains p-TEFb, a kinase that phosphorylates RNA polymerase II to promote RNA elongation. Some of the LEC and SEC target genes are induced in fly ALS/FTLD models, including U12 snRNA and the long non-coding RNA Hsrω, linking transcriptional activation and TDP-43 in neurodegenerative disease. Furthermore, TDP-43 is involved in miRNA abundance and biogenesis. It interacts with the nuclear protein Drosha and specific primary miRNAs to facilitate the production of some precursor miRNAs [110]. Cytoplasmic TDP-43 also interacts with the Dicer complex and precursor miRNAs to enhance their processing, demonstrating that TDP-43 regulates RNA decay and turnover.

TDP-43 and dsRNA Processing

Many of the TDP-43 associated functions involve dsRNA structures, whether as precursors, intermediates, or products. Along this line, previous work has demonstrated that TDP-43 restricts dsRNA accumulation. Loss of the TDP-43 homologue, TDP-1, in *Caenorhabditis elegans,* results in the accumulation of dsRNAs including antisense overlapping transcripts, transposons, and intronic sequences [111]. Furthermore, TDP-43 siRNA depletion in human HeLa cells, and in M17 and SH-SY5Y neuroblastoma cells induces dsRNA accumulation, demonstrating a conserved function of TDP-43 [112]. Here, the accumulated dsRNAs was comprised of numerous RNAs species, including repetitive sequences and intronic regions.

Interestingly, loss of TDP-43 has also been shown to induce expression of specific repetitive elements. One example is the induction of *Alu* elements, a family of repetitive

elements that comprise ~11% of the human genome [113–116]. What impact these induced *Alus* have on cellular processes, however, have not been determined. In addition, loss of nuclear TDP-43 in post-mortem frontotemporal degeneration-amyotrophic sclerosis (FTD-ALS) human brain specimens results in chromatin decondensation [117]. Decondensation around long interspersed nuclear elements (LINEs) lead to increased LINE expression and retrotransposition, overall demonstrating that TDP-43 inhibits the expression of several repetitive elements that can form dsRNA structures.

Section IV Summary

TDP-43 is a highly conserved and ubiquitous RNA binding protein that facilitates numerous stages of RNA metabolism. Given the prominence of dsRNAs as activators of RLR-dependent interferon responses, I sought to investigate whether TDP-43 is required to prevent RLR activation due to endogenous RNAs. This thesis determines that loss of TDP-43 induces cytoplasmic immunostimulatory dsRNA accumulation, triggering a lethal RIG-I-dependent Type I and III IFN response. Collectively, this study describes a role for TDP-43 in preventing the accumulation of endogenous dsRNAs and uncovers an intricate relationship between the control of cellular gene expression and interferon-mediated cell death.

CHAPTER 1:

FUS negatively regulates Kaposi's Sarcoma-Associated Herpesvirus gene expression

Viruses **2018**, *10*, 359, doi: 10.3390/v10070359. PMCID: PMC6070805.

William Dunker[1†], Yu Song[1,2,†], Yang Zhao[1], John Karijolich[1,3,#]

[1] Department of Pathology, Microbiology, and Immunology, Vanderbilt University School of Medicine, Nashville, TN. 37232
[2] College of Pharmacy, Xinxiang Medical University, Xinxiang 453000, China.
[3] Vanderbilt-Ingram Cancer Center, Vanderbilt University Medical Center, Nashville, TN. 37232
[†] These authors contributed equally to this work.
[#] Corresponding author: john.karijolich@vanderbilt.edu

Abstract:

Kaposi's sarcoma-associated herpesvirus (KSHV) is a human gammaherpesvirus and the etiological agent of Kaposi's sarcoma. KSHV is also causally associated with the development of lymphoproliferative diseases, including primary effusion lymphoma (PEL). KSHV reactivation from latency plays an integral role in the progression to KSHV-associated disease as several lytic proteins have angiogenic and anti-apoptotic functions essential to the tumor microenvironment. Thus, restriction of KSHV reactivation represents an attractive therapeutic target. Here, I demonstrate that the cellular protein Fused-in-sarcoma (FUS) restricts KSHV lytic reactivation in PEL and in an epithelial cell-based model. Depletion of FUS significantly enhances viral mRNA and protein expression, resulting in increased viral replication and production of infectious virions.

Chromatin immunoprecipitation analyses demonstrates that FUS is present at several KSHV lytic cycle genes during the latent stage of infection. I further demonstrate that FUS interacts with RNA polymerase II and negatively affects Serine-2 phosphorylation of its C-terminal domain at the KSHV RTA gene, decreasing nascent RNA synthesis. Knockdown of FUS increases transcription of RTA, thus driving enhanced expression of KSHV lytic genes. Collectively, these data reveal a novel role for FUS in regulating viral gene expression and are the first to demonstrate its role as a viral restriction factor.

Keywords: KSHV; RTA; Viral Lytic Reactivation; FUS; RNA Polymerase II; Restriction Factor

Introduction:

Kaposi's sarcoma-associated herpesvirus (KSHV) is a double-stranded DNA herpesvirus and belongs to the gammaherpesvirus subfamily. KSHV is an AIDS-associated opportunistic pathogen and the etiological agent of Kaposi’s sarcoma (KS), a multicentric, angioproliferative spindle cell tumor that is the most prevalent cancer in untreated AIDs patients [118–121]. The virus is also linked to various B cell lymphoproliferative diseases, including primary effusion lymphoma (PEL) and multicentric Castleman's disease [122,123]. Similar to other herpesviruses, KSHV has two distinct phases of its lifecycle, latency and the lytic cycle. Latency is characterized by the persistence of an episome and expression of a limited number of viral genes [9]. In contrast, during viral reactivation, all viral genes are expressed, resulting in viral DNA replication and the production of infectious virions [124,125].

The latent to lytic transition is implicated in KSHV-associated disease progression, with both phases likely making unique contributions. For instance, latently expressed viral proteins have been shown to subvert cellular mechanisms which normally protect cells from aberrant proliferation, as is the case with latency-associated nuclear antigen (LANA), which can bind and inhibit tumor suppressors such as p53 and retinoblastoma protein [126,127]. Additionally, an anti-apoptotic transcriptional program is important for KSHV latency and the latent protein vFLIP has also been shown to activate the anti-apoptotic transcription factor NF-κB [128–131]. The importance of this gene expression program is highlighted by the essential nature of vFLIP for the survival of latent PEL cells [128]. While latent proteins have oncogenic properties, latency itself is not immortalizing, suggesting that lytic replication has a role. Consistent with this, clinical studies have shown the successful prevention as well as treatment of KSHV-associated malignancies with therapeutics that inhibit lytic replication [132–136]. It is now well appreciated that the presence of lytic cells is required for the production of angiogenic and anti-apoptotic viral products, which are essential to the tumor microenvironment [137–139].

The main driver of reactivation is the viral encoded replication and transcription activator (RTA/ORF50), which functions as a transcription factor and initiates expression of lytic cycle genes [140]. RTA is both necessary and sufficient to promote lytic gene expression [140,141]. Recombinant viruses that lack RTA, while capable of establishing latency, are unable to reactivate [142]. RTA is a sequence-specific transcriptional activator, consisting of an amino-terminal basic DNA-binding domain, a central leucine zipper motif, and a carboxy-terminal acidic activation domain [141]. RTA's amino-terminal DNA-binding domain is capable of directly binding RTA-responsive elements within viral

gene promoters with high affinity [143]. The amino-terminal domain and leucine zipper also promotes RTA's interaction with cellular proteins, including Oct-1, RBP-Jκ, and K-RBP, that aid in viral promoter specification and transactivation by RTA [144–148]. The carboxy-terminal acidic activation domain is also required for RTA-mediated lytic reactivation and binds to cellular SWI/SNF and TRAP/Mediator complexes [149]. Despite low sequence homology within the carboxyl transcriptional activation domain among RTA homologs of gammaherpesviruses, the RTA, SWI/SNF, and TRAP/Mediator interactions are conserved in herpesvirus saimiri and murine gammaherpesvirus 68, highlighting the importance of cellular proteins in gammaherpesvirus reactivation [149].

Given RTA's requirement for KSHV reactivation, it is perhaps not surprising that cellular proteins target RTA to prevent lytic replication. In fact, several proteins have been demonstrated to inhibit the transcriptional activation of RTA or limit RTA's ability to transactivate lytic promoters. For instance, ADP-ribosylation and phosphorylation of RTA by PARP-1 and hKFC, respectively, result in the suppression of its recruitment to RTA-regulated lytic promoters [150]. Additionally, cellular KAP-1 associates with RTA-dependent lytic promoters and represses their expression, and depletion of KAP-1 is sufficient to induce KSHV reactivation [151].

It is likely other unidentified proteins affect RTA-mediated KSHV reactivation. Indeed, the human genome encodes numerous proteins that influence the dynamics of cellular transcription, and some have been tangentially associated with antiviral processes. For example, the cellular protein Fused-in-sarcoma (FUS) is involved in cellular transcription, and has also been demonstrated to be a component of cytoplasmic stress granules, which are important components of the host anti-viral response [46,152–

154]. However, a role for FUS in the antiviral response has not been determined. Here, I demonstrate that FUS is a negative regulator of KSHV reactivation in PEL and in an epithelial cell-based model of KSHV infection. Loss of FUS leads to enhanced viral RNA and protein expression, resulting in an increase in the production of infectious virions. Chromatin immunoprecipitation (ChIP) analyses demonstrated that FUS is present at several KSHV loci, including RTA. Lytic reactivation promotes FUS eviction from many lytic cycle genes, however, FUS remains associated with RTA. Knockdown studies coupled with ChIP of RNA polymerase II (RNAP II) indicate that FUS negatively regulates phosphorylation on the C-terminal domain (CTD) of RNAP II at the RTA locus. Consistent with this, FUS knockdown increases RNAP II phosphorylation and increases nascent RNA expression of RTA, thus enhancing viral reactivation. These results demonstrate that FUS is an important cellular protein that negatively regulates viral gene expression and reveal a previously unknown antiviral role for FUS.

Materials and Methods:

Cells and Viruses.

iSLK.219 [155], iSLK.BAC16 [156], iSLK.Control [155], HEK293T (ATCC) were maintained in Dulbecco's modified Eagle medium (DMEM; Invitrogen) supplemented with 10% fetal bovine serum (FBS; Invitrogen). TREx-BCBL1-RTA [157] were grown in RPMI 1640 medium (Invitrogen) supplemented with 10% fetal bovine serum (FBS; Invitrogen) and 2 mM L-glutamine (Invitrogen). All cells were maintained with 100 U of penicillin/ml and 100 µg of streptomycin/ml (Invitrogen) at 37 °C under 5% CO_2. iSLK.219, iSLK.BAC16, iSLK.Control, and TREx-BCBL1-RTA cells were reactivated with 1 µg/ml of doxycycline (Fisher Scientific).

Sirna Knockdowns.

iSLK.219 cells were transfected at 60-80% confluency with 40 nM siRNA (FUS: 5' rCrGrGrArCrAUrGrGrCrCUrCrArArArCrGrAdTdT) or MISSION siRNA Universal Negative Control #1 (Sigma) using Lipofectamine RNAiMax (Invitrogen). 48 h post-transfection cells were reactivated as described above. siRNAs were microporated into TREx-BCBL1-RTA cells using the Neon transfection system (Invitrogen) at 1,600 v, 10 ms pulse width, and 3 pulses. 18 h post-microporation cells were reactivated as described above, with the addition of 100μM sodium butyrate (Sigma).

Genome Replication.

TREx-BCBL1-RTA cells were treated with FUS siRNA for 18 h, and reactivated with doxycycline and sodium butyrate for 48 h. The virus and cells were pelleted at 20,000 G for 2 h at 4ºC. Viral genomes were quantified by qPCR using serially diluted BAC16 as a standard curve.

Supernatant Transfer.

iSLK.219 cells were reactivated with doxycycline for 72 h, after which the supernatant was collected. The supernatant was added to HEK293T cells with 8 μg/ml of polybrene (Sigma) and spun at 1,000 rpm for 1 h at room temperature. Fresh media was then added and the cells were incubated for 48 h, followed by analysis.

Cloning, Lentiviral Production and Infection.

FUS was PCR amplified from pENTR4-FLAG FUS (Addgene) and Gateway cloned into pLenti-CMV-tight-blast-dest vector (Addgene).

Lentivirus was prepared in HEK293T cells. Cells were transfected at 50-60% confluency with recombinant FUS, psPAX2 (lentiviral packaging), and pMD2.G (lentiviral envelope) (Addgene) using polyjet (SignaGen). 72 h post-transfection the supernatant was collected, mixed with 8 µg/ml of polybrene, and iSLK.219 cells were spinfected as described above. Cells were selected for 2 weeks in media containing 5 µg/ml blasticidin (Invivogen).

Nucleic Acid Isolation and Measurement.

For analysis of gene expression by RT-qPCR, total RNA was isolated with TRIzol (Invitrogen) in accordance with the manufacturer's instructions. RNA was DNase I (NEB) treated at 37 °C for 20 minutes and inactivated with EDTA at 70 °C for 10 minutes. cDNA was synthesized from DNase-treated RNA with random 9-mer (Integrated DNA Technologies) and M-MLV RT (Promega). qPCR was performed using the PowerUp SYBR Green qPCR kit (Thermo Scientific) with appropriate primers.

4su. Labeling.

iSLK.219 cells were treated with 500 µM 4sU (Abcam) for 3 min prior to isolating RNA with TRIzol as described above. DNase-treated 4sU-containing RNA (50 µg) was incubated in biotinylation buffer (10 mM Tris [pH 7.4], 1 mM EDTA), and 5 µg MTSEA-biotin-XX (Biotium) with constant rotation in the dark at room temperature for 2 h. RNA was then phenol-chloroform extracted and precipitated with isopropanol. The pellet was resuspended in nuclease-free water and mixed with 50 µl Dynabeads MyOne streptavidin C1 (Invitrogen) that had been pre-washed twice with nuclease-free water. Samples were rotated in the dark for 1 h at RT with high salt buffer (100 mM Tris [pH 7.5], 10 mM EDTA, 1 M NaCl, 0.1% Tween 20), then washed 4X with high salt wash buffer. Samples were

eluted with fresh 5% β-mercaptoethanol, and the RNA was precipitated with ethanol prior to RT-qPCR.

Subcellular Fractionation and Western Blotting.

Subcellular fractionation was performed using the REAP method with the minor modification of using one 10-cm plate for each fractionation condition [158].

Cell lysates were prepared with lysis buffer (50 mM Tris [pH 7.6], 150 mM NaCl, 0.5% NP-40) and quantified by Bradford assay. Equivalent amounts of each sample were resolved by SDS-PAGE, electrotransferred to PVDF membrane, and blotted for the indicated proteins. Antibodies: FUS (Santa Cruz; diluted 1:5000), GAPDH (Invitrogen; diluted 1:5000), H3 (Millipore; diluted 1:1000), Hsp90 (Cell Signaling; diluted 1:1000), RNAPII (Millipore; 1:1000), Ser2 RNAPII (Abcam; diluted 1:1000), RTA (diluted 1:10,000), ORF57 (diluted 1:1000), and bZIP (diluted 1:2000). Primary antibodies were followed by AlexaFluor 680-conjugated anti-rabbit and anti-mouse secondary antibodies (Life Technologies; 1:5000) and visualized by Li-Cor Odyssey.

Immunoprecipitation (IP).

iSLK.219 cells were reactivated for the indicated time with doxycycline. Cells were washed in PBS, collected, and lysed in lysis buffer (50 mM Tris [pH 7.6], 150 mM NaCl, 0.5% NP-40, 10% glycerol). 3 μg of RNAP II antibody (8WG16, Millipore) or control IgG (Cell Signaling) were incubated with SureBeads Protein G magnetic beads (Bio-Rad) at room temperature for 10 minutes, then added to the cell lysate. IPs were performed overnight at 4 °C with gentle rotation. Beads were washed three times in lysis buffer, followed by elution in 1X Laemmli buffer at 70 °C for 10 minutes.

Phosphonoacetic Acid (PAA) Treatment.

iSLK.219 cells were transfected with FUS-siRNA (40 nM) at 60%–70% confluency. 38 h post-siRNA treatment cells were treated with phosphonoacetic acid (PAA) (Alfa Aesar; final concentration: 0.5mM). 4 h later, the cells were reactivated with doxycycline. Cells were harvested 24 and 48 h after induction, and viral gene expression was quantified by RT-qPCR.

Immunofluorescence Microscopy.

iSLK.BAC16 cells, cultured on glass coverslips, were fixed in 4% paraformaldehyde (Ted Pella) for 15 minutes, permeabilized in ice cold methanol for 1 h, blocked in blocking buffer (1% Triton X-100, 0.5% Tween-20, 3% BSA, 5% normal goat serum (Invitrogen)) for 30 minutes, and incubated in primary antibody overnight (FUS: diluted 1:250). Slides were incubated with Rhodamine red anti-mouse secondary antibody (Thermo Scientific; diluted 1:750). Cells were imaged with an Olympus FV1000 confocal microscope.

Chromatin Immunoprecipitation (ChIP).

ChIP was performed as described previously [159], with the following modifications: chromatin was sheared by using a tip sonicator (Fisher Scientific) for 25 rounds of 20 second pulses with 20 Amplitude and 40 second off. Chromatin was diluted in ChIP dilution buffer (0.01% [w/v] SDS, 1.1% [v/v] Triton X-100, 1.2 mM EDTA, 16.7 mM Tris-HCl pH 8.1, 167 mM NaCl). ChIP was performed overnight at 4 °C using 5 µg RNAP II antibody (8WG16, Millipore), FUS (J2516, Santa Cruz), Ser2 RNAPII (5095, Abcam), with Control IgG (Cell Signaling) and rotated overnight at 4 °C. DNA was isolated after crosslink reversal using a QIAGEN PCR clean up kit prior to qPCR.

Results:

FUS Knockdown Increases KSHV Lytic Gene Expression and Virion Production

FUS participates in the regulation of gene expression at multiple levels, including transcriptional regulation, and has also been implicated in B cell biology, the main latent reservoir of KSHV [46,152,153,160,161]. I hypothesized that given the extensive rewiring of gene expression during KSHV reactivation that FUS impacts the viral lytic phase. To test the role of FUS in KSHV B cell lytic reactivation I depleted FUS in TREx-BCBL1-RTA cells, a patient-derived PEL cell line harboring a doxycycline-inducible lytic transactivator RTA, using siRNA. 18 h post-siRNA transfection, cells were reactivated with doxycycline and sodium butyrate for 48 h. FUS-targeted siRNA reduced its levels by 93.5% compared to the nontarget-siRNA (Figure 1.1A). Using RT-qPCR, I quantified the expression of KSHV genes representing different viral kinetic classes. FUS depletion resulted in a significant increase in the steady state levels of several KSHV-encoded mRNAs as well as the long noncoding RNA PAN (Figure 1.1B). Furthermore, I verified that protein levels of RTA, bZIP, and ORF57 were increased in FUS-depleted cells relative to control lytic cells (Figure 1.1C). A small percentage of PEL cells undergo spontaneous lytic reactivation at steady state. To investigate the role of FUS in spontaneous lytic reactivation of PEL cells, I depleted FUS in TREx-BCBL1-RTA cells with siRNA and quantified lytic transcript abundance by RT-qPCR. Depletion of FUS promoted a minor increase in expression of three lytic genes, presumably in the population of PEL cells undergoing spontaneous lytic reactivation (Figure 1.1D). Given the increase in viral lytic gene expression, I predicted that knockdown of FUS would affect virion production. Virus was harvested from the supernatant and cell pellets of induced TREx-BCBL1-RTA cells

treated with control- or FUS-specific siRNA and quantified by qPCR. Indeed, knockdown of FUS resulted in a significant increase in viral genomes/mL increase in viral production (Figure 1.1E).

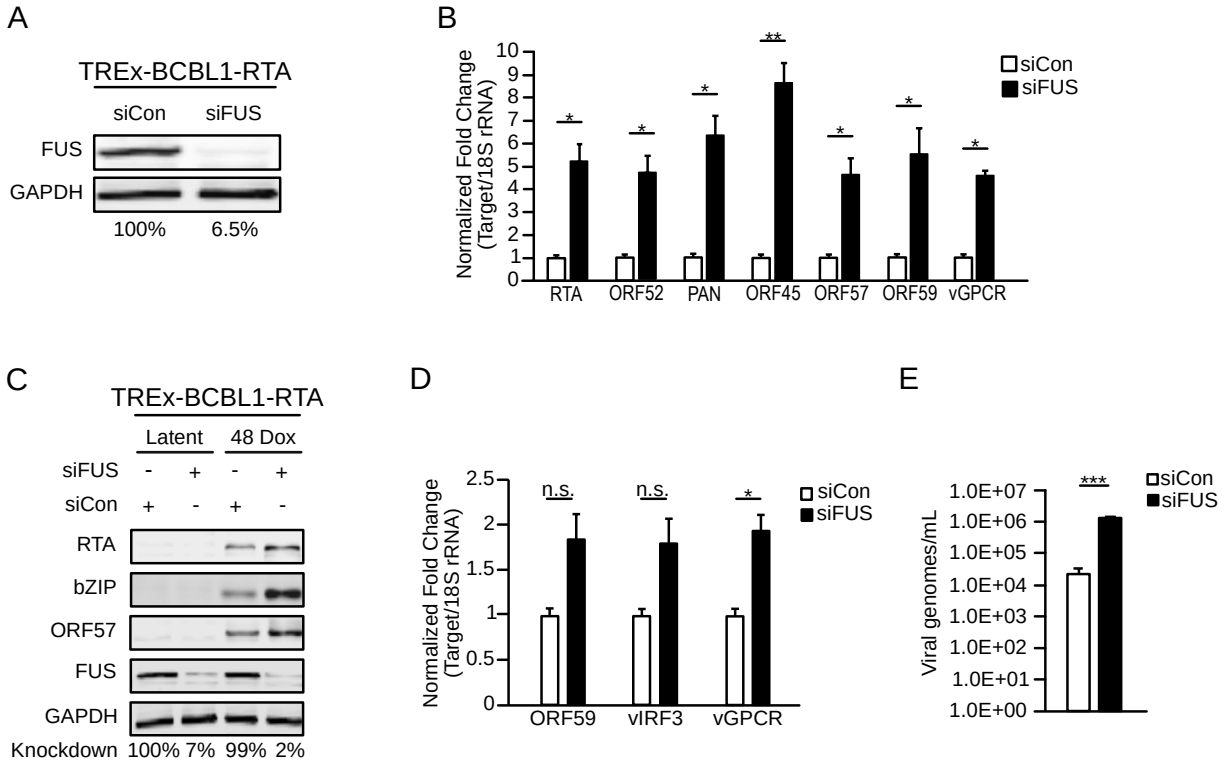

Figure 1.1: FUS represses KSHV reactivation in PEL cells. **(A)** Western blot analysis of FUS expression 48 h post reactivation in TREx-BCBL1-RTA cells treated with the indicated siRNAs. Knockdown efficiency is indicated beneath each lane. **(B)** RT-qPCR of viral transcripts from cells in (A). All samples were normalized to 18S and siCon levels set to 1. **(C)** Western blot of viral proteins from cells in (A). **(D)** TREx-BCBL1-RTA cells were transfected with the indicated siRNAs for 18 h prior to RNA isolation and RT-qPCR. All samples were normalized to 18S and siCon levels set to 1. **(E)** TREx-BCBL1-RTA cells were depleted of FUS for 18 h, followed by reactivation with doxycycline and sodium butyrate for 48 h. Virus and cells were centrifuged, total DNA isolated and subjected to qPCR with ORF52 primers. All samples were normalized to GAPDH, and siCon set to 1. Student t-test used to determine statistical significance *p≤ 0.05. **p≤ 0.005. ***p≤0.0005.

I also investigated the role of FUS in iSLK.219 cells. iSLKs are a clear-cell renal-cell carcinoma cell line (SLK) that stably maintains the KSHV.219 episome (iSLK.219) [155,162]. The recombinant KSHV.219 virus constitutively expresses green fluorescent protein (GFP) from the EF-1 alpha promoter and can be used as a proxy for the presence of KSHV within cells. The KSHV.219 virus also encodes red fluorescent protein (RFP) under the control of a viral lytic promoter. Similar to TREx-BCBL1-RTA cells, iSLK cells contain a doxycycline-inducible version of the lytic transactivator RTA. siRNA-depletion of FUS in iSLK.219 cells during latency and 48 h post-reactivation was efficient, reducing FUS levels by 91.5% and 94.9%, respectively (Figure 1.2A). 48 h post-reactivation GFP and RFP positive cells were analyzed by fluorescence microscopy in FUS- and control-siRNA-treated cells. FUS depletion resulted in a marked increase in the number of RFP positive cells, suggesting more efficient entry into the lytic cycle (Figure 1.2B). Using RT-qPCR I quantified the expression of nine lytic genes. All viral transcripts analyzed were expressed greater than 4-fold more in FUS-depleted cells relative to control-siRNA treated cells (Figure 1.2C). Additionally, protein levels of RTA, bZIP, and ORF57 were increased in FUS-depleted lytic iSLK.219 cells relative to control-siRNA treated cells (Figure 1.2D).

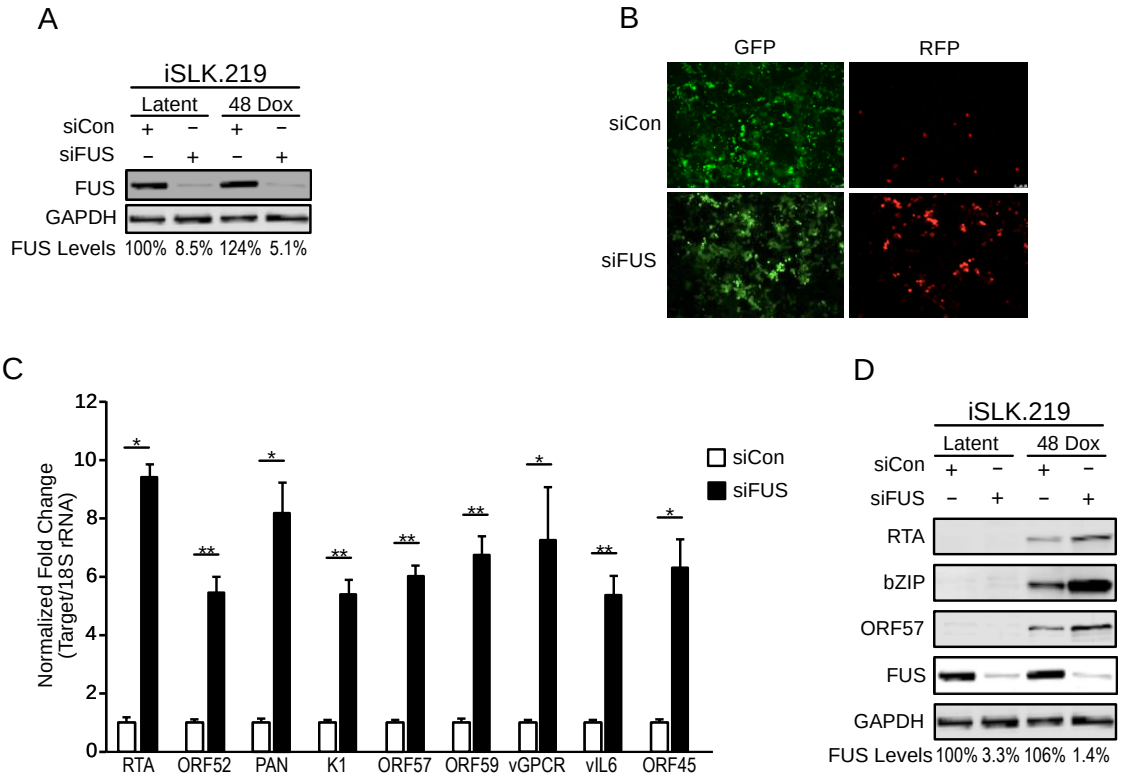

Figure 1.2: FUS represses KSHV reactivation in iSLK.219 cells. **(A)** iSLK.219 cells were treated with siRNA against FUS for 48 h, followed by doxycycline-induced reactivation of KSHV for 48 h. Knockdown efficiency in latency and 48 h post-reactivation was determined by western blot and is indicated beneath each lane. GAPDH was used as a loading control. **(B)** Fluorescent microscopy of iSLK.219 cells depleted of FUS by siRNA in (A). **(C)** RT-qPCR of viral transcripts from FUS-depleted iSLK.219 cells in (A). All samples were normalized to 18S and siCon levels set to 1. **(D)** Western blot of viral proteins from cells in (A). GAPDH was used as a loading control. Student t-test used to determine statistical significance *p≤ 0.05. **p≤ 0.005

To test whether the observed FUS phenotype was due to off-target effects of siRNA-mediated knockdown, I examined the effect of a second FUS-siRNA on KSHV reactivation. This second FUS- siRNA was highly effective, depleting levels of FUS to 0.75% relative to control-siRNA treated cells (Figure 1.3A). 48 h post-reactivation, cells depleted with the second FUS-siRNA exhibited greater RFP fluorescence than cells treated with control siRNA, suggesting more efficient lytic reactivation upon FUS depletion (Figure 1.3B). Indeed, RT-qPCR quantification of viral gene expression revealed

increased PAN, ORF57, ORF59, and vGPCR expression in FUS-depleted cells relative to control siRNA treatment (Figure 1.3C).

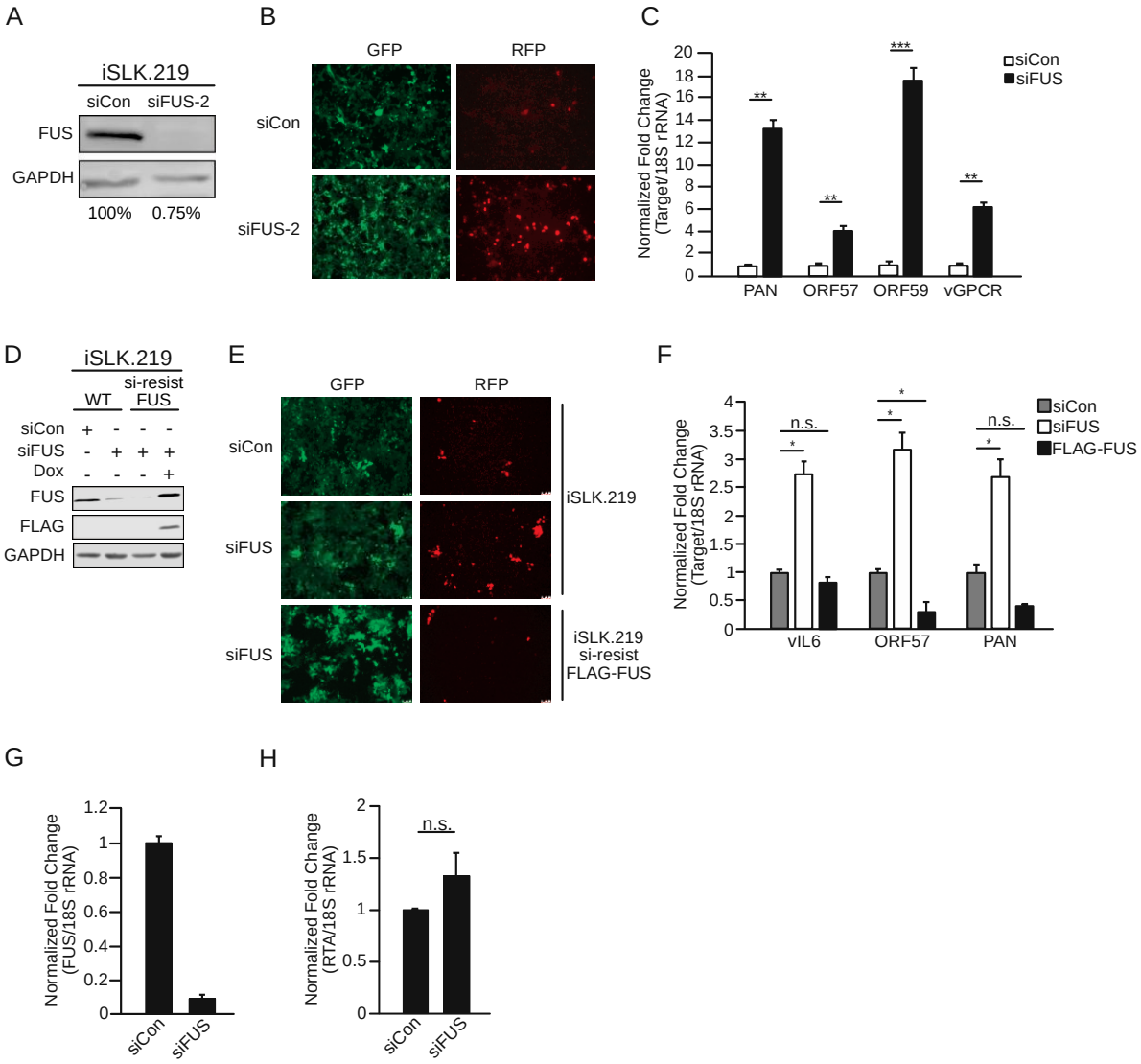

Figure 1.3: **Independent verification of FUS-siRNA specificity**. **(A)** iSLK.219 cells were depleted of FUS with a second FUS-siRNA and induced with doxycycline for 48 h. Knockdown efficiency was determined by western blot analysis and is indicated beneath each lane. **(B)** Fluorescent microscopy of iSLK.219 cells depleted of FUS in (A). **(C)** Quantification of viral gene expression in cells described in (A) by RT-qPCR. All samples were normalized to 18S and siCon set to 1. **(D)** Western blot analyses of protein extracts from WT iSLK.219 and iSLK.219 cells transduced with siRNA-resistant FLAG-tagged FUS. Cells were treated with either control or FUS-siRNA and induced for 48 h with doxycycline. **(E)** Fluorescent microscopy of cells in (D). **(F)** RT-qPCR of viral gene expression in cells described in (D). All samples were normalized to 18S and siCon set to 1. **(G)** Uninfected iSLK control cells, which harbor the doxycycline-inducible RTA, were depleted of FUS with siRNA for 48 h, followed by doxycycline treatment for 24 h. FUS knockdown was determined by RT-qPCR. **(H)** Quantification of RTA mRNA levels from cells in (G). Student t-test used to determine statistical significance *p≤ 0.05. **p≤ 0.005. ***p≤0.0005.

To further demonstrate specificity of the FUS siRNA, I used lentiviral transduction to establish iSLK.219 cells harboring doxycycline-inducible, FLAG-tagged siRNA-resistant FUS, and quantified the effect of FUS siRNA treatment on KSHV lytic reactivation. Western blot analysis demonstrated that while endogenous FUS was significantly depleted by FUS-siRNA, siRNA-resistant FLAG-tagged FUS was not (Figure 1.3D). Importantly, expression of siRNA-resistant FUS in iSLK.219 cells abrogated the increased viral reactivation and gene expression observed in WT iSLK.219 cells treated with siRNA targeting FUS (Figure 1.3E, F).

The RT-qPCR primers to quantify RTA expression are specific to KSHV encoded RTA, however, given that both TREx-BCBL1-RTA and iSLK.219 cells are reactivated by doxycycline-induced expression of RTA, I verified that FUS depletion did not influence the expression of the doxycycline-inducible RTA. To investigate this, I treated iSLK cells that do not contain KSHV with control or FUS-specific siRNA and quantified their effect on doxycycline-induced RTA expression. With 91% depletion of FUS, I did not observe a significant change in RTA expression (Figure 1.3G, H).

Having confirmed the specificity of the FUS-siRNA and the effect of its depletion on lytic gene expression, I next leveraged the fact that the KSHV.219 virus constitutively expresses GFP and quantified infectious virion production using a supernatant transfer assay. Following FUS- or control-siRNA treatment, iSLK.219 cells were reactivated for 72 h, whereupon supernatants were collected and used to infect HEK293T cells (Figure 1.4A). Infection of HEK293T cells using supernatants from iSLK.219 cells treated with FUS-specific siRNA resulted in a 4-fold increase in GFP-positive cells compared to supernatants from control-siRNA treated cells (Figure 1.4B). Additionally, I quantified the

expression of the latent viral transcript LANA by RT-qPCR. Consistent with the number of GFP-positive cells, significantly more LANA was expressed in HEK293T cells infected with virions from FUS-siRNA treated iSLK.219 cells compared to control-siRNA treated cells (Figure 1.4C). Collectively, these results establish that FUS restricts KSHV reactivation and production of infectious virions in both PEL and iSLK.219 cells. This is the first demonstration of an antiviral role for FUS.

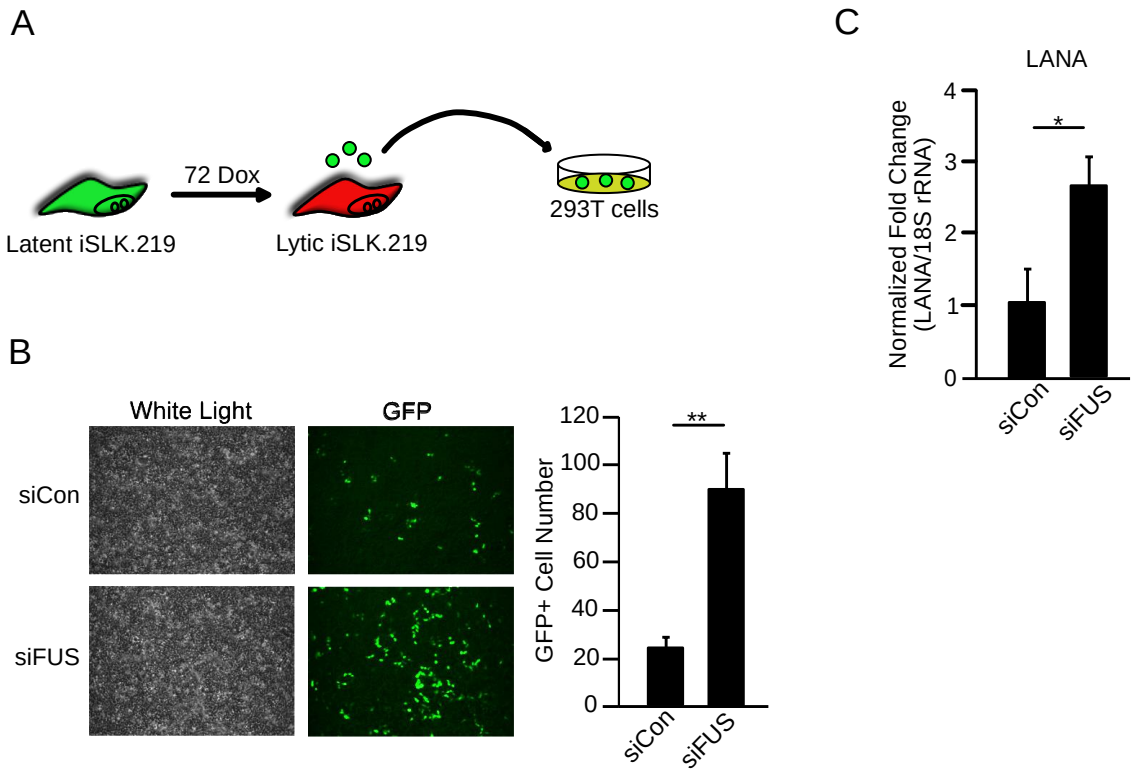

Figure 1.4: FUS restricts KSHV virion production in iSLK.219 cells. (A) Schematic of supernatant transfer. **(B)** KSHV-infected HEK293T cells following supernatant transfer from FUS-depleted iSLK.219. GFP-positive cells were infected with the virus. Quantification of GFP-positive cells is to the right. Values represent four independent views of the infected cells. **(C)** LANA mRNA levels from HEK293T cells in (B). Student t-test used to determine statistical significance *p≤ 0.05. **p≤ 0.005.

FUS Depletion Enhances KSHV Gene Expression Prior to Viral DNA Replication

We next sought to determine at which stage of lytic reactivation FUS affects KSHV gene expression. Herpesvirus gene expression occurs in a transcriptional cascade, wherein immediate-early genes are first transcribed, followed by early gene expression and viral DNA replication, and then late gene expression (Figure 1.5A). To determine where in the transcriptional cascade FUS affects viral gene expression, FUS- and control-siRNA treated iSLK.219 cells were treated with the viral DNA polymerase inhibitor phosphonoacetic acid (PAA), and viral early and late gene expression was quantified following reactivation. PAA treatment resulted in a significant decrease in the expression of the KSHV late gene ORF52, consistent with the dependency of late gene expression on viral replication (Figure 1.5A, B). Viral gene expression was significantly increased in FUS-siRNA treated cells compared to control-siRNA treated cells, and PAA treatment did not reduce the effect of FUS-siRNA (Figure 1.5C). These results indicate FUS restricts KSHV reactivation early during reactivation, prior to viral DNA replication and independent of late gene expression.

FUS is Nuclear Localized throughout KSHV Viral Reactivation

The early effect of FUS on KSHV reactivation led me to hypothesize that FUS regulates the early transcriptional dynamics on the KSHV genome. However, FUS is a nucleocytoplasmic shuttling protein and can reside in either the cytoplasm or nucleus depending on the cellular state, and stress has been shown to promote its cytoplasmic relocalization [154,163]. Thus, I monitored FUS localization in TREx-BCBL1-RTA cells during latency and lytic reactivation by subcellular fractionation. Western blot analyses

demonstrated that FUS predominantly localized to the nucleus in both latency and 48 h post-lytic reactivation (Figure 1.6A).

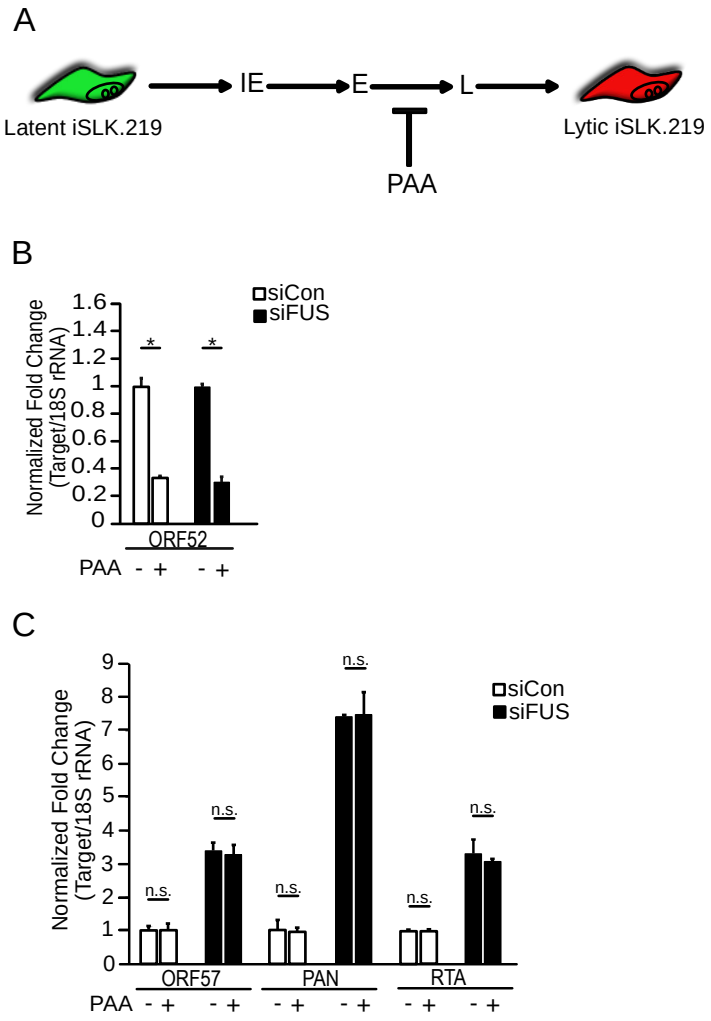

Figure 1.5: FUS restricts viral reactivation prior to DNA replication. **(A)** Schematic of the herpesviral gene expression cascade. Phosphonoacetic acid (PAA) treatment blocks viral DNA replication, thereby blocking late viral gene expression. **(B)** Total RNA isolated from iSLK.219 cells reactivated for 48 h and transfected with either siCon or siFUS and treated with PAA, was subjected to RT-qPCR to monitor expression of ORF52. All samples were normalized to 18S. The non-PAA treated samples for both siCon and siFUS were normalized to 1 and compared to the PAA treated samples. **(C)** RT-qPCR of ORF57, PAN, and RTA viral genes from iSLK.219 cells treated with same conditions as (B) and collected at 24 h post reactivation. All samples were normalized to 18S. For each condition and gene, siCon was set to 1. Student t-test used to determine statistical significance *p<0.05.

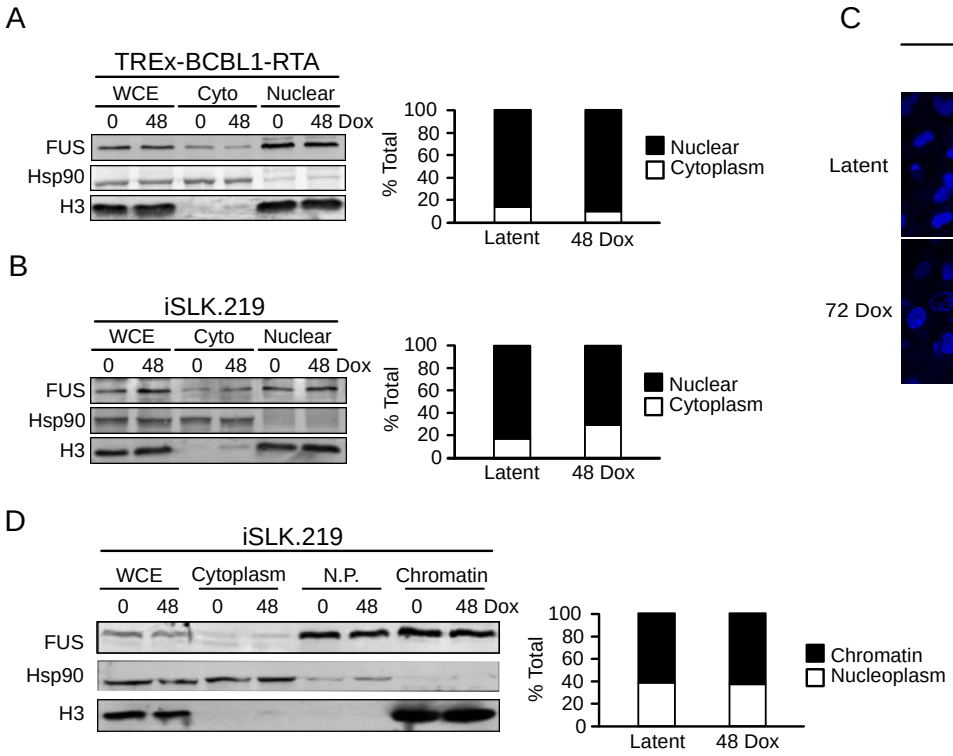

Figure 1.6: FUS is predominately nuclear in KSHV-infected cells. **(A)** TREx-BCBL1-RTA cells were fractionated at latency and 48 h post-reactivation. WCE: Whole Cell Extract. Cyto: Cytoplasm. Hsp90 is a cytoplasmic control, H3 is a nuclear control. Quantification is to the right of the western blot. **(B)** Fractionation of iSLK.219 cells. **(C)** IF of iSLK.BAC16 cells at latency and 72 h post-reactivation. DAPI is a nuclear marker. **(D)** Chromatin fractionation of iSLK.219 cells at latency and 48 h post-reactivation. WCE: whole cell extract. N.P.: nucleoplasm. Hsp90 is a cytoplasmic control, H3 a nuclear control. Quantification is to the right of the Western blot.

I also monitored FUS localization in iSLK.219 cells in both latency and lytic reactivation. Similar to TREx-BCBL1-RTA cells, FUS was predominately nuclear, and no cytoplasmic redistribution was detected upon lytic reactivation (Figure 1.6B). FUS localization was also determined in iSLK.BAC16 cells by immunofluorescence (IF) microscopy, which confirmed my biochemical fractionation data indicating a nuclear residence (Figure 1.6C). These cells are similar to iSLK.219 cells, however they do not express RFP upon lytic reactivation. Within the nucleus FUS has been demonstrated to associate with chromatin, thus I further fractionated the iSLK.219 nuclear fractions into

soluble nucleoplasm and chromatin-bound fractions [46,152,153,161]. Western blot analyses demonstrated that approximately 60% of FUS fractionated with chromatin in both latency and the lytic cycle (Figure 1.6D). Collectively, these results demonstrate that FUS is nuclear localized in KSHV infected cells and its subcellular localization is not altered upon lytic reactivation.

FUS Affects RNA Polymerase II CTD Phosphorylation and Nascent RNA Transcription

Prompted by the presence of FUS in the chromatin fraction, we tested whether FUS is present on the viral genome. We performed ChIP on FUS in both latent and 48 h post-reactivation lytic iSLK.219 cells and quantified its levels at select viral genes. FUS was present at several loci, including RTA, ORF57, PAN, and vIL6 in latent cells (Figure 1.7A). Interestingly, during lytic reactivation, the levels of FUS decreased at ORF57 and PAN, while quantitatively it was not significantly altered at the RTA and vIL6 loci. However, the decrease at vIL6 was trending towards significance.

RNAP II transcription is regulated by a dynamic cycle of post-translational modifications, including phosphorylation of the C-terminal domain (CTD) [164]. Interestingly, FUS has been demonstrated to interact with RNAP II and prevent Serine (Ser)2 CTD phosphorylation, a mark associated with elongation, at select cellular genes [152,153]. The recruitment of FUS to the RTA locus prior to reactivation, coupled with its maintenance during reactivation, could allow FUS to interact with RNAP II and influence Ser2 phosphorylation and thus RTA expression. To test this hypothesis, I first examined the interaction between FUS and RNAP II in latent and reactivated iSLK.219 cells by immunoprecipitation and western blotting. I observed a robust interaction in nuclear extracts between FUS and RNAP II, confirming that this interaction can occur in the

context of KSHV latency and lytic reactivation (Figure 1.7B). Next, we monitored the presence of Ser2 phosphorylated RNAP II on the viral genome by ChIP. The levels of Ser2 phosphorylated RNAP II were normalized to the total levels of RNAP II. We observed that Ser2 phosphorylation was increased at the RTA locus, as well as at ORF57, PAN, and vIL6 in FUS-siRNA treated cells relative to control-siRNA treated cells (Figure 1.7C). Furthermore, consistent with the ChIP data, I observed a significant increase in nascent RNA synthesis of RTA, PAN, ORF57, and vIL6 in FUS-depleted cells relative to control-siRNA treated cells by 4-thiouridine (4sU) pulse labeling and purification coupled to RT-qPCR (Figure 1.7D, E). Quantification of the housekeeping gene GAPDH from purified 4sU-labeled RNA showed no change in nascent RNA synthesis (Figure 1.7E). Collectively, these results are consistent with a mechanism whereby FUS recruitment and maintenance at the RTA locus reduces its expression, thus restricting KSHV reactivation.

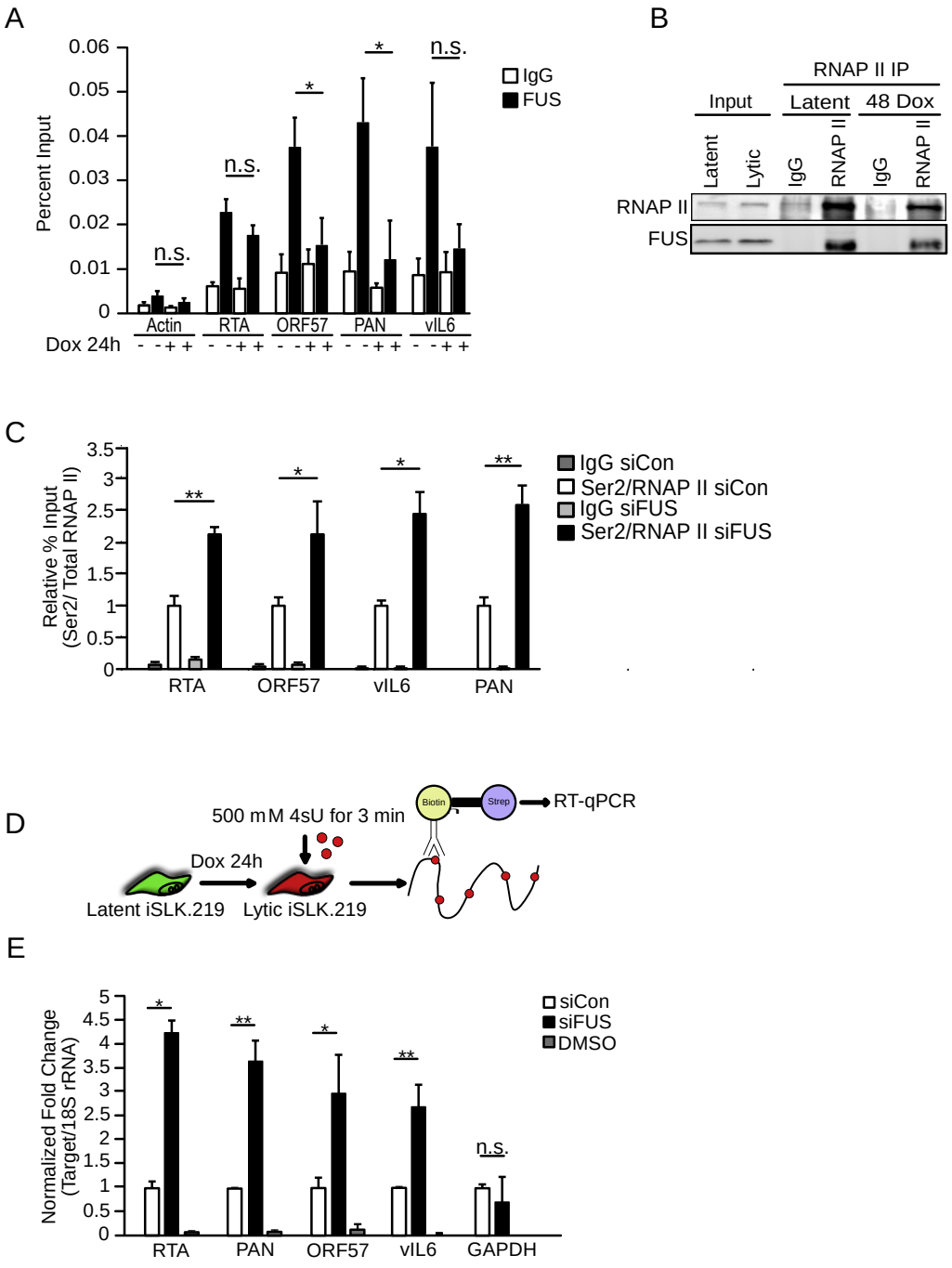

Figure 1.7: FUS regulates RTA nascent RNA expression. **(A)** FUS occupancy of the indicated viral genes was analyzed by ChIP in iSLK.219 cells 24 h post-reactivation. IgG was used as a negative control. **(B)** Western blot of RNAP II immunoprecipitation (IP) from iSLK.219 cells at latency and 48 h post-reactivation. **(C)** Ser2 RNAP II occupancy was determined at the indicated viral genes by ChIP 48 h post-reactivation in iSLK.219 cells treated with either siCon or siFUS. Ser2 levels were normalized to total RNAP II present at each genomic loci as determined by ChIP. siCon ratio set at 1. **(D)** Schematic representation of the assay employed to measure nascent RNA synthesis. **(E)** RT-qPCR of nascent viral and host transcripts. Values were normalized to 18S. DMSO was added in place of 4sU as a negative control. Student t-test used to determine statistical significance *p≤ 0.05. **p≤ 0.005.

Discussion:

Reactivation from latency is necessary for the continual seeding of new infected cells, transmission of the virus to other individuals, and progression to KSHV-associated disease. As such, preventing or limiting lytic reactivation represents an attractive target for cellular restriction factors. Here, I demonstrate that the cellular protein FUS limits KSHV lytic reactivation in PEL and iSLK.219 cells. Although stress can promote nucleocytoplasmic shuttling of FUS, in the context of lytic reactivation, FUS remains predominately nuclear with a significant portion associated with chromatin [154,163]. FUS has previously been shown to interact with RNAP II and regulate CTD phosphorylation, and our immunoprecipitation and ChIP analyses suggests that FUS interacts with RNAP II and reduces Ser2 CTD phosphorylation at the RTA locus [152,153]. Consistent with FUS negatively affecting Ser2 CTD phosphorylation, siRNA-mediated knockdown of FUS robustly stimulates RTA nascent RNA production. These data put forth a model whereby FUS regulates RNAP II elongation at the RTA locus, and thus inhibits expression of the KSHV major lytic transactivator. This study is the first to demonstrate an antiviral role for FUS and establish that it imposes a restriction on KSHV reactivation at the level of viral gene transcription.

Myself and others have demonstrated that nuclear FUS is able to regulate gene transcription [152,161,165]. While recruitment of FUS to the genome can occur through interactions with the CTD of RNAP II, how FUS is recruited to the viral episome during latency is unclear. However, FUS does have the ability to directly bind nucleic acids, including both single-stranded and double-stranded DNA and RNA, and these interactions could facilitate FUS occupancy on the KSHV genome [166]. If FUS

recruitment was mediated via RNA, this could occur through either cis- or trans mechanisms. In cis, overlapping transcription of latent and lytic genes could provide the necessary RNAs, while in trans the RNA can be derived from either the cellular or viral genome. Investigations into how FUS is recruited to viral DNA are underway and should reveal novel insight into its newly described antiviral function.

Previously, work from Schwartz et al. identified a role for FUS in regulating Ser2 CTD phosphorylation [152]. Ser2 phosphorylation can be catalyzed by multiple kinases, including the positive transcription elongation factor b (P-TEFb), CDK12, and dual-specificity tyrosine-regulated kinase (DYRK1A), and *in vitro* FUS directly inhibits the ability of P-TEFb to phosphorylate GST-CTD [152,167–169]. The mechanism by which FUS limits Ser2 CTD phosphorylation on the viral genome has not been elucidated. However, P-TEFb has been demonstrated to be present on the viral genome, and thus FUS inhibition of Ser2 CTD phosphorylation at viral genes may occur through P-TEFb inhibition, as proposed for select cellular genes [170]. Interestingly, Tsai et al. demonstrated that RTA is a target of CDK9, a kinase within the P-TEFb complex, and this phosphorylation is important for RTA-mediated transactivation [171]. Whether FUS also affects RTA-mediated transactivation via preventing P-TEFb mediated phosphorylation of RTA is worth pursuing.

FUS is an important regulator of B cell development and activation, and considering B cells are the main reservoir of KSHV latency, it will be interesting to determine how KSHV infection impacts the role of FUS in these processes [160]. Furthermore, mutations in FUS are associated with a range of diseases including cancer and ALS. In the case of ALS, FUS mutations have been described that promote its

relocalization to the cytoplasm [172]. My work demonstrates that FUS restricts KSHV lytic reactivation within the nucleus at the level of viral transcription. Thus, I would predict KSHV reactivation would be significantly enhanced within cells harboring FUS mutations associated with ALS.

Beyond KSHV, this study raises the question of whether FUS restricts other viral pathogens. Epstein-Barr virus (EBV) is a closely related gammaherpesvirus and shares a similar tropism and lifecycle to KSHV. Whether FUS interacts with the latent EBV episome to regulate gene expression will be interesting to investigate. Similarly, other members of the Herpesviridae family establish latency as an episome. It is intriguing to speculate that FUS may function as a general restriction factor for this class of viruses. Collectively, this work has identified the cellular protein FUS as a novel KSHV restriction factor negatively regulating viral gene transcription.

CHAPTER 2:

TDP-43 prevents endogenous RNAs from triggering a lethal RIG-I-dependent interferon response

Cell Reports **2021**, *35(2)*, 108976, doi: 10.1016/j.celrep.2021.108976.

William Dunker [1], Xiang Ye [1], Yang Zhao [1], Lanxi Liu [1], Antiana Richardson [1], John Karijolich [1,2,3,4,5*]

[1] Department of Pathology, Microbiology, and Immunology, Vanderbilt University Medical Center, Nashville, TN 37232-2363, USA, [2] Department of Biochemistry, Vanderbilt University School of Medicine, Nashville, TN 37232-2363, [3] Vanderbilt-Ingram Cancer Center, Nashville, TN 37232-2363, USA, [4] Vanderbilt Institute for Infection, Immunology and Inflammation, Nashville, TN 37232-2363, USA. [5] Vanderbilt Center for Immunobiology, Nashville, TN 37232-2363, USA. *Corresponding author: John.karijolich@vanderbilt.edu;

Abstract:

RIG-I-like receptors (RLRs) are involved in the discrimination of self vs non-self via the recognition of dsRNA. Emerging evidence suggests that immunostimulatory dsRNAs are ubiquitously expressed yet they are disrupted or sequestered by cellular RNA binding proteins (RBPs). TDP-43 is an RBP associated with multiple neurological disorders and is essential for cell viability. Here, I demonstrate that TDP-43 regulates the accumulation of immunostimulatory dsRNA. The immunostimulatory RNA was identified as RNA Polymerase III transcripts, including 7SL and *Alu* retrotransposons, and I demonstrate that the RNA binding activity of TDP-43 is required to prevent immune stimulation. The dsRNAs activate a RIG-I-dependent interferon response which promotes necroptosis.

Genetic inactivation of the RLR-pathway rescues the interferon-mediated cell-death associated with loss of TDP-43. Collectively, this study describes a role for TDP-43 in preventing the accumulation of endogenous immunostimulatory dsRNAs and uncovers an intricate relationship between the control of cellular gene expression and IFN-mediated cell-death.

Keywords: TDP-43, double-stranded RNA, RIG-I-like receptors, RNA binding protein, necroptosis, gene expression

Introduction:

The regulation of innate immune double-stranded RNA (dsRNA) sensors is paramount for initiating a robust antimicrobial gene expression response as well as preventing an aberrant immune response to endogenous dsRNA. The primary cell intrinsic dsRNA sensors include the RIG-I-like Receptors (RLRs), Toll-like receptor 3 (TLR3), protein kinase R (PKR), and the 2'-5'-oligoadenylate synthetase (OAS) proteins [173–177]. Activation of these receptors induces an antimicrobial gene expression response including the production of interferon (IFN) and other proinflammatory cytokines.

The RLR family members retinoic acid-inducible gene I (RIG-I) and melanoma differentiation-associated protein 5 (MDA5) recognize distinct structural and chemical moieties of RNAs. For example, RIG-I preferentially recognizes short (<1000 bp) 5'-triphosphorylated (5'ppp) blunt dsRNAs, although it can also recognize 5'ppp single-stranded RNA (ssRNA) and circular RNAs at a lower affinity [60–66]. Conversely, MDA5 binds long (>1000bp) dsRNA independent of 5'-end phosphorylation status [61,68].

Activation of either receptor drives their association with the adapter protein mitochondrial antiviral-signaling protein (MAVS). Signaling through MAVS promotes the activation and nuclear translocation of the transcription factor complexes interferon regulatory factor (IRF) and nuclear factor kappa-light-chain-enhancer of activated B cells (NF-κB) resulting in the expression of IFNs and cytokines [176,177].

Immunostimulatory dsRNAs are generally not present within the host transcriptome as their presence would activate an interferon gene expression response potentially resulting in lethality. To circumvent their production cells employ a diverse collection of incompletely understood mechanisms. Recent studies have identified RNA binding proteins (RBPs) that regulate essential junctions of RNA biogenesis whose deletion results in dsRNA sensor activation. For example, depletion of heterogenous ribonucleoprotein (hnRNP) C, which regulates pre-mRNA splicing through the binding of proximal *Alu* elements, results in RIG-I-dependent cell death due to the generation of dsRNA hairpins formed between inverted *Alu* repeats [70–72]. Additionally, adenosine deaminase RNA specific (ADAR) enzymes recognize and deaminate adenosine to inosine within dsRNA generating imperfect dsRNA structures, and loss of this activity results in RLR-dependent sensing of endogenous dsRNA [73–78]. These connections between RBPs and RLR-dependent innate responses hint towards a deep connection between the proper control of gene expression and cell-intrinsic immune mechanisms.

TAR-DNA binding protein 43 (TDP-43) is an RNA binding protein that participates in multiple steps of RNA metabolism including transcription, splicing and transport of mRNA, as well as microRNA metabolism [101–103,106,109,110,178]. The misregulation of RNA processing has been described in a growing number of neurological diseases and

TDP-43 is implicated in amyotrophic lateral sclerosis (ALS) and frontotemporal lobar dementia (FTLD) [35,87]. However, the mechanisms by which TDP-43 contributes to disease are not completely understood.

Many of the TDP-43 associated functions involve dsRNA structures, whether as products or as intermediates. Along this line, previous work has demonstrated that loss of the TDP-43 homologue, TDP-1, in *Caenorhabditis elegans,* as well as siRNA depletion of TDP-43 in HeLa and M17 neuroblastoma cells results in dsRNA accumulation [111,112]. However, the physiological relevance of these dsRNAs is unknown. Given the prominence of dsRNAs as activators of RLR-dependent interferon responses I sought to investigate whether TDP-43 is required to prevent the activation of an RLR response to endogenous RNAs. Here, I demonstrate that loss of TDP-43 induces cytoplasmic immunostimulatory dsRNA accumulation, triggering a RIG-I-dependent Type I and III IFN response. RIG-I activation is driven in part by the upregulation and mislocalization of TDP-43 bound RNA polymerase III (RNAPIII) transcribed noncoding RNAs, including *Alu* retrotransposons. Moreover, I demonstrate that cell death associated with loss of TDP-43 can be prevented by CRISPR/Cas9 knockout (KO) of either the RLR-pathway or the type I IFN receptor IFNAR1. IFN signaling induces expression of the pore-forming protein Mixed Lineage Kinase Domain Like Pseudokinase (MLKL) leading to cell death, thus uncovering a previously undescribed link between RBP-mediated control of gene expression and necroptosis. Collectively, this study describes a role for TDP-43 in preventing the accumulation of endogenous immunostimulatory dsRNAs and uncovers an intricate relationship between the control of cellular gene expression and IFN-mediated cell death.

Methods and Materials:

Cell Culture

786-O (ATCC), HEK293T (ATCC), and iSLK.BAC16 [179] were maintained in Dulbecco's modified Eagle medium (DMEM; Invitrogen) supplemented with 10% fetal bovine serum (FBS; Invitrogen). SH-SY5Y (ATCC) were grown in 50:50 DMEM: Ham's F-12 nutrient mixture (Invitrogen) medium supplemented with 10% fetal bovine serum (FBS; Invitrogen). All cells were maintained with 100 U of penicillin/ml and 100 μg of streptomycin/ml (Invitrogen) at 37 °C under 5% CO_2.

Viruses.

KSHV virions were isolated from iSLK.BAC16 cells that were reactivated with 1 μg/ml of doxycycline (Fisher Scientific) for 120 h by pelleting virus at 20,000 G for 2 h at 4ºC. KSHV virions were resuspended in PBS.

siRNA Knockdown.

SH-SY5Y and 786-O cells were transfected at 60-80% confluency with 50 nM siRNA or MISSION siRNA Universal Negative Control #1 (Sigma) using Lipofectamine RNAiMax (Invitrogen). 48 h post-transfection cells were collected.

Immunofluorescence Microscopy.

SH-SY5Y cells, cultured on poly-L-lysine treated glass coverslip, were transfected at 60-80% confluency with siRNAs for 48 h. Cells were fixed in 4% paraformaldehyde, permeabilized in 0.25% Triton-X, blocked in blocking buffer (3% BSA, 5% Normal Goat Serum (Thermo), 0.1% Tween) and incubated in primary antibody (TDP-43: 1:400; J2: 1:100). Slides were incubated with Rhodamine red anti-mouse and Cyanine 5 anti-rabbit

secondary antibodies (Thermo Scientific; diluted 1:750) and were mounted in mounting media (Thermo). Cells were imaged with an Olympus FV1000 confocal microscope.

J2 Immunoprecipitation (IP).

SH-SY5Y cells were transfected with siRNAs for 48 h. Cells were washed in PBS and RNA was isolated by TRIzol (Invitrogen) in accordance with the manufacturer's instructions. RNA was DNase I (NEB) treated at 37 °C for 20 minutes and inactivated with EDTA at 70 °C for 10 minutes followed by phenol chloroform extraction. 15 μg of RNA was incubated with 2 μg of J2 antibody (Scicons) or control IgG (Cell Signaling) in binding buffer (50 mM Tris [pH 8.0], 150 mM NaCl, 1mM EDTA, 1% NP-40, 5mM MgCl2) with Ribo-lock (Thermo) at 4°C overnight. IPs were incubated with SureBeads Protein G magnetic beads (Bio-rad) at 4°C for 4 h, washed five times in binding buffer, and RNA was eluted in TRIzol. J2-isolated RNA was either Mock or CIAP (Promega)-treated at 37 °C for 1 h, followed by PCA extraction. 100 ng of RNA was transfected into 786-O cells at 60-80% confluency with Lipofectamine RNAiMax. 24 h post-transfection cells were collected and analyzed by RT-qPCR.

Nucleic Acid Isolation and Measurement.

For analysis of gene expression by RT-qPCR, total RNA was isolated with TRIzol (Invitrogen) in accordance with the manufacturer's instructions. RNA was DNase I (NEB) treated at 37 °C for 20 minutes and inactivated with EDTA at 70 °C for 10 minutes. cDNA was synthesized from DNase-treated RNA with random 9-mer (Integrated DNA Technologies) and M-MLV RT (Promega). qPCR was performed using the PowerUp SYBR Green qPCR kit (Thermo Scientific) with appropriate primers.

Subcellular Fractionation and Western Blotting.

Subcellular fractionation was performed using the REAP method with the minor modification of using one 10-cm plate for each fractionation condition [180].

Cell lysates were prepared with lysis buffer (50 mM Tris [pH 7.6], 150 mM NaCl, 0.5% NP-40) and quantified by Bradford assay. Equivalent amounts of each sample were resolved by SDS-PAGE, electrotransferred to PVDF membrane, and blotted for the indicated proteins (Table S1). Primary antibodies were followed by AlexaFluor 680-or -800 conjugated anti-rabbit and anti-mouse secondary antibodies (Life Technologies; 1:5000) and visualized by Li-Cor Odyssey.

KSHV Infection.

SH-SY5Y and 786-O cells were treated with siRNA for 48 h prior to infection. KSHV virions were added to the media and supplemented with 2% polyethylene glycol (PEG(VWR)) and 8 μg/ml of polybrene (Sigma). Cells were spun at 1,000 rpm for 30 min at room temperature. Fresh media was then added, and the cells were incubated for 24 h, followed by analysis by RT-qPCR.

CRISPR/Cas9 Cloning, Lentiviral Production, and Infection.

Single-guide RNAs (sgRNAs) were selected by inputting gene sequences into the Broad Institute GPP sgRNA CRISPR KO Designer. Two high-score sgRNAs were selected for each gene. sgRNA oligos were cloned into the lentiCRISPR V2 (Addgene) lentiviral plasmid according to depositor instructions.

Lentivirus was prepared in HEK293T cells. Cells were transfected at 50-60% confluency with lentiCRISPR V2, psPAX2 (lentiviral packaging), and pMD2.G (lentiviral envelope) (Addgene) using polyjet (SignaGen). 72 h post-transfection the supernatant was

collected, mixed with 8 μg/ml of polybrene and 1% PEG, and added to SH-SY5Y, 786-O, or HEK293T cells that were spinfected at 1,000 rpm for 1 h at room temperature. Cells were selected for 2 weeks in media containing either 300 μg/ml hygromycin B (Invitrogen; rtTA doxycycline-inducible element), 5 μg/ml blasticidin (Invivogen; inducible RIG-I), or 5 μg/ml puromycin (Sigma; lentiCRISPR V2 knockouts).

Knockout Generation.

Cells were infected with lentivirus. Following puromycin selection, single cell clones were grown out in 48-well plates. The knockout was verified by Western blot of the respective protein. CRISPR/Cas9 induced mutations were identified by isolation of genomic DNA (Promega), PCR of the genomic region where the guide RNA targets, TOPO cloning, and Sanger sequencing of the PCR product (Mutations listed in Table 2.1). For select knockouts, 100 ng/ml of the RIG-I ligand 3p-hpRNA (Invivogen) was transfected into cells for 6 h, followed by RNA isolation and RT-qPCR. For IFNAR1 knockouts, recombinant IFN α and β were added to cells for 8 h, followed by RNA isolation and RT-qPCR.

Cloning and Cell Line Generation.

RIG-I pLenti-CMVtight-FL-HA-DEST-Blast [28] underwent site-directed mutagenesis (SDM) to mutate the RIG-I sgRNA recognition sequence to prevent CRISPR/Cas9 cleavage. Lentivirus was produced and used to transduce SH-SY5Y and 786-O RIG-I knockout cells followed by antibiotic selection. Cells were then transduced with lentiviral particles produced from pLenti CMV rtTA3 Hygro (Addgene) to create a Tet-On inducible system, followed by antibiotic selection.

DUSP11 was PCR amplified from SH-SY5Y mRNA and Gateway cloned into the pLenti-CMV-tight-blast-dest vector. MLKL was PCR amplified from MLKL pF-TRE3G-PGK-puro (generously provided by Dr. James Murphy [181]) and Gateway cloned into pLenti-CMV-tight-blast-dest vector. HEK293T, 786-O, and SH-SY5Y cells were transduced with lentiviral particles produced from pLenti CMV rtTA3 Hygro (Addgene) to create a Tet-On inducible system, followed by antibiotic selection. RIG-I, DUSP11, and MLKL lentivirus was then produced and used to transduce either HEK293T rtTA3 cells (RIG-I), or 786-O and SH-SY5Y rtTA3 cells (DUSP11, MLKL) followed by antibiotic selection. FLAG-TDP-43 pcDNA3 WT and mutRRM (with W113A/R151A mutations) plasmids were generously provided by Dr. J. Paul Taylor [182].

RNA Sequencing.

SH-SY5Y RIG-I complement cells were treated with siRNA for 48 h. Doxycycline was added to induce RIG-I expression for the final 24 h. Total RNA was isolated using TRIzol, DNase treated, and rRNA depleted (NEB). RNA sequencing libraries were generated using the Collibri Stranded RNA library prep kit (Thermo) according to the manufacture recommendations. Libraries were then subjected to paired-end sequencing on a NovaSeq 6000 at the Vanderbilt Technologies for Advanced Genomics (VANTAGE). Data are submitted in SRA and will be available upon publication.

RNA Sequencing Data Analysis.

Raw read quality was assessed using FastQC (v0.11.5). STAR (v2.7.3a) was used to align reads to the human genome (GRCh38). The transcript quantification was done using featureCounts using the pair-end mode to count both reads that uniquely mapped. Differentially expressed genes were called using edgeR (v2.26.5) with Benjamini-

Hochberg adjusted p-value < 0.01 and log2FoldChange > 2. R package clusterProfiler (v3.12.0) was used for the gene set over-representation analysis with the KEGG database. K-means clustering was applied to gene expression values (normalized by count per million) using R function kmeans (from R package stats) and the number of clusters was determined by total within sum of square. Heatmaps were generated using pheatmap (v1.0.12). For making IGV figures, the bam files were first transformed into bigwig file with a bin size of 10bp and normalized by CPM (count per million). Then the bigwig files were loaded into IGV viewer to view the read distribution on target genes.

Northern Blot.

SH-SY5Y RIG-I complement cells were treated with siRNA for 48 h. Doxycycline was added to induce RIG-I expression for the final 24 h. Total RNA was isolated using TRIzol followed by 1h DNase treatment and PCA extraction. 25 μg of RNA was mixed with loading buffer (Formamide, bromophenol blue, xylene cyanol, EDTA), denatured at 90°C for 2min, loaded on a 10% TBE-urea gel, and run at 20W for ~2 h. RNA was transferred onto nylon membrane in TBE buffer at 4°C overnight followed by twice crosslinking at 254 nm. The membrane was incubated with the hybridization buffer (1M sodium phosphate [pH 6.5], 20X SSC, 50X Denhardts, 20% SDS) at 42°C for 1h, replaced with fresh hybridization buffer, and supplemented with 10% PEG. Labeled probes were added to the buffer and incubated at 42°C overnight. The membrane was washed 3X in wash buffer (0.5X SSC, 0.1%SDS) followed by exposure on a film. The film was developed on the Typhoon FLA 7000 (GE Healthcare).

Endogenous TDP-43 Immunoprecipitation.

SH-SY5Y cells were washed twice in cold PBS, crosslinked with 0.5% formaldehyde for 10 min in PBS, quenched with 0.3M glycine for 5min, and washed twice with cold PBS. Cells were resuspended in RIP buffer (150 mM KCl, 25mM Tris [pH 7.4], 5mM EDTA, 0.5mM DTT, 0.5% NP-40) and kept on ice for 20min followed by sonication. Protein G beads (Biorad) were washed in RIP buffer, followed by the addition of 2.5 μg of IgG (Thermo) or TDP-43 antibody (Proteintech) and incubated at room temp for 30min. Excess antibody was removed. Soluble cell extract was added to bead-antibody complex and incubated at 4°C for 3 h. Beads were washed three times for 10 min with RIP buffer followed by DNAse treatment. Protein-RNA crosslinks were reversed by adding reverse crosslink buffer (100 mM Tris [pH 8], 10mM EDTA, 1% SDS, 0.5% DTT) to samples and heated at 70°C for 45 min. RNA was recovered by TRIzol extraction followed by isopropanol precipitation and RT-qPCR analysis. Protein was recovered in 300mM glycine [pH 2.5] at RT for 15 min and analyzed by Western blot.

RIG-I RNA Immunoprecipitation.

SH-SY5Y RIG-I complement cells were treated with siRNA for 48 h. Doxycycline was added to induce RIG-I expression for the final 24 h. Cells were washed twice in cold PBS, crosslinked with 0.5% formaldehyde for 10 min in PBS, quenched with 0.3M glycine for 5min, and washed twice with cold PBS. Cells were resuspended in RIPA buffer (50mM Tris [pH 8.0], 0.5% sodium deoxycholate, 0.05% SDS, 1mM EDTA, 150mM NaCl, 1mM DTT, 1% NP-40) and kept on ice for 20min followed by sonication. Anti-Flag M2 magnetic resin (Sigma) was washed in RIPA buffer followed by the addition of soluble extract and incubation at 4°C for 3 h. Beads were washed three times for 10 min at 4°C and then two

times for 5 min at room temperature in RIPA buffer with 0.1%SDS, 1M NaCl, and 1M urea. Resin was eluted with 1X FLAG peptide (Sigma) in RIPA buffer for 45 min at 4°C. Crosslinks were reversed by adding 100 mM Tris [pH 8], 10mM EDTA, 1% SDS and 2% DTT to samples and heated at 70°C for 45 min. RNA was recovered by TRIzol extraction, isopropanol precipitation, DNase treatment, PCA extraction, and ethanol precipitation. Bound RNAs were analyzed by RT-qPCR.

Cell Viability Assays.

SH-SY5Y and 786-O cells were treated with siRNAs for 120 h and 96 h, respectively. Trypan Blue: Cells were trypsinized (Gibco) and diluted 1:1 with trypan blue stain. The mixture was incubated for 1 min, followed by counting by Cell Countess II. CellTiter-Glo: Cells were equilibrated at room temperature for ~30 min. An equal volume of CellTiter-Glo reagent (Promega) was added to wells, mixed and lysed for 2 min, incubated for 10 min, and luminescence was read.

Small Molecular Inhibitor Treatment.

Cells were treated with 100 μM RNAPIII inhibitor CAS 577784-91-9 (Millipore) or vehicle at the same time as siRNA treatment. Cells were collected 24 h post transfection followed by RT-qPCR analysis.

RNA Decay.

SH-SY5Y: Cells were transfected with siCON/siTDP-43 for 48h. 100 μM RNAPIII inhibitor was added after 48h and cells were collected at indicated time points. RNA was isolated and followed by RT-qPCR analysis. HEK293T TDP-43 KO: Cells were transfected with pcDNA3, WT TDP-43, or TDP-43 RRM for 24h. 100 μM RNAPIII inhibitor was added and

cells were collected at indicated time points. RNA was isolated and followed by RT-qPCR analysis.

Results:

Loss of TDP-43 is associated with the accumulation of immunostimulatory dsRNA

Knockdown of TDP-43 in HeLa and M17 neuroblastoma cells results in dsRNA accumulation [111,112]. However, their impact on cellular homeostasis has yet to be determined. Given that dsRNA can serve as a potent activator of a cell intrinsic interferon response I hypothesized that loss of TDP-43 would result in the accumulation of immunostimulatory dsRNA. To test this, I depleted TDP-43 using siRNA in the SH-SY5Y neuroblastoma cell line and analyzed dsRNA accumulation 48 h post knockdown by immunofluorescence (IF) microscopy using the J2 dsRNA-specific antibody. The J2 antibody is commonly used to visualize and isolate dsRNA as it recognizes RNA helices equal or greater than 40 bp in a sequence-independent manner [183]. Poly(I:C), a synthetic analog of dsRNA, was transfected as a positive control. Consistent with previous results in HeLa and M17 cells, TDP-43 depletion in SH-SY5Y cells resulted in dsRNA accumulation when compared to the nontarget-siRNA (siCON) treated cells (Figure 2.1A). The J2-postive dsRNA was only observed in the cytoplasm.

To determine whether the dsRNA is immunostimulatory I performed J2 or control IgG immunoprecipitations (IPs) on total RNA extracted from cells treated with either siCON or siTDP-43 and transfected the immunopurified RNAs into a reporter cell line followed by quantification of IFN β mRNA levels by RT-qPCR (Figure 2.1B, C). While transfections of RNA purified by the control IgG did not induce IFN β regardless of siRNA

treatment, J2-purified RNAs from siTDP-43-treated cells resulted in a significant increase in IFN β expression when compared to siCON-treated cells (Figure 2.1C). Additionally, removal of 5' phosphate structures by phosphatase (CIAP)-treatment prevented IFN β induction.

Given that the J2 IP enriched immunostimulatory dsRNA I next sought to determine whether depletion of TDP-43 resulted in the induction of an interferon gene expression response. SH-SY5Y cells were treated with siCON or siTDP-43 for 48 h prior to RNA extraction and quantification of interferon expression (Figure 2.1D, E). As a positive control I transfected poly(I:C). TDP-43 depletion resulted in expression of the type I interferon, IFN β, and the type III interferons, IFN λ1 and 2/3 (Figure 2.1E). In contrast, the type I interferon, IFN α, and type II interferon, IFN γ, were not induced. These results mirror the IFN expression profile upon poly(I:C) transfection. To further assess the effects of TDP-43 depletion on gene expression I quantified the expression of several interferon stimulated genes (ISGs) as well as downstream targets of NF-κB. TDP-43 knockdown induced expression of several ISGs (Figure 2.1F). Interestingly, while poly(I:C) induced the expression of multiple NF-κB targets, knockdown of TDP-43 did not (Figure 2.1G).

I next sought to investigate whether the interferon response associated with loss of TDP-43 was neuronal specific or also observed in cell lines derived from other tissue. To test this, 786-O clear cell renal cell carcinoma (ccRCC) cells were transfected with siCON or siTDP-43 and the interferon gene expression response was quantified by RT-qPCR. Importantly, I observed that loss of TDP-43 induced an IFN and ISG expression profile identical to that observed in SH-SY5Y cells (Figure S2.1A-D). Collectively, these

results demonstrate that loss of TDP-43 results in the accumulation of dsRNA that activates an interferon gene expression response.

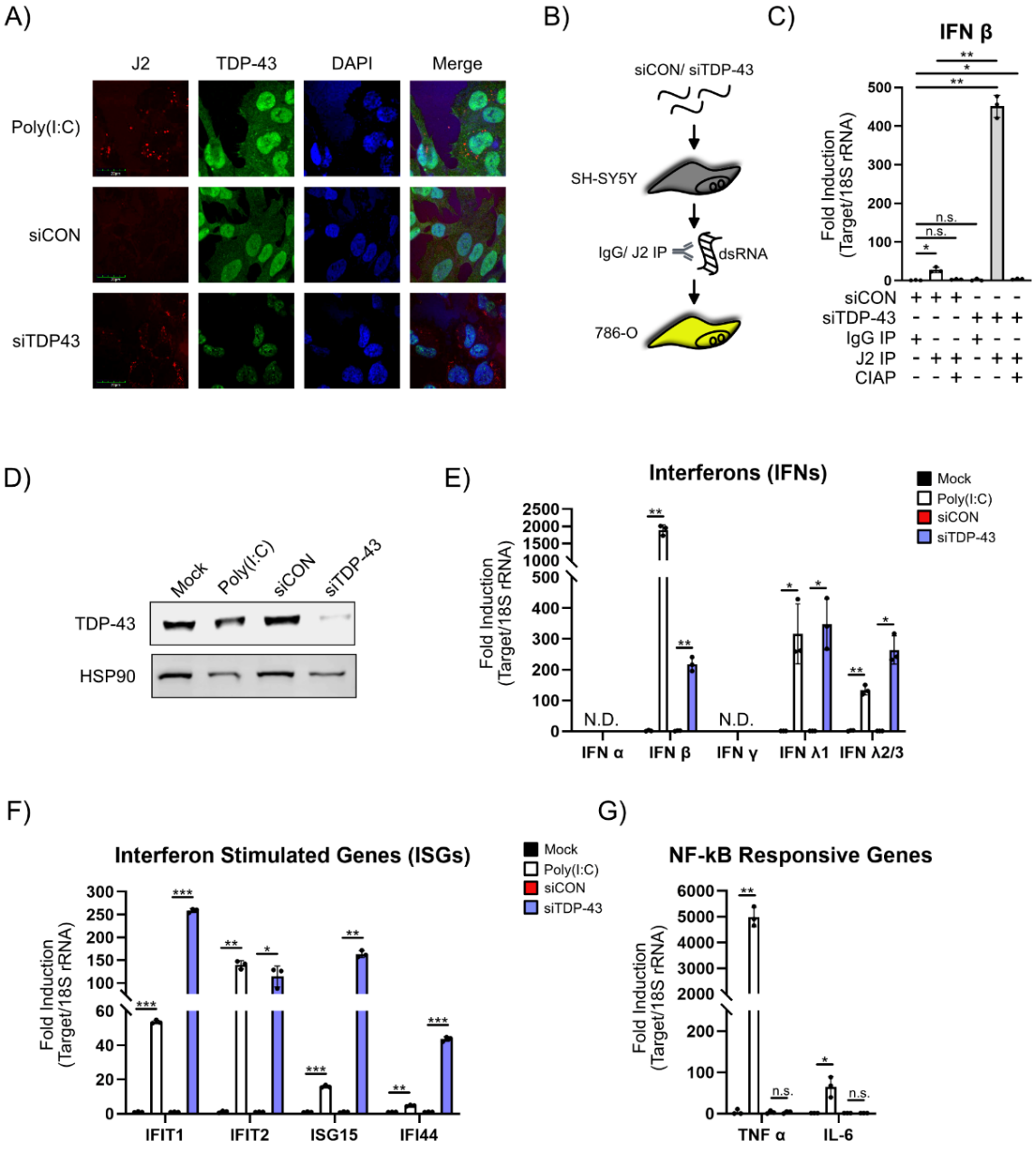

Figure 2.1: **TDP-43 depletion induces cytoplasmic immunostimulatory dsRNA accumulation and a Type I and III interferon response. (A)** Immunofluorescence microscopy of SH-SY5Y cells treated with siCON/siTDP-43 for 48 h. Poly(I:C) was transfected as a dsRNA positive control. Scale bars: 20 μm. **(B)** Schematic of IgG/J2 immunoprecipitation (IP) from siCON/siTDP-43-treated SH-SY5Y cells followed by transfection into 786-O cells. **(C)** RT-qPCR analysis of IFN β levels from 786-O cells transfected with IgG/J2 IP'd dsRNA for 24h. J2-purified RNA was either Mock or CIAP treated prior to transfection. siCON IgG was set to 1. **(D)** Western blot analysis of SH-SY5Y cells treated with siCON/siTDP-43 for 48 h. **(E, F, G)** RT-qPCR analysis of interferons (IFNs) (E), interferon stimulated genes (ISGs) (F), and NF-kB responsive genes (G) from cells in D. All samples were normalized to 18S rRNA and Mock/siCON levels were set to 1. Student t test was used to determine statistical significance * $p \leq 0.05$; ** $p \leq 0.005$; *** $p \leq 0.0005$; ns: not significant.

TDP-43 knockdown activates a RIG-I-dependent immune response

To test whether the interferon response was dependent on RLR signaling I generated CRISPR/Cas9 knockouts (KO) of the essential RLR components MAVS, RIG-I, and MDA5 in the SH-SY5Y cell line (Figure 2.2A-C). Full-length (FL) and truncated (mini) MAVS isoforms can regulate an immune response thus guide RNAs were designed to target both isoforms [184,185]. Western blot analysis confirmed knockout of both FL and mini-MAVS (Figure 2.2B). RIG-I and MDA5 are interferon-inducible proteins thus depletion of TDP-43 induced their expression in WT cells but not in the knockout cell lines (Figure 2.2C). I further validated the KOs by identifying the CRISPR/Cas9 induced mutations by Sanger sequencing of the genomic loci from single cell clones (Table 2.1).

To investigate the interferon response, I treated the WT and KO cells with siCON or siTDP-43 for 48 h and quantified IFN and ISG gene expression by RT-qPCR (Figure 2.2D, E). While siTDP-43 resulted in robust IFN and ISG expression in WT and MDA5 KO cells their expression was completely abrogated in both MAVS and RIG-I KOs (Figure 2.2D, E). These results suggest that TDP-43 depletion induces a RIG-I-dependent IFN response.

To rule out potential off-target effects of the RIG-I sgRNA I complemented the RIG-I KO with a doxycycline (DOX)-inducible guide RNA-resistant FLAG-tagged RIG-I and evaluated the IFN response in cells transfected with siCON or siTDP-43 (Figure 2.2F, G). Western blot analysis confirmed that DOX treatment resulted in FLAG-RIG-I expression (Figure 2.2F). Consistent with a requirement for RIG-I in sensing the accumulated dsRNA, IFN β expression was only observed in cells treated with DOX and siTDP-43 (Figure 2.2G). To determine whether RIG-I was similarly required for the IFN response in 786-O cells I generated MAVS, RIG-I, and MDA5 KO cells and quantified IFN and ISG expression by RT-qPCR in siCON and siTDP-43 treated 786-O cells. Consistent with results obtained in the SH-SY5Y cells, IFN and ISG expression was only observed in WT and MDA5 cells (Figure S2.2A-G).

I further investigated the impact of dsRNA accumulation in HEK293T cells as they do not express RIG-I. To test the dependency of the interferon response on RIG-I in HEK293T cells I generated cells harboring a DOX-inducible FLAG-RIG-I. Culturing of HEK293T cells harboring the DOX-inducible RIG-I transgene, iRIG-I cells, revealed leaky RIG-I expression (Figure 2.2H). RIG-I ligand transfection demonstrated that WT HEK293T cells do not mount an interferon response while leaky RIG-I expression in iRIG-I cells was sufficient for IFN β induction (Figure 2.2I). WT and iRIG-I cells were then treated with siCON or siTDP-43 for 48 h and IFN β expression was quantified by RT-qPCR (Figure 2.2J). Consistent with a role for RIG-I sensing the accumulated dsRNA, IFN β was only observed in siTDP-43 treated iRIG-I cells. Collectively, these results demonstrate that loss of TDP-43 activates a RIG-I dependent interferon response.

Lastly, to determine whether the IFN expression resulted in a functional antiviral response I treated SH-SY5Y and 786-O cells with siCON or siTDP-43 for 48 h followed by infection with Kaposi's sarcoma-associated herpesvirus (KSHV), an oncogenic DNA herpesvirus [186] The abundance of the KSHV transcript LANA was used to quantify infection. Loss of TDP-43 significantly reduced LANA levels compared to siCON-treated cells (Figure S2.3A, B). Importantly, TDP-43 depletion in the MAVS KO cell lines did not reduce LANA abundance, demonstrating that it is an antiviral interferon response and not TDP-43 regulating KSHV infection.

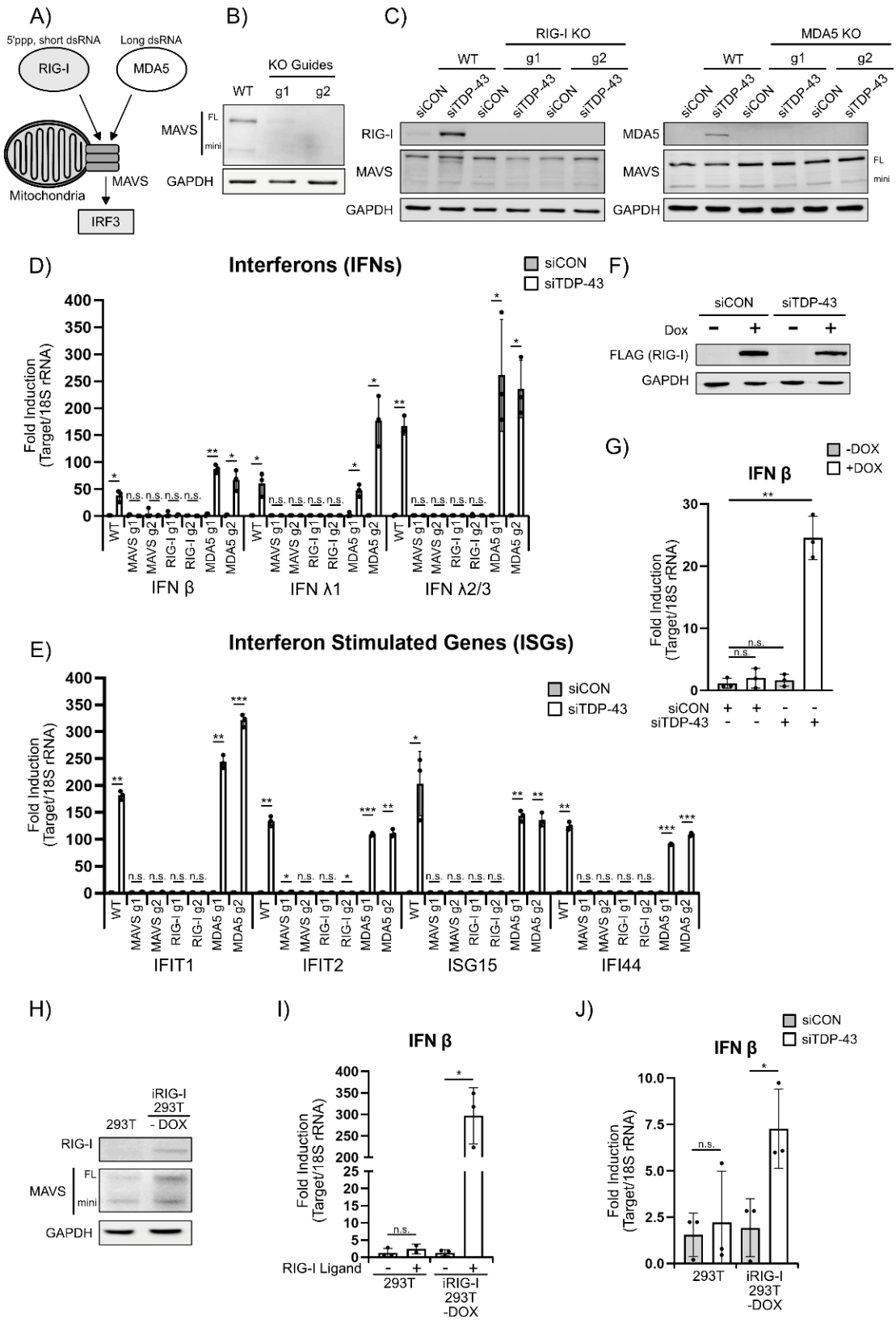
A)
5'ppp, short dsRNA
Long dsRNA
RIG-I
MDA5
MAVS
Mitochondria
IRF3
B)
KO Guides
WT
g1
g2
MAVS
FL
mini
GAPDH
C)
RIG-I KO
MDA5 KO
WT
g1
g2
siCON
siTDP-43
RIG-I
MDA5
MAVS
GAPDH
D)
Interferons (IFNs)
siCON
siTDP-43
Fold Induction (Target/18S rRNA)
WT
MAVS g1
MAVS g2
RIG-I g1
RIG-I g2
MDA5 g1
MDA5 g2
IFN β
IFN λ1
IFN λ2/3
n.s.
F)
siCON
siTDP-43
Dox
FLAG (RIG-I)
GAPDH
G)
-DOX
+DOX
IFN β
Fold Induction (Target/18S rRNA)
siCON
siTDP-43
E)
Interferon Stimulated Genes (ISGs)
IFIT1
IFIT2
ISG15
IFI44
H)
293T
iRIG-I 293T - DOX
RIG-I
MAVS
FL
mini
GAPDH
I)
IFN β
Fold Induction (Target/18S rRNA)
RIG-I Ligand
293T
iRIG-I 293T -DOX
J)
siCON
siTDP-43
IFN β
Fold Induction (Target/18S rRNA)
293T
iRIG-I 293T -DOX

Figure 2.2: TDP-43 knockdown activates a RIG-I and MAVS-dependent interferon response. (A) Schematic of RIG-I-like Receptor (RLR) signaling pathway. **(B)** Western blot analysis of SH-SY5Y MAVS knockout (KO) cells. Two independent guide RNAs are shown, and full length (FL) and mini-MAVS (mini) are depicted. **(C)** Western blot analysis of SH-SY5Y RIG-I and MDA5 KO cells. Cells were treated with siCON/siTDP-43 for 48h. **(D, E)** RT-qPCR analysis of IFNs (D) and ISGs (E) following siCON/siTDP-43 treatment for 48h. **(F)** Western blot analysis of SH-SY5Y RIG-I KO cells complemented with DOX-inducible FLAG-tagged RIG-I. Cells were treated with siCON/siTDP-43 for 48h and DOX for final 24h. **(G)** RT-qPCR analysis of IFN β levels from cells in F. **(H)** Western blot analysis of HEK293T and DOX-inducible RIG-I (iRIG-I) HEK293T cells. **(I)** RT-qPCR analysis of IFN β levels following RIG-I ligand transfection into cells in H for 6h. **(J)** RT-qPCR analysis of IFN β levels following siCON/siTDP-43 treatment of HEK293T and iRIG-I HEK293T cells for 48h. All samples were normalized to 18S rRNA and siCON/ Mock levels were set to 1. Student t test was used to determine statistical significance * $p \leq 0.05$; ** $p \leq 0.005$; *** $p \leq 0.0005$; ns: not significant.

IRF3 is required for the IFN and ISG response observed in TDP-43 depleted cells

RIG-I activation of an interferon response canonically proceeds through the adapter protein MAVS which further recruits and activates the transcription factor interferon regulatory factor 3 (IRF3). I generated a 15bp in frame deletion of IRF3 in SH-SY5Y cells that prevents it from activating IFN expression following transfection of a RIG-I ligand (Figure 2.3A, B; Table 2.1). To investigate the role of IRF3 I transfected WT or truncated IRF3 SH-SY5Y cells with siCON or siTDP-43 and quantified IFN and ISG expression by RT-qPCR. While TDP-43 depletion in WT cells resulted in a robust IFN and ISG response, inactivation of IRF3 completely prevented IFN and ISG expression (Figure 2.3C, D). Moreover, I generated an IRF3 KO in 786-O cells and observed a similar requirement for IRF3 in the IFN and ISG response (Figure S2.4A-E). Collectively, these data demonstrate that the loss of TDP-43 activates a RIG-I, MAVS, and IRF3-dependent type I and III IFN response.

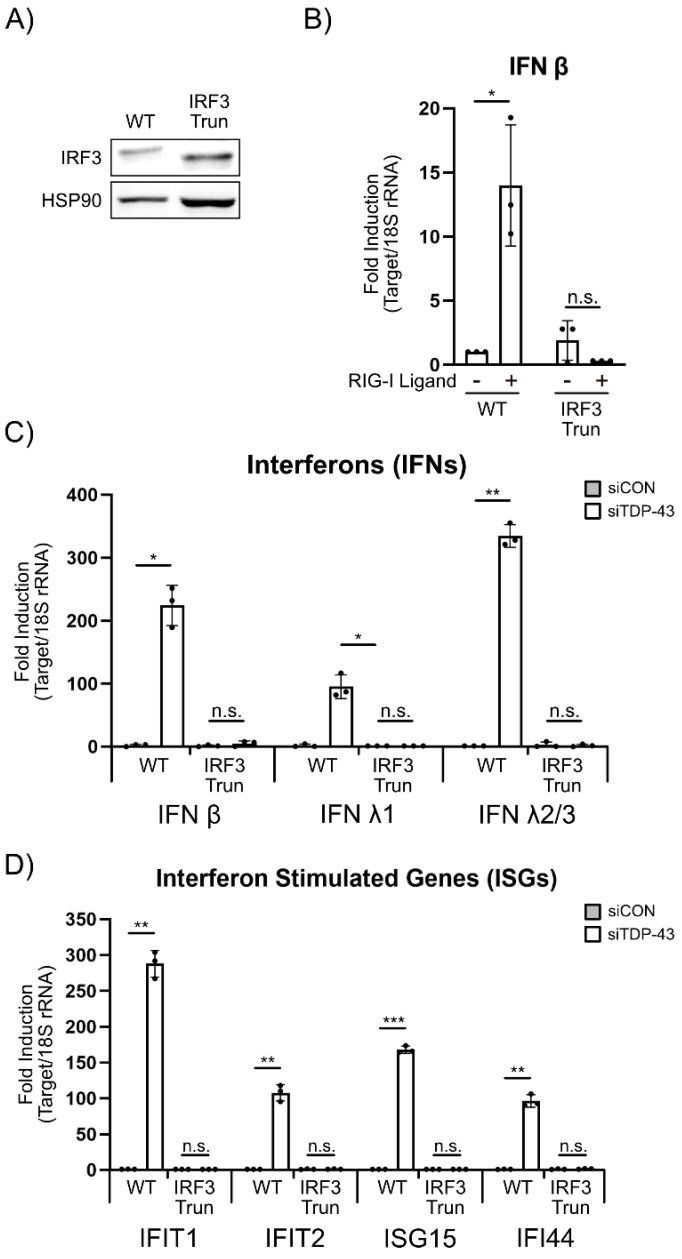

Figure 2.3: IRF3 is responsible for the TDP-43 depletion-induced interferon response. (A) Western blot analysis of truncated IRF3 (IRF3 trun) cells. **(B)** RT-qPCR analysis of IFN β levels following RIG-I ligand transfection for 6h. **(C, D)** RT-qPCR analysis of IFNs (C) and ISGs (D) levels following siCON/siTDP-43 treatment for 48h. All samples were normalized to 18S rRNA and Mock/ siCON levels were set to 1. Student t test was used to determine statistical significance * $p \leq 0.05$; ** $p \leq 0.005$; *** $p \leq 0.0005$; ns: not significant.

TDP-43 knockdown increases the levels of multiple RNAPIII RNAs

I next sought to determine how loss of TDP-43 affects cellular gene expression. Leveraging RNA-sequencing we defined the transcriptome of FLAG-RIG-I complemented RIG-I KO SH-SY5Y cells treated with either siCON or siTDP-43 (Figure 2.4A). Differential gene expression analysis revealed two distinct clusters of up- and down-regulated genes (Figure 2.4B). While multiple ontological terms are present within these clusters, many of the most significant terms present among the upregulated genes are involved in RNA Polymerase III (RNAPIII) transcription. RNAPIII transcribes housekeeping noncoding RNAs such as tRNAs and a variety of small non-coding RNAs, including 7SK snRNA (RN7SK), 7SL RNA (RN7SL), and *Alu* retrotransposons, which are in the short interspersed repetitive elements (SINEs) class of retrotransposons [187]. Aberrant expression of RNAPIII transcripts, including 7SL and *Alu* RNAs, has previously been shown to activate a RIG-I-dependent interferon response [70,79]. Inspection of my RNA-sequencing data revealed that indeed 7SK snRNA, 7SL RNA, and the H1 RNA component of RNase P were expressed significant higher in cells depleted of TDP-43, and RT-qPCR further confirmed these findings (Figure 2.4C, D). Additionally, *Alu* loci with clear increased expression were identified and RT-qPCR analysis confirmed their increased expression. As *Alu* elements are frequently located within introns and untranslated regions of mRNA I also assessed the expression of independently transcribed *Alu* RNA by northern blot analysis using an oligonucleotide directed at a consensus *Alu* motif. Consistent with my previous analyses, using the consensus *Alu* motif oligonucleotide I observed increased expression of an RNA migrating at ~300 nt, the expected length of independently transcribed *Alu* RNA (Figure 2.4D-F).

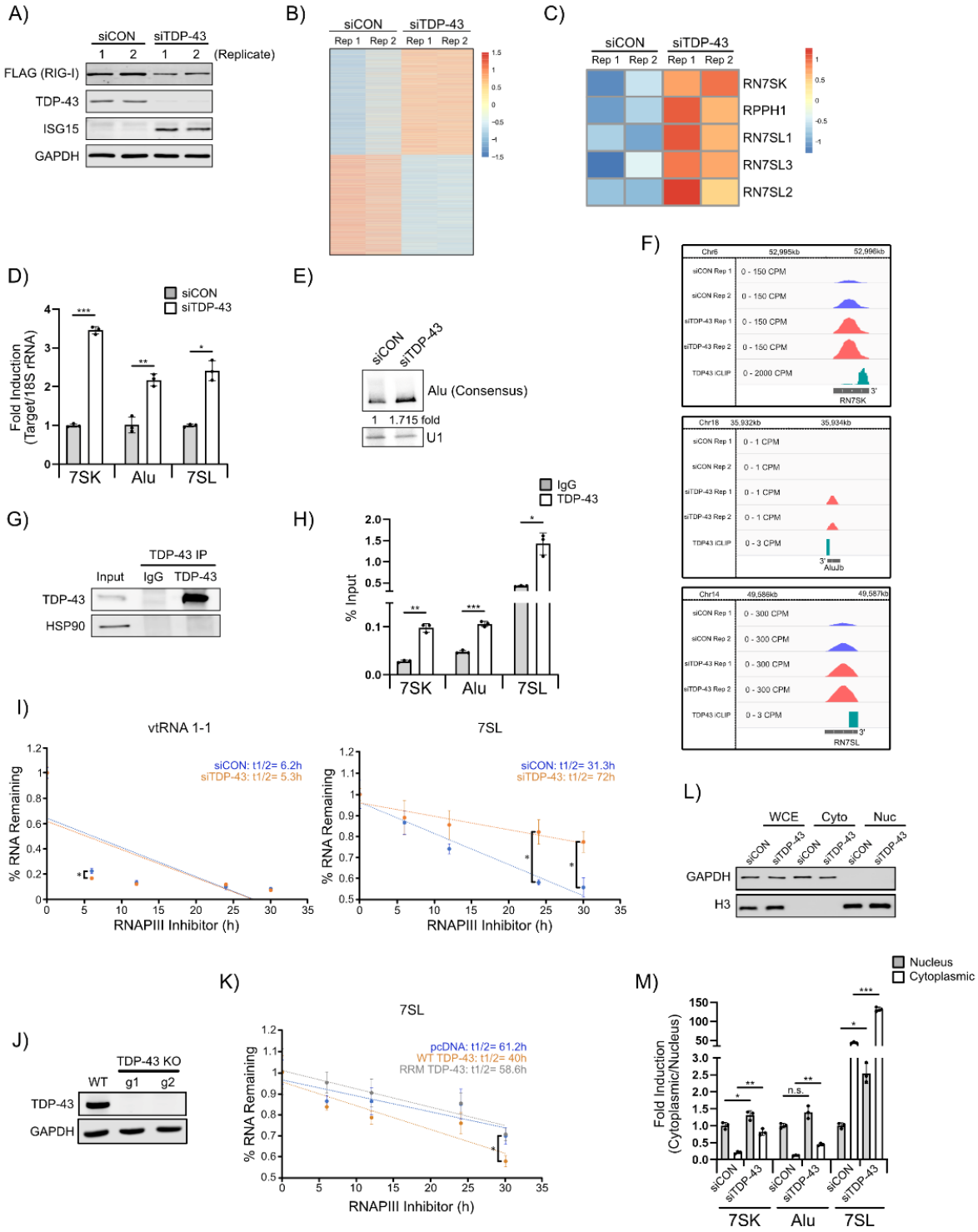
A)
siCON
siTDP-43
1 2 1 2 (Replicate)
FLAG (RIG-I)
TDP-43
ISG15
GAPDH
B)
siCON
siTDP-43
Rep 1 Rep 2 Rep 1 Rep 2
C)
siCON
siTDP-43
Rep 1 Rep 2 Rep 1 Rep 2
RN7SK
RPPH1
RN7SL1
RN7SL3
RN7SL2
D)
siCON
siTDP-43
Fold Induction (Target/18S rRNA)
7SK
Alu
7SL
E)
siCON
siTDP-43
Alu (Consensus)
1 1.715 fold
U1
F)
siCON Rep 1
siCON Rep 2
siTDP-43 Rep 1
siTDP-43 Rep 2
TDP43 iCLIP
RN7SK
AluJb
RN7SL
G)
TDP-43 IP
Input IgG TDP-43
TDP-43
HSP90
H)
IgG
TDP-43
% Input
7SK
Alu
7SL
I)
vtRNA 1-1
siCON: t1/2= 6.2h
siTDP-43: t1/2= 5.3h
7SL
siCON: t1/2= 31.3h
siTDP-43: t1/2= 72h
% RNA Remaining
RNAPIII Inhibitor (h)
L)
WCE
Cyto
Nuc
siCON
siTDP-43
GAPDH
H3
J)
TDP-43 KO
WT g1 g2
TDP-43
GAPDH
K)
7SL
pcDNA: t1/2= 61.2h
WT TDP-43: t1/2= 40h
RRM TDP-43: t1/2= 58.6h
% RNA Remaining
RNAPIII Inhibitor (h)
M)
Nucleus
Cytoplasmic
Fold Induction (Cytoplasmic/Nucleus)
n.s.
7SK
Alu
7SL

Figure 2.4: TDP-43 represses RNAPIII-transcribed RNAs to prevent cytoplasmic relocalization. (A) Western blot analysis of SH-SY5Y RIG-I complement cells treated with siCON/siTDP-43 for 48h and DOX treatment for 24h. Two replicates are shown for each condition. **(B, C)** Heat map of global up and down-regulated transcripts (B) and RNAPIII-transcribed genes (C) from A. **(D)** RT-qPCR analysis of RNAPIII transcripts from SH-SY5Y cells treated with siCON/siTDP-43. Samples were normalized to 18S rRNA and siCON levels were set to 1. **(E)** Northern blot analysis of consensus *Alu* from RNA in D. U1 snRNA was used as a loading control. **(F)** IGV view of RNAPIII-transcribed RNAs combined with TDP-43 iCLIP data. The 3' end of the genes are marked. **(G, H)** Western blot analysis (G) and RT-qPCR analysis of bound RNAs (H) from endogenous TDP-43 immunoprecipitation (IP) from SH-SY5Y cells. IgG was used as a control. Fold enrichment was computed by percent input. **(I)** RT-qPCR analysis of vtRNA 1-1 and 7SL RNA decay from SH-SY5Y cells treated with siCON/siTDP-43 for 48h. Cells were treated RNAPIII inhibitor for indicated time before collection. 0h time point was set at 1. **(J)** Western blot analysis of HEK293T TDP-43 KO cells. Two independent guide RNAs were used. **(K)** RT-qPCR analysis of 7SL RNA decay from 293T TDP-43 KO cells transfected with indicated plasmids for 24h. 0h time point was set at 1. **(L, M)** Western blot analysis (L) and RT-qPCR analysis of RNAs (M) from fractionated SH-SY5Y cells treated with siCON/siTDP-43 for 48h. Fold induction was calculated by comparing nuclear levels to cytoplasmic levels. siCON cytoplasmic-to-nuclear levels were set at 1. Student t test was used to determine statistical significance * $p \leq 0.05$; ** $p \leq 0.005$; *** $p \leq 0.0005$; ns: not significant.

Using previously published TDP-43 individual-nucleotide resolution UV-crosslinking and immunoprecipitation (iCLIP) sequencing data we observed that many of the upregulated RNAPIII transcripts have prominent TDP-43 iCLIP tags near their 3'-end (Figure 2.4F) [102]. To verify the iCLIP data I performed IPs using either anti-TDP-43 or control IgG antibodies and quantified the enrichment of 7SK, 7SL, and a consensus *Alu* sequence (Figure 2.4G, H). Consistent with the iCLIP data I observed a significant enrichment of all three RNAPIII transcripts over the control IgG (Figure 2.4H).

Although TDP-43 has not been associated with the regulation of RNAPIII transcript stability it has been linked to the regulation of mRNA half-life. Thus, I investigated whether the increased expression of select RNAPIII transcripts was due to alterations in RNA half-life. To test this, I determined the half-life of 7SL RNA and a control RNAPIII transcript, vault RNA 1-1, that did not exhibit increased expression in TDP-43 depleted cells. Loss of TDP-43 extended the half-life of 7SL RNA whereas the half-life of vault RNA was not

affected (Figure 2.4I). I next investigated whether TDP-43 RNA binding was necessary for regulating 7SL RNA half-life. To test this, I generated HEK293T TDP-43 KO cells and transfected them with either an empty vector, WT TDP-43, or an RNA binding defective TDP-43 (mutRRM; W113A/R151A) (Figure 2.4J). While expression of wild-type TDP-43 reduced 7SL half-life relative to the empty vector control, the half-life of 7SL RNA was not altered by expression of the RNA binding defective TDP-43 (Figure 2.4K). These results demonstrate a role for TDP-43 in the regulation of select RNAPIII transcript stability and suggest this contributes to changes in the transcriptome in TDP-43 depleted cells.

I also examined the nuclear/cytoplasmic localization of the TDP-43 bound RNAPIII transcripts by RT-qPCR as TDP-43 has previously been linked to nuclear export of mRNA [105]. Following whole cell fractionation into nuclear and cytoplasmic fractions I observed a significant cytoplasmic relocalization of the primarily nuclear 7SK snRNA in TDP-43 depleted cells (Figure 2.4L, M). Moreover, although *Alu* and 7SL RNAs are normally present in the cytoplasm I observed an increase in cytoplasmic levels of both RNAs (Figure 2.4M). Collectively, these results demonstrate that TDP-43 affects the expression, localization, and decay of select RNAPIII transcribed RNAs.

RNAPIII RNAs are associated with and activate RIG-I upon loss of TDP-43

7SL and *Alu* RNAs have previously been demonstrated to activate a RIG-I-dependent interferon response [70,79]. To test whether RNAPIII transcription is required to promote activation of RIG-I upon loss of TDP-43 I treated cells with siCON or siTDP-43 in the presence of an RNAPIII specific inhibitor and assessed IFN β expression by RT-qPCR. Inhibition of RNAPIII transcription was confirmed by measuring the levels of cellular vault RNA 1-1 (Figure 2.5A). Strikingly, inhibition of RNAPIII transcription

completely prevented the induction of IFN β expression when TDP-43 was depleted (Figure 2.5A). These results indicate that RNAPIII transcription is required for activating RIG-I.

Next, I tested whether TDP-43 RNA binding was required to prevent IFN β expression. HEK293T TDP-43 KO cells were co-transfected with RIG-I and either an empty vector, WT TDP-43, or an RNA binding defective TDP-43 (mutRRM; W113A/R151A) and IFN β expression was quantified by RT-qPCR (Figure 2.5B, C). Supporting my evidence that RIG-I is required to sense dsRNA that accumulates when TDP-43 is absent I observed IFN β expression in TDP-43 KOs transfected with RIG-I and an empty vector (Figure 2.5C). Furthermore, I observed IFN β expression in cells that expressed RNA-binding defective TDP-43 whereas expression of WT TDP-43 rescued IFN β expression. These data demonstrate that the RNA-binding capacity of TDP-43 is required to prevent IFN β expression.

As my data implicate RNAPIII activity as well as the ability of TDP-43 to bind RNA in the induction of IFN β expression I evaluated whether RIG-I interacts with TDP-43-target RNAs by IP-RT-qPCR (Figure 2.5D, E). TDP-43 knockdown resulted in an increased association between RIG-I and several of its RNAPIII transcribed RNA binding partners, including 7SK snRNA, 7SL RNA, and *Alu* RNA (Figure 2.5E). In contrast, the binding of RIG-I to TDP-43 associated spliceosomal snRNAs, noncoding RNAs, and mRNAs were not affected by TDP-43 depletion (Figure 2.5E). These results demonstrate that loss of TDP-43 facilitates RIG-I recognition of select RNAPIII-transcribed RNAs that can be bound by TDP-43.

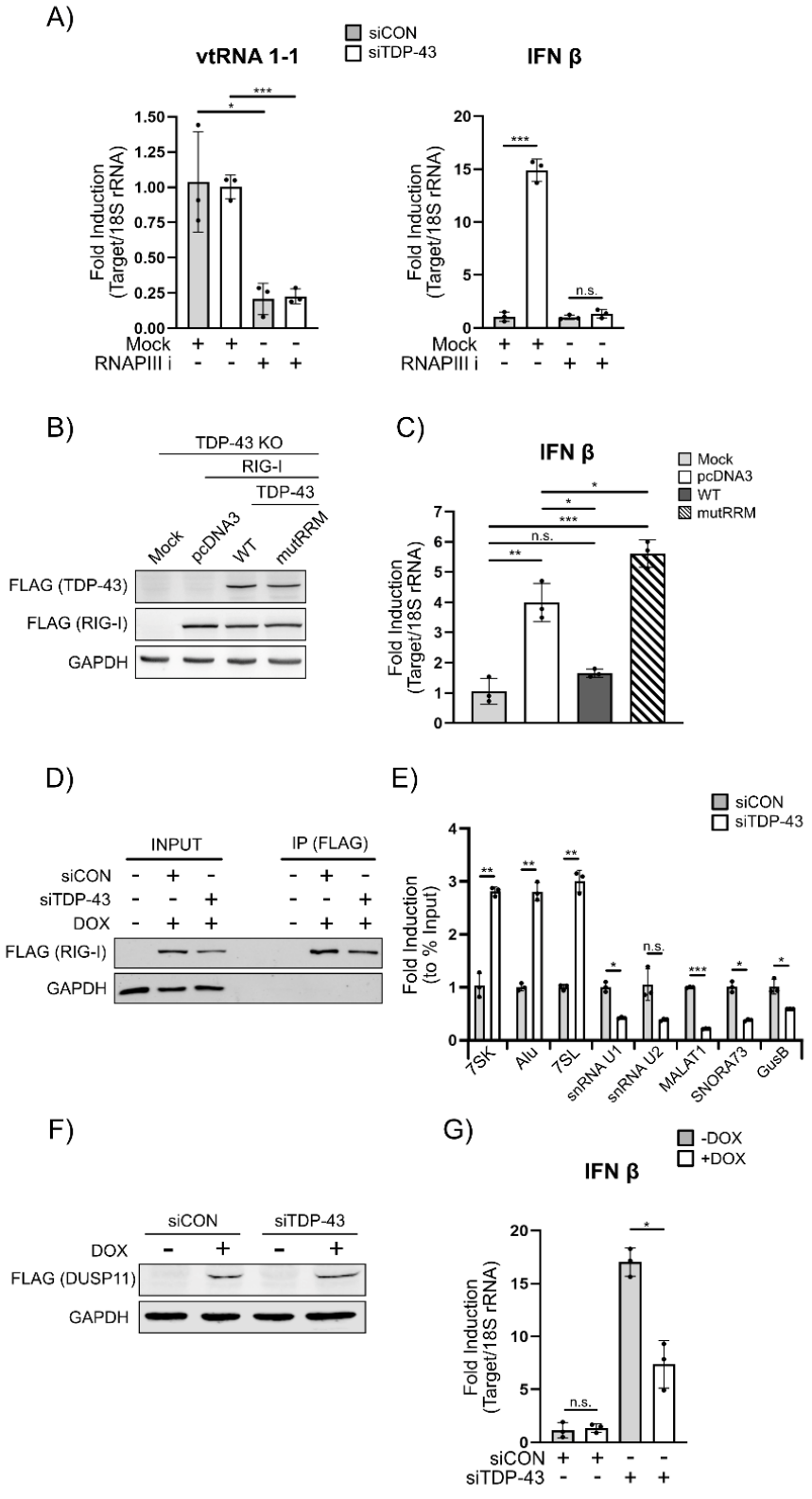
A)
siCON
siTDP-43
vtRNA 1-1
IFN β
Fold Induction (Target/18S rRNA)
Mock
RNAPIII i
n.s.
B)
TDP-43 KO
RIG-I
TDP-43
Mock
pcDNA3
WT
mutRRM
FLAG (TDP-43)
FLAG (RIG-I)
GAPDH
C)
IFN β
Mock
pcDNA3
WT
mutRRM
Fold Induction (Target/18S rRNA)
n.s.
D)
INPUT
IP (FLAG)
siCON
siTDP-43
DOX
FLAG (RIG-I)
GAPDH
E)
siCON
siTDP-43
Fold Induction (to % Input)
n.s.
7SK
Alu
7SL
snRNA U1
snRNA U2
MALAT1
SNORA73
GusB
F)
siCON
siTDP-43
DOX
FLAG (DUSP11)
GAPDH
G)
-DOX
+DOX
IFN β
Fold Induction (Target/18S rRNA)
n.s.
siCON
siTDP-43

Figure 2.5: Induced RNAPIII transcripts bind RIG-I to activate an IFN response that is rescued by exogenous TDP-43 expression in an RNA binding-dependent manner. (A) RT-qPCR analysis of vtRNA 1-1 and IFN β levels following siCON/siTDP-43 and RNAPIII inhibitor treatment for 24h. **(B, C)** Western blot analysis (B) and RT-qPCR analysis (C) of HEK293T TDP-43 KO cells transfected with FLAG-tagged RIG-I and FLAG-tagged TDP-43 plasmids for 24h. **(D, E)** Western blot analysis (D) and RT-qPCR analysis of bound RNAs (E) from FLAG-RIG-I IP of SH-SY5Y RIG-I complement cells treated with siCON/siTDP-43 for 48h and DOX treatment for 24h. Fold enrichment was computed by percent input and siCON was set to 1. **(F, G)** Western blot analysis (F) and RT-qPCR analysis (G) of DOX-inducible FLAG-DUSP11 treated with siCON/siTDP-43 and DOX for 48h. All samples were normalized to 18S rRNA and Mock/siCON levels were set to 1. Student t test was used to determine statistical significance * $p \leq 0.05$; ** $p \leq 0.005$; *** $p \leq 0.0005$; ns: not significant.

A defining feature of many RIG-I substrates is the presence of a 5'-triphosphate. Dual specificity phosphatase 11 (DUSP11) is an RNA triphosphatase that acts on several RNAPIII-derived RNAs and a reduction in its activity has been shown to activate a RIG-I-dependent interferon response [28,188,189]. Although we did not observe a reduction in DUSP11 expression in our transcriptomic data I hypothesized the significant increase in RNAPIII RNA levels may result in some transcripts escaping the activity of DUSP11 thus enabling their engagement by RIG-I. To test this, I transduced SH-SY5Y cells with a DOX-inducible DUSP11 transgene and quantified IFN expression in siCON and siTDP-43 depleted cells (Figure 2.5F, G). Consistent with my previous observations, knockdown of TDP-43 resulted in the expression of IFN β mRNA when cells were grown in the absence of DOX (Figure 2.5G). While I still observed IFN β mRNA expression when DUSP11 was overexpressed I observed a ~50% reduction in IFN β mRNA levels indicating that some of the immunostimulatory RNAs are triphosphorylated. Together, these data demonstrate that select RNAPIII transcripts are associated with RIG-I upon TDP-43 depletion as well as reveal a role for TDP-43 in limiting the accumulation of triphosphorylated RNAs.

Genetic inactivation of the RLR pathway rescues the interferon-mediated cell death associated with loss of TDP-43.

Cell culture and animal models have demonstrated that TDP-43 is essential for viability and multiple mechanisms have been proposed, including the dysregulation of Rho family GTPases, an accumulation of dsDNA breaks, and defects in autophagy [88,89,190–192]. Based on my observations I hypothesized that TDP-43 depletion induced an immune-mediated cell death. To test this, I treated SH-SY5Y WT, RIG-I KO, MDA5 KO, MAVS KO, and IRF3 truncation cells with either siCON or siTDP-43 and measured cell viability five days post-transfection by trypan blue staining and ATP production using a CellTiter-Glo assay (Figure 2.6A, B). TDP-43 knockdown reduced cell viability and ATP production in WT and MDA5 KO cells (Figure 2.6A, B). In contrast, in MAVS and RIG-I KOs, and IRF3 truncation cells, depletion of TDP-43 did not reduce cell viability or ATP production when compared to siCON treatment. (Figure 2.6A-D). Importantly, TDP-43 depletion-mediated cell death was also rescued in the 786-O MAVS KO, RIG-I KO, and IRF3 KO cells (Figure S2.5A-D).

As inactivation of IRF3 rescued cell death I hypothesized that the IRF3-dependent type I or III IFNs induce cell death via signaling through either the interferon alpha and beta receptor 1 (IFNAR1) or interferon lambda receptor 1 (IFNLR1), respectively. RT-qPCR analysis determined that IFNAR1 was expressed at significantly higher levels than IFNLR1 in both SH-SY5Y and 786-O cells (Figure 2.6E; Figure S2.5E). To test whether signaling through IFNAR1 contributed to the cell death phenotype I generated IFNAR1 KO cells using CRISPR/Cas9 (Figure 2.6F; Figure S2.5F). Treatment of WT and IFNAR1 KO cells with IFN α or β confirmed that the KO cells do not respond to extracellular IFNs

(Figure 2.6G; Figure S2.5G). Similar to results obtained with the RLR and IRF3 KOs, inactivation of IFNAR1 signaling rescued cell viability associated with loss of TDP-43 (Figure 2.6H, I; Figure S2.5H, I). Collectively, these results demonstrate that cell death associated with loss of TDP-43 is mediated in an RLR- and IFNAR1-dependent manner.

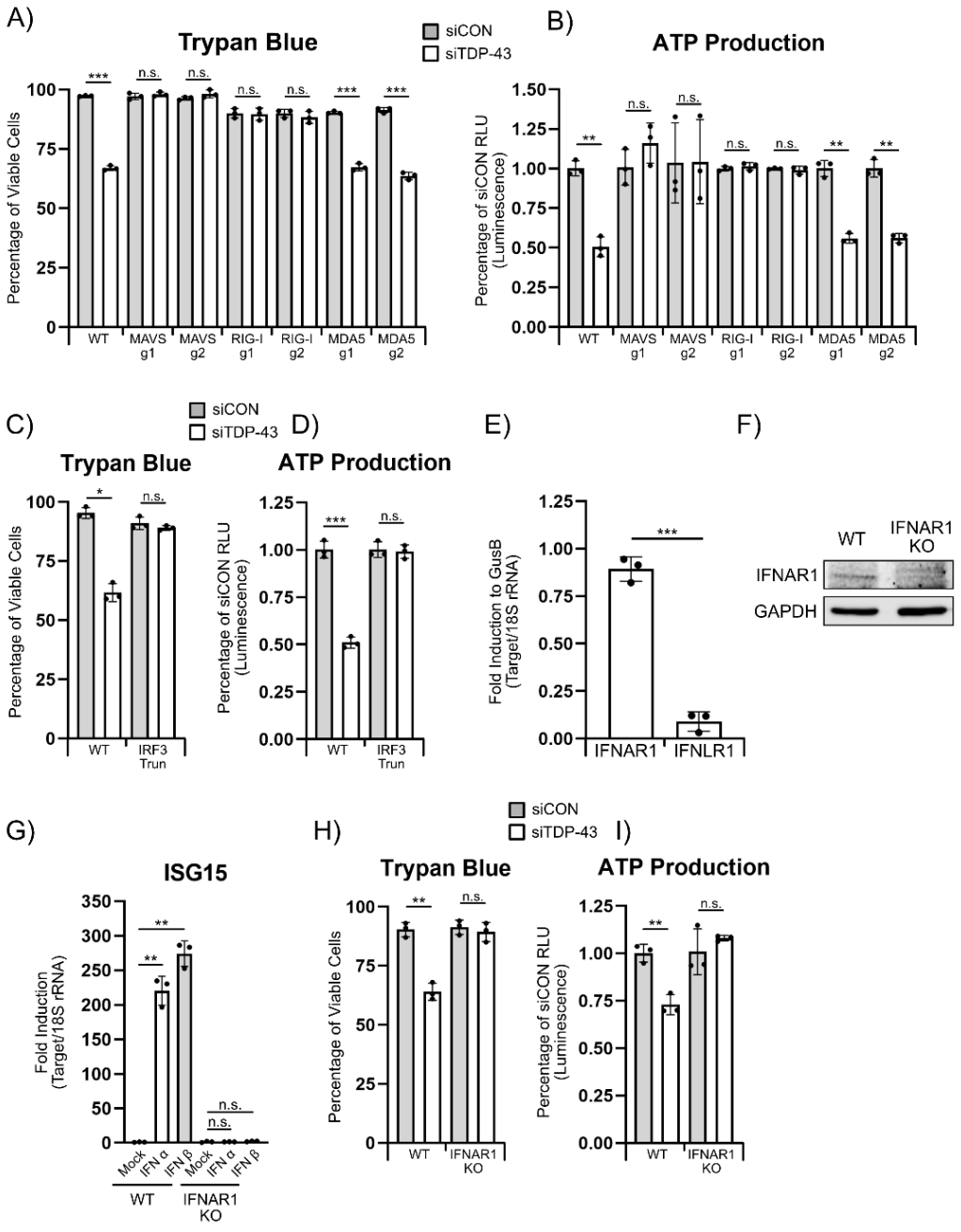

Figure 2.6: TDP-43 depletion-induced cell death requires activation of the RLR signaling pathway and type I interferon signaling. (A, B) Trypan blue staining (A) and cell titer glo analysis (B) of SH-SY5Y KO cells treated with siCON/siTDP-43 for 96h. **(C, D)** Trypan blue staining (C) and cell titer glo (D) of SH-SY5Y truncated IRF3 cells similar to A and B. **(E)** RT-qPCR analysis of IFNAR1 and IFNLR1 levels from SH-SY5Y cells. All samples were normalized to 18S rRNA, followed by the housekeeping gene GusB where GusB levels were set to 1. **(F)** Western blot analysis of IFNAR1 KO SH-SY5Y cells. **(G)** RT-qPCR analysis of ISG15 levels from WT and IFNAR1 KO SH-SY5Y cells treated with IFN α or β for 8h. Mock levels were set to 1. **(H, I)** Trypan blue staining (H) and cell titer glo analysis (I) of SH-SY5Y IFNAR1 KO cells similar to A and B. Student t test was used to determine statistical significance * $p \leq 0.05$; ** $p \leq 0.005$; *** $p \leq 0.0005$; ns: not significant.

IFNAR1 signaling promotes MLKL-dependent necroptosis

Type I IFN-mediated cell death can occur through a variety of mechanisms. IFN-dependent necroptosis is one such pathway and is activated via IFNAR1 signaling and requires the serine/threonine-protein kinase 1/3 (RIPK1/3) and the necroptotic effector mixed lineage kinase domain like pseudokinase (MLKL). Activated MLKL oligomerizes and forms cell membrane pores to facilitate cell death [83,84]. I evaluated the expression of MLKL by western blot analysis of extracts from SH-SY5Y cells treated with either siCON or siTDP-43 and observed a striking increase in its levels in TDP-43-depleted cells (Figure 2.7A). MLKL is interferon-inducible and its overexpression has recently been observed to promote cell death [193–196]. Indeed, MLKL upregulation upon TDP-43 knockdown was only observed in WT and MDA5 KO cells, but not in the MAVS KO, RIG-I KO, IFNAR1 KO, or IRF3 truncation cells (Figure 2.7B). These results were corroborated in the 786-O WT and KO cell lines (Figure S2.6A, B).

To determine whether MLKL overexpression is sufficient to promote cell death I generated DOX-inducible FLAG-tagged MLKL SH-SY5Y and 786-O cell lines. DOX-treatment induced FLAG-MLKL expression (Figure 2.7C; Figure S2.6C). 48 h post-DOX treatment I observed ~25-40% reduced cell viability when compared to the no DOX

control (Figure 2.7D; Figure S2.6D). In addition, I observed ~50% reduction in ATP production by CellTiter Glo (Figure 2.7E; Figure S2.6E). Next, I generated MLKL KOs in SH-SY5Y and 786-O cells and quantified cell viability in siCON and siTDP-43 treated cells (Figure 2.7F; Figure S2.6F). While siTDP-43 resulted in a ~40% reduction in cell viability in WT cells, there was only a ~20% decrease in cell viability in MLKL KO cells (Figure 2.7G; Figure S2.6G). Moreover, MLKL KO significantly restored ATP production in cells treated with siTDP-43 (Figure 2.7H; Figure S2.6H). These results demonstrate that MLKL expression is IFN-inducible and that its overexpression is sufficient to induce cell death in both SH-SY5Y and 786-O cells. Moreover, necroptosis contributes significantly to the mechanism behind cell death in TDP-43 deficient cells.

In summary, loss of TDP-43 results in the accumulation of immunostimulatory dsRNA that activate RIG-I and culminate in IFN-mediated necroptotic cell death.

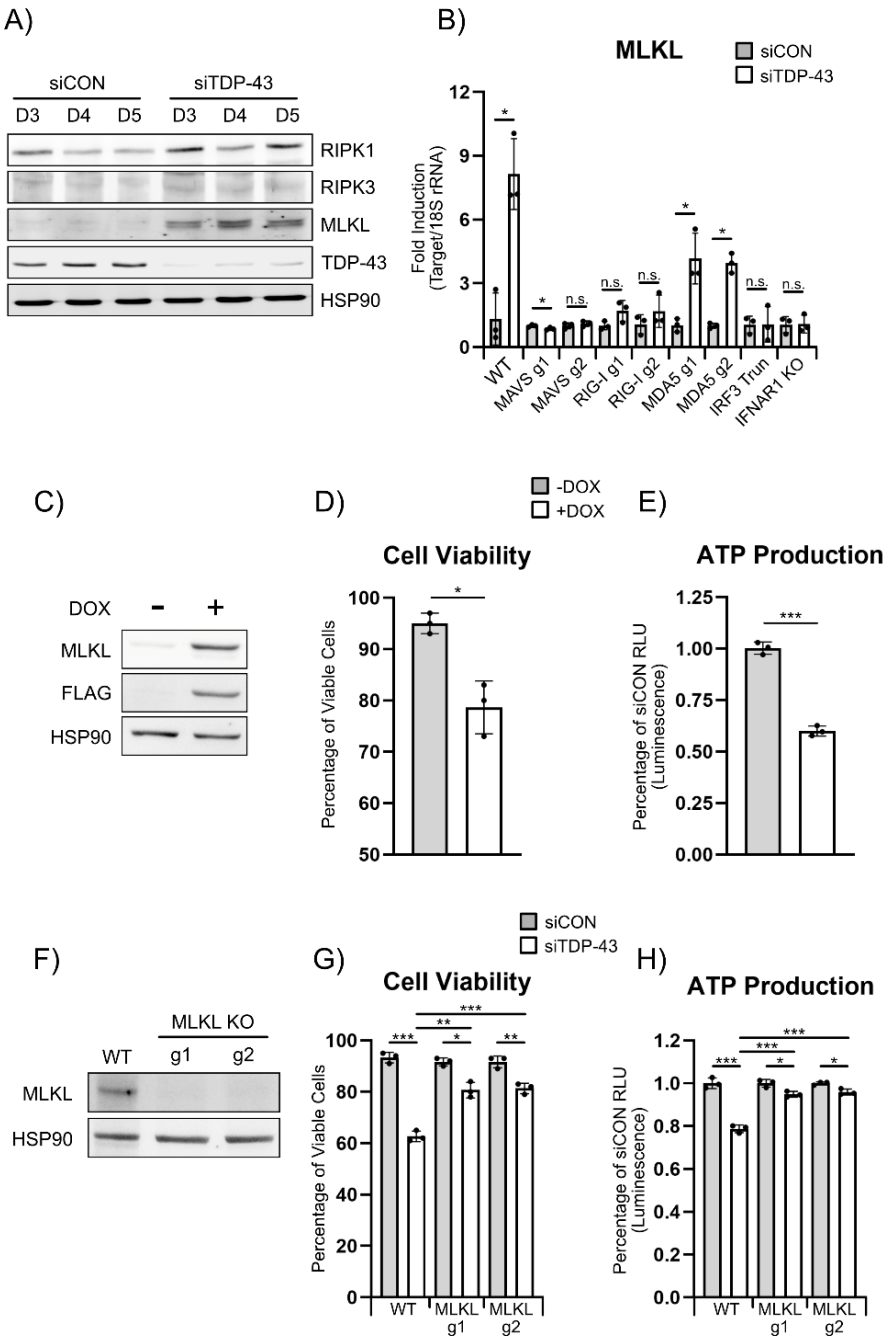

Figure 2.7: TDP-43 knockdown induces MLKL overexpression to activate necroptosis. (A) Western blot analysis of MLKL levels from SH-SY5Y cells treated with siCON/siTDP-43. **(B)** RT-qPCR analysis of MLKL levels from SH-SY5Y WT and KO cells treated with siCON/siTDP-43 for 48h. All samples were normalized to 18S rRNA and siCON levels were set to 1. **(C)** Western blot of inducible MLKL SH-SY5Y cells where doxycycline was added for 24h. **(D, E)** Trypan blue staining (D) and cell titer glo analysis (E) of cells in D. DOX was added for 48h. **(F)** Western blot of MLKL KO SH-SY5Y cells. **(G, H)** Trypan blue staining (G) and cell titer glo analysis (H) of MLKL KO cells treated with siCON/siTDP-43 for 96h. Student t test was used to determine statistical significance * $p \leq 0.05$; ** $p \leq 0.005$; *** $p \leq 0.0005$; ns: not significant.

Discussion:

While best characterized in the context of host-defense, RLRs are also important contributors to the efficacy of various anti-cancer approaches and their inappropriate activation is associated with the development of autoimmunity [81,197,198]. Thus, the ability to control RLR activation is of importance across multiple facets of cellular and organismal homeostasis. TDP-43 is an essential RNA-binding protein implicated in the development of various pathologies including ALS and FTLD [199]. Here, I demonstrate that loss of TDP-43 results in increased expression and mislocalization of several RNAPIII noncoding RNAs. Increased RNAPIII activity facilities a RIG-I-dependent interferon response that can be partially suppressed by overexpression of the cellular triphosphatase DUSP11, indicating the accumulated immunostimulatory dsRNAs are triphosphorylated. Moreover, RIG-I-dependent IFN β production promotes MLKL-dependent necroptosis which can be rescued via the genetic inactivation of the RLR pathway. Thus, this study uncovers an underappreciated and intricate relationship between the control of cellular gene expression and IFN-mediated cell death.

I have determined that TDP-43 regulates the accumulation of immunostimulatory dsRNA. While we did not attempt to identify the J2-postiive RNAs in SH-SY5Y cells, previous work in M17 neuroblastoma cells identified an enrichment of J2-binding in highly structured intronic regions of RNA as well as across the human endogenous retrovirus K (HERV-K) transcript in TDP-43 depleted cells [111]. I anticipate that some of the J2-positive signal I observe is derived from RNAs previously identified. I have determined that J2-postive RNAs are immunostimulatory and that loss of TDP-43 potentiates a RIG-I-dependent interferon response. RIG-I primarily discriminates RNA on the basis of a 5’-

di or triphosphate structure at the end of RNAs and thus it is unlikely that J2-enriched HERV-K or intronic regions previously identified contribute significantly to RIG-I activation [60,62–65]. In support of this, the RIG-I-dependent interferon response is blunted by increasing the expression of the cellular RNA triphosphatase DUSP11.

We observed a significant remodeling of cellular gene expression in TDP-43 depleted cells. Among the most significant ontological terms associated with the upregulated genes were RNAPIII transcription. Indeed, by RT-qPCR I confirmed the expression of many RNAPIII noncoding RNAs, including 7SL and *Alu* RNA, were significantly higher in cells lacking TDP-43. Increased RNAPIII-derived RNAs may stem from effects of TDP-43, either directly or indirectly, on chromatin modification and therefore RNAPIII transcription. For example, in human post-mortem brain tissue loss of TDP-43 is associated with decondensation of intergenic chromatin [117]. A reduction in H3K9me3, a repressive chromatin mark for repetitive elements such as *Alus* and long interspersed elements (LINEs) was also observed. Interestingly, analysis of previously published TDP-43 iCLIP-seq data revealed that many of the upregulated RNAPIII transcripts are bound by TDP-43 [102]. Moreover, I demonstrated that TDP-43 regulates the half-life of the RNAPIII transcript 7SL RNA and that this regulation requires the ability of TDP-43 to bind RNA. While TDP-43 has been linked to the regulation of mRNA stability these are the first data suggesting that TDP-43 is involved in noncoding RNA decay [200]. Whether this occurs co- or post-transcriptionally as well as which RNA decay machineries are involved is unknown and future studies will clarify this. Collectively, this suggests that increased RNAPIII transcripts in TDP-43 depleted cells result from a combination of alterations on transcription and RNA stability.

In TDP-43 depleted cells I observed an increase in the cytoplasmic localization of several RNAPIII transcribed RNAs. While 7SL RNA and *Alu* RNAs are normally cytoplasmic, the levels of the primarily nuclear 7SK snRNA were also increased in the cytoplasm. TDP-43 has been demonstrated to participate in the transport and localization of mRNPs in neuronal and dendritic cells, however a role for it in 7SK snRNA localization has not been identified [105,106,201,202]. Additional studies are required to determine the mechanism by which TDP-43 influences 7SK snRNA expression and nuclear retention.

Regardless of the mechanism facilitating enhanced RNAPIII noncoding RNA expression, my work demonstrates that RNAPIII transcription is required for the interferon response in TDP-43 depleted cells. Although RNAPIII has been identified as a cytoplasmic DNA sensor capable of activating RIG-I via the transcription of promoter-independent triphosphorylated RNAs I do not anticipate this contributing too significantly to the cell-intrinsic immune response observed [56,57]. Rather, my data supports a model in which RNAPIII-derived noncoding RNAs that can be bound by TDP-43 are engaged by RIG-I to facilitate activation of MAVS and an IRF3-dependent interferon response. I speculate that the enhanced expression of RNAPIII transcripts results in a failure of their proper processing and/or localization, which in turn facilities RIG-I activation. However, I cannot exclude the possibility that TDP-43 shields the select RNAPIII transcripts from RIG-I sensing. Indeed, the unshielding of *7SL* RNA and *RNA5SP141* transcripts due to loss of their RBPs results in a RIG-I-dependent interferon response [79,80].

TDP-43 is associated with multiple neurological disorders including ALS and FTLD. Interestingly, elevated IFN levels have been reported in the brains of ALS and

FTLD patients as well as in animal models [94–97]. Multiple lines of evidence support a role for IFN signaling in neurodegeneration, including observations that high dose interferon treatment can cause neurological abnormalities. Moreover, patients with Aicardi-Goutieres, an interferonopathy caused by mutations in MDA5, present with childhood neurodegeneration and dysfunction. My demonstration that TDP-43 plays a critical role in regulating immunostimulatory dsRNA accumulation suggests that activation of the RLR pathway may play a prominent role in initiating the neurological dysfunction observed in ALS and FTLD.

My results here expand on an emerging theme in RLR activation that host encoded RNAs can be prominent RLR ligands, and that cellular RBPs can function as cell-intrinsic checkpoints or barriers to RLR activation. Given these observations I hypothesize that gene expression is inherently a dangerous process, not only in that alterations in gene expression programs can cause disease, but that the RNA structures involved in orchestrating the programs as well as the intermediates of RNA processing reactions can be immunostimulatory. Moreover, this can be viewed as a proverbial double-edged sword in that mechanisms which limit immunostimulatory dsRNAs may be pathogenic in the context of mutations but also leveraged therapeutically in conditions in which increased IFN signaling is desirable. Thus, I anticipate that continued investigations into mechanisms of gene expression will provide additional significant insight into the control of RLR activation by endogenous RNAs.

Gene	Sequence
MAVS Guide 1 WT	GCCC**TCAGCCCTCTGACCTCCAGCG**GGCA
MAVS Guide 1 SH-SY5Y	GCCC **- - - - - - - TCTGACCTCCAGCG**GGCA
MAVS Guide 1 786-O	GCCC **- - - - - - - - - - - - - - -TCCAGCG**GGCA
MAVS Guide 2 WT	CTGC**AGGGGCTGCAGAGGGTA - AAC**AGGG
MAVS Guide 2 SH-SY5Y	CTGC**AGGGGCTGCAGAGGGTAAAAC**AGGG
MAVS Guide 2 786-O	CTGC**AGGGGCTGCAGAGGGTA - - AC**AGGG
RIG-I Guide 1 WT	CCCT**TGT -TGTTTTTCTCAGCCTG**AATA
RIG-I Guide 1 SH-SY5Y	CCCT**TGTTTGTTTTTCTCAGCCTG**AATA
RIG-I Guide 1 786-O	CCCT**TGTTTGTTTTTCTCAGCCTG**AATA
RIG-I Guide 2 WT	AAGC**CACGGAACCAGCCTTCCTC**CTGG
RIG-I Guide 2 SH-SY5Y	AAGC**CACGGAACCAGCCTT - CTC**CTGG
RIG-I Guide 2 786-O	AAGC**CACGGAACCAGC - - - - - - -** CTGG
MDA5 Guide 1 WT	TCTC**TGAGAAAGAAAGATGTC - - - - - - - - - - - - - - - - - - GAA**TGGGTATT
MDA5 Guide 1 SH-SY5Y	TCTC**TGAGAAAGAAAGATGTATATAATACCCTTCTCTGAGAA**TGGGTATT
MDA5 Guide 1 786-O	TCTC**TGAGAAAGAAAGATGTC - - - - - - -** TATT
MDA5 Guide 2 WT	CCAC**CTGGATGTACATTTTC - ACCC**TGGC
MDA5 Guide 2 SH-SY5Y	CCAC**CTGGATGTACATTCTCAACCC**TGGC
MDA5 Guide 2 786-O	CCAC**CTGGATGTACATT - - - - - CCC**TGGC
IRF3 WT	GGGC**AGGGCTCAGGGGCTACA - GCC**AGGCTTGGGGGTCCCG
IRF3 SH-SY5Y	GGGC**AGGGCTCAGGGGCTACA - - -** - - - - - - - - - - - - - CCCG
IRF3 786-O	GGGC**AGGGCTCAGGGGCTACAAGCC**AGGCTTGGGGGTCCCG
IFNAR1 WT SH-SY5Y	CGAC**GACCCTAGTGCTCGTCGCCG**TGGC
IFNAR1 KO SH-SY5Y	CGAC**GACCCTAGTGCTCGT - - CCG**TGGC
IFNAR1 WT 786-O	GCCA**TGGGTGTTGTCCGCAGCCGC**AGGT
IFNAR1 KO 786-O	GCCA**T - - - - GTTGTCCGCAGCCGC**AGGT
TDP-43 Guide 1 WT	CCAG**GGGCGTGTGGGCTTCGCTAC**AGGA
TDP-43 Guide 1 HEK293T	CCAG**GGGCGTGTGGGCTTCG - - - -** - - - A
TDP-43 Guide 2 WT	GAAA**ACATCCGATTTAATAGT- GTT**GGGT
TDP-43 Guide 2 HEK293T	GAAA**ACATCCGATTTAATAGTTGTT**GGGT
MLKL Guide 1 WT	CTCC**ATGACAATGGAGAATTGAGG**CGGA
MLKL Guide 1 SH-SY5Y	CTCC**ATGACAATGGAGAATT - AGG**CGGA
MLKL Guide 1 786-O	ATCC**ATG - - - - - - - - - - - - - - - - - G**CGGA
MLKL Guide 2 WT	CATG**CCTGTTTCACCCATAAGCCA**AGGA
MLKL Guide 2 SH-SY5Y	CATG**CCTGTTTCACCCATA - - CCA**AGGA
MLKL Guide 2 786-O	CATG**CCTGTTTCACCCATA - - CCA**AGGA

Table 2.1: CRISPR-Cas9 induced mutations

Guide RNA recognition sites are in bold

CHAPTER 3:

Discussion:

RNA processing is a tightly regulated cellular process that is essential for life. Defects in this regulation, whether by changes in the expression, localization, or activity of regulatory factors, can have major consequences that may induce cellular stress and death. RNA binding proteins (RBPs) facilitate numerous RNA processing events, starting from transcription and concluding in RNA decay, demonstrating that they are involved throughout the RNA "life-cycle." Apart from regulating RNA processing events, RBPs are also involved in physiological relevant conditions, such as viral infection and activation of an innate immune response. Unfortunately, the mechanisms that RBPs employ to regulate these conditions are not completely understood. Therefore, my thesis aimed to determine how RBPs regulate KSHV infection and double-stranded RNA sensing. The first chapter demonstrates that the RBP FUS restricts KSHV reactivation by regulating RNAPII CTD phosphorylation on viral promoters to restrict transcriptional elongation. The second chapter determined that the RBP TDP-43 prevents a lethal RIG-I-like receptor-dependent interferon response by regulating RNAPIII transcript abundance and cytoplasmic localization. Based on these findings, I conclude that RBPs function beyond their canonical role in regulating RNA metabolism and are involved in restricting viral infection and activation of an innate immune response. My thesis demonstrates that by

identifying RBP function in infection and nucleic acid sensing, additional insight is revealed into their cellular activity apart from their previously reported functions.

The first chapter of my thesis determined that FUS restricts KSHV reactivation. FUS is involved in several stages of RNA biogenesis and defects in FUS expression, localization, or mutations are associated with diseases such as ALS and FTLD. KSHV is an oncogenic human herpesvirus that establishes latency upon infection of certain cell types and can later be reactivated into the lytic phase. I proposed to investigate how FUS regulates KSHV reactivation as FUS is necessary for B cell development, which is the primary latent reservoir for the virus. I demonstrated that FUS restricts KSHV reactivation from a patient-derived, latently infected B cell line and a model ccRCC cell line as siRNA depletion of FUS increased viral gene expression, protein expression, and infectious virion production. I was able to rescue the FUS-depletion induced increase in reactivation by exogenous expression of siRNA-resistant FUS, validating the on-target effect of the siRNA. Furthermore, FUS restricted reactivation prior to viral DNA replication and was predominantly nuclear in latency and the lytic cycle. Finally, we demonstrated that FUS interacts with RNA polymerase II, localized to the viral episome, and restricted Serine-2 phosphorylated RNA polymerase II transcription on the episome to inhibit RNA synthesis of viral genes such as RTA. Overall, my first chapter identified FUS as a restriction factor for KSHV infection and was the first to demonstrate that restriction of viral gene transcriptional elongation is an antiviral host defense.

My study reveals several interesting viewpoints on how FUS and other RBPs impact RNA metabolism to restrict viral infection. FUS regulation of RNA polymerase II elongation on viral promoters is a novel mechanism for inhibiting infection. It remains to

be determined whether this is a common means of restriction for other viruses. KSHV is a human herpesvirus and is specifically classified as a γ-herpesvirus. It is interesting to speculate that FUS and the regulation of RNAPII phosphorylation may restrict the other human herpesviruses as they share several features and characteristics such as being dsDNA viruses, establish latency, and reactivate into a lytic phase. It is also possible that the antiviral function is restricted to γ-herpesviruses, such as EBV and the murine virus MHV68, as these viruses have unique features such as longer replication cycles and more restricted cellular and tissue tropism. Many host restriction factors are antagonized by viral products to prevent their activity during an infection. As FUS restricts KSHV reactivation, I hypothesize that the virus may encode proteins that impact FUS restriction. The Karijolich lab possesses a KSHV ORFeome library that contains all viral ORFs on expression plasmids. It would be interesting to use the library and screen the viral proteins to determine if any interact with FUS and determine if they inhibit its antiviral activity. The viral ORF may be antagonizing FUS through a variety of mechanisms, including the prevention of FUS interaction with the episome or blocking the interaction with RNA polymerase II. Finally, FUS regulates similar RNA processes as several other RBPs, including the hnRNPs. Whether additional RBPs also restrict KSHV or other viruses by inhibiting RNA polymerase II elongation has yet to be determined.

Although my thesis has identified a new function of FUS in restricting KSHV, there are several areas that will benefit from future studies. We have demonstrated that FUS binds the viral episome at some promoters in latency. How FUS is recruited, what impact it has on viral chromatin structure, and what role it has in maintaining latency are interestingly questions. I have shown that FUS restricts RNA polymerase II Ser2

phosphorylation on viral genes, although the mechanism behind this has not be identified. Furthermore, FUS is involved in B cell development and KSHV establishes latency primarily in B cells. Additional research is required to determine if KSHV-infected B cells impact FUS function during development. Finally, FUS mutations are associated with ALS and FTLD. The significance of these mutations on KSHV infection and reactivation, as well as on the relationship between KSHV and ALS or FTLD patients, will require further investigation.

The second chapter of my thesis determined that the RBP TDP-43 regulates RNA polymerase III transcript abundance to prevent a lethal RIG-I-dependent interferon response. TDP-43 regulates numerous stages of RNA metabolism including splicing, RNA export, and transcription, and its misregulation and mutations are implicated in diseases such as ALS, FTLD, cancer, and myopathy. The RIG-I-like receptors (RLR) include the dsRNA sensors RIG-I and MDA5 that bind distinct and unique dsRNA ligands. RLR signaling induces an antimicrobial interferon and inflammatory response to a variety of infections and autoimmune diseases. I determined to investigate how TDP-43 regulates RLR activation as TDP-43 is involved in several RNA processes that have dsRNA intermediates or final products. I demonstrated that loss of TDP-43 induces the accumulation of immunostimulatory dsRNA and a subsequent interferon response in SH-SY5Y neuroblastoma and 786-O clear-cell renal cell carcinoma (ccRCC) cell lines. The interferon response was RIG-I, MAVS, and IRF3 dependent as TDP-43 depletion in a RIG-I, MAVS, and IRF3 CRISPR/Cas9 knockout prevented interferon induction. Furthermore, TDP-43 repressed RNAPIII transcript accumulation and cytoplasmic relocalization to prevent RIG-I activation in an RNA binding-dependent manner. Finally, I

demonstrated that loss of TDP-43 induces cell death via RLR, IRF3, and IFNAR1 signaling, leading to the induction of MLKL overexpression to facilitate necroptosis. Overall, my second chapter identified TDP-43 as a regulator of dsRNA accumulation and RLR signaling and determined why TDP-43 depletion induces lethality.

My study reveals several interesting viewpoints on gene expression, TDP-43 expression in disease, and how RBPs regulate RNA processing to restrict RLR activation. I have shown that TDP-43 regulates RNAPIII transcript abundance to prevent RLR activation, clearly demonstrating that defects in gene expression are dangerous and can induce cell death. These findings are in accordance with loss or dysregulation of other RNA processing proteins, such as ADAR, activating RLRs. Additional research is required to determine how errors in other stages of RNA metabolism can activate an immune response. As mentioned in the introduction, TDP-43 mutations, changes in expression, and mislocalization are associated with several diseases, including ALS. My findings demonstrate that loss of TDP-43 induces a lethal interferon response, the accumulation of RNAPIII-transcribed ncRNAs, and the cytoplasmic relocalization of these transcripts. How these consequences of TDP-43 nuclear depletion contribute to TDP-43 associated disease remain to be investigated. Current research has indicated that RIG-I activation is necessary for a robust response to checkpoint inhibitor immunotherapy [197,198]. By determining that loss of TDP-43 activates RIG-I, my research may suggest that TDP-43 is a potential drug target to enhance checkpoint inhibition therapy. Finally, TDP-43 and other RBPs including hnRNPs regulate several shared RNA processes. Previous TDP-43 mass spectrometry experiments reveal that it interacts with several other RBPs, suggesting that it may form a complex to regulate dsRNA accumulation. Indeed, I have

performed an initial siRNA screen of select RBPs to identify other proteins that prevent an innate immune response. Through this screen, I have identified other RBPs whose depletion induces IFN β expression and the Karijolich lab is continuing this research. I would hypothesize that some of these proteins also restrict RLR activation by facilitating proper RNA biogenesis in a complex with TDP-43.

My thesis has identified a new role of TDP-43 in restricting RLR activation. However, there are several areas of this work that are open to further investigations by our lab or other groups. I have demonstrated that TDP-43 depletion induces cytoplasmic immunostimulatory dsRNA accumulation. The identity of these dsRNA species remains to be determined as well as why they are immunostimulatory. I have shown that loss of TDP-43 leads to the accumulation of RNAPIII-transcribed ncRNAs due to their increased stability in an RNA binding-dependent manner. This suggests that TDP-43 is involved in a novel ncRNA decay pathway. Interestingly, previous TDP-43 mass spectrometry experiments have determined that it interacts with RNA decay factors, such as SKIV2L2 and RRP6. Therefore, I hypothesize that TDP-43 is facilitating RNAPIII transcript decay by binding the RNA and recruiting it to the RNA decay machinery. I am very intrigued by this finding and am excited for the Karijolich lab to identify the mechanism of how TDP-43 promotes decay as it would reveal a new RNA decay pathway. Furthermore, TDP-43 depletion induced cytoplasmic relocalization of the RNAPIII transcripts that then activate RIG-I. The mechanism by which TDP-43 regulates ncRNA export is unknown, although it does interact with the mRNA export nucleoporin TPR and regulates export of several mRNAs [105,106,201]. Finally, my findings reveal that loss of TDP-43 in a RLR, IRF3, or IFNAR knockout prevent cell death while TDP-43 depletion is lethal in wild-type cells.

These findings suggest that a TDP-43 KO may be viable if generated in a RLR KO background. I have already generated RLR KOs in both the SH-SY5Y and 786-O cell lines. I hypothesize a TDP-43/RLR double knockout cell line would live while a TDP-43 KO in wild-type cells would die. I am also interested in determining if a TDP-43/RLR double knockout can be generated *in* vivo. MAVS KO mice are available for purchase. Hence, additional work will determine whether a TDP-43 knockout can be generated in mice using a MAVS knockout background to further our understanding of TDP-43 function.

Throughout my thesis, I have determined that RNA binding proteins regulate viral infection and dsRNA sensing. The notion that RBPs impact viral and immune processes in addition to their known role in RNA biogenesis is important for understanding how RNA metabolism regulates disease. I have determined that FUS restricts KSHV reactivation by impacting RNA polymerase II elongation of viral genes. The findings not only identify FUS as a novel restriction factor, but also demonstrates that the host can regulate transcription elongation as a defense mechanism against viral infection. I also demonstrated that TDP-43 regulates dsRNA accumulation to prevent a lethal RIG-I-dependent interferon response. The results exemplify how defects in RNA processing are dangerous and demonstrate why TDP-43 is essential for life. My thesis results are in line with and provide additional information to recent findings in the field that describe how RNA binding proteins regulate and are involved in cellular processes and physiological relevant conditions that are beyond their canonical roles in gene expression.

Appendix:

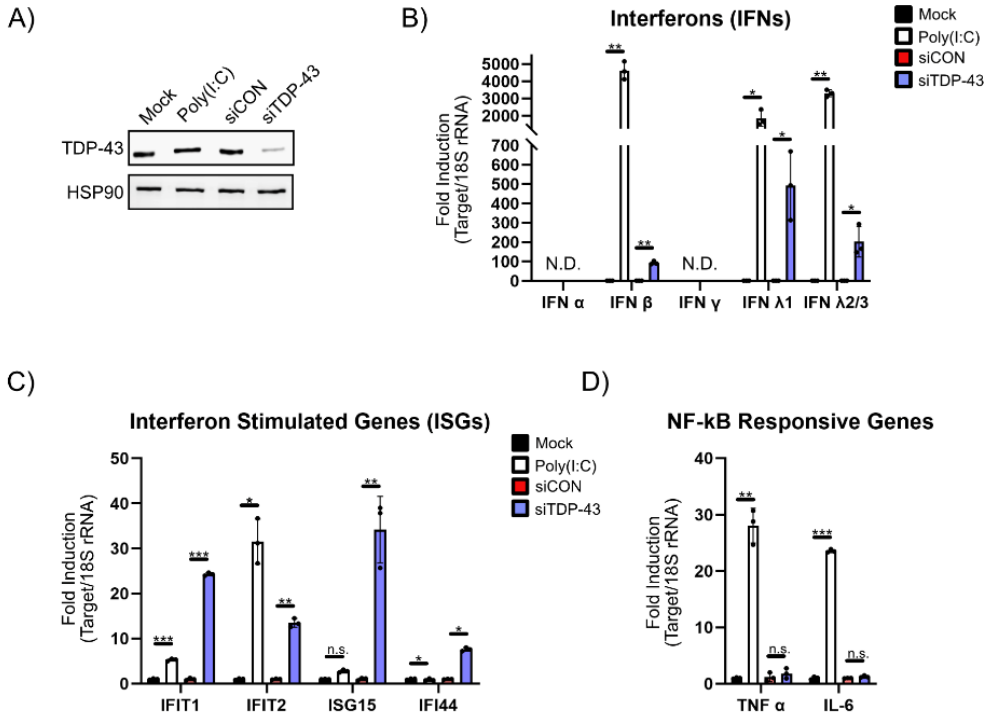

Figure S2.1: TDP-43 knockdown activates a Type I and III IFN response in 786-O cells. (A) Western blot analysis of 786-O cells treated with siCON/siTDP-43 for 48 h. **(B, C, D)** RT-qPCR analysis of the IFNs (B), ISGs (C), and NF-kB responsive genes (D) from cells in A. All samples were normalized to 18S rRNA and Mock/ siCON levels were set to 1.Student t test was used to determine statistical significance * $p \leq 0.05$; ** $p \leq 0.005$; *** $p \leq 0.005$; *** $p \leq 0.0005$; ns: not significant.

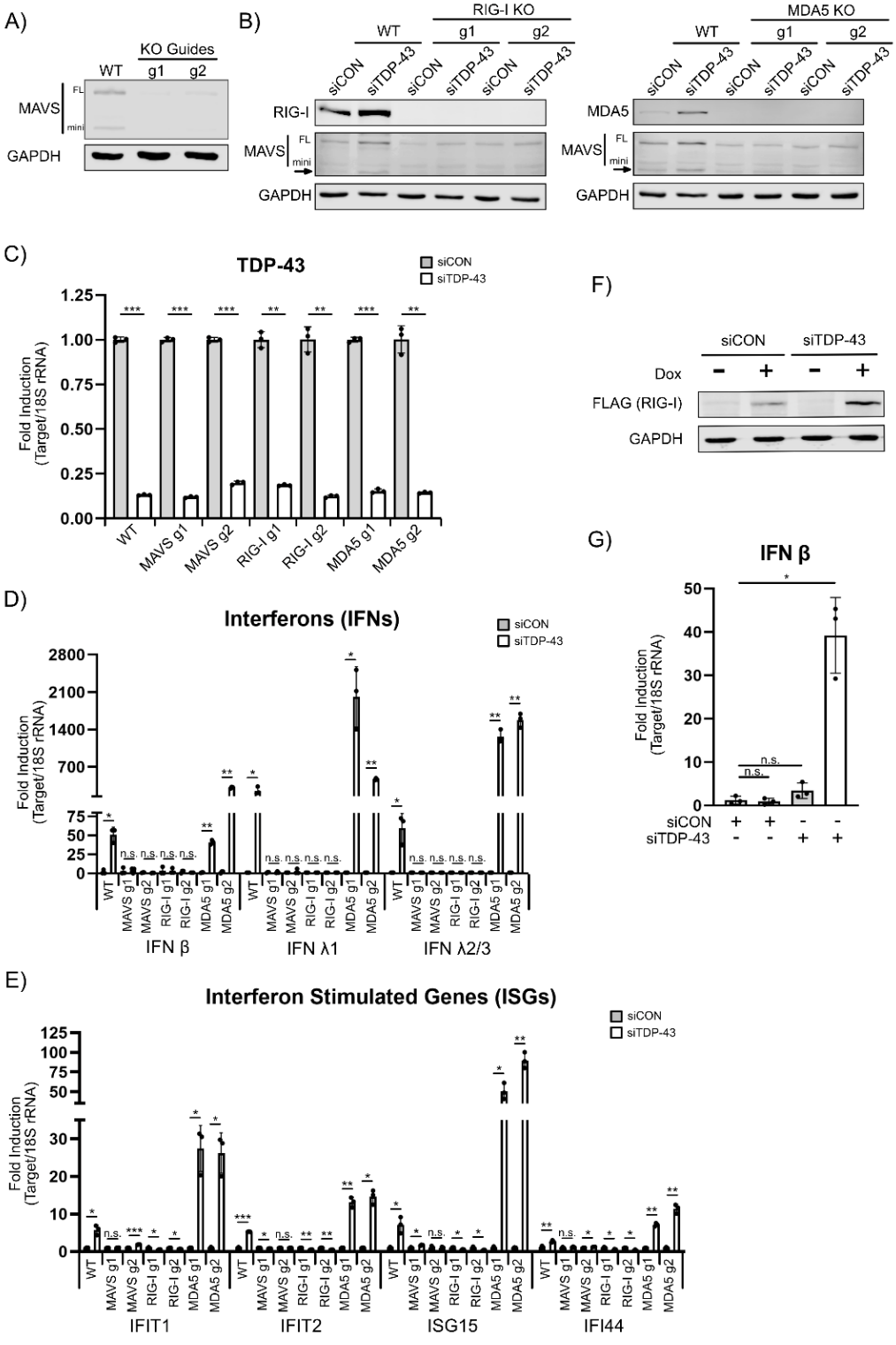
A)
KO Guides
WT
g1
g2
MAVS
FL
mini
GAPDH
B)
RIG-I KO
MDA5 KO
WT
g1
g2
siCON
siTDP-43
RIG-I
MDA5
MAVS
FL
mini
GAPDH
C)
TDP-43
siCON
siTDP-43
Fold Induction (Target/18S rRNA)
1.25
1.00
0.75
0.50
0.25
0.00
***
**
WT
MAVS g1
MAVS g2
RIG-I g1
RIG-I g2
MDA5 g1
MDA5 g2
D)
Interferons (IFNs)
siCON
siTDP-43
Fold Induction (Target/18S rRNA)
2800
2100
1400
700
75
50
25
0
n.s.
IFN β
IFN λ1
IFN λ2/3
E)
Interferon Stimulated Genes (ISGs)
siCON
siTDP-43
Fold Induction (Target/18S rRNA)
125
100
75
50
30
20
10
0
IFIT1
IFIT2
ISG15
IFI44
F)
siCON
siTDP-43
Dox
FLAG (RIG-I)
GAPDH
G)
IFN β
Fold Induction (Target/18S rRNA)
50
40
30
20
10
0
n.s.
siCON
siTDP-43

Figure S2.2: TDP-43 knockdown activates a RIG-I and MAVS-dependent interferon response in 786-O cells. (A) Western blot analysis of 786-O MAVS knockout (KO) cells. Two independent guide RNAs are shown, and full length (FL) and mini-MAVS (mini) are depicted. **(B)** Western blot analysis of 786-O RIG-I and MDA5 KO cells. Two independent guide RNAs are shown and cells were treated with siCON/siTDP-43 for 48h. **(C, D, E)** RT-qPCR analysis of TDP-43 (C), IFNs (D), and ISGs (E) following siCON/siTDP-43 treatment for 48h. **(F)** Western blot analysis of 786-O RIG-I KO cells complemented with DOX-inducible FLAG-tagged RIG-I. Cells were treated with siCON/siTDP-43 for 48h and DOX for final 24h. **(G)** RT-qPCR analysis of IFN β levels from cells in F. Student t test was used to determine statistical significance * $p \leq 0.05$; ** $p \leq 0.005$; *** $p \leq 0.0005$; ns: not significant.

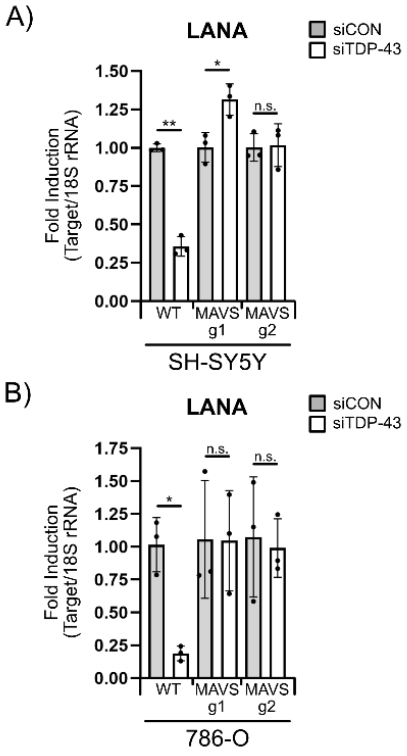

Figure S2.3: Loss of TDP-43 induces a MAVS-dependent antiviral IFN response. (A) RT-qPCR analysis of LANA levels in SH-SY5Y WT and MAVS KO cells 24h post KSHV infection. **(B)** RT-qPCR analysis of LANA levels in 786-O WT and MAVS KO cells 24h post KSHV infection. All samples were normalized to 18S rRNA and siCON levels were set to 1. Student t test was used to determine statistical significance * $p \leq 0.05$; ** $p \leq 0.005$; *** $p \leq 0.0005$; ns: not significant.

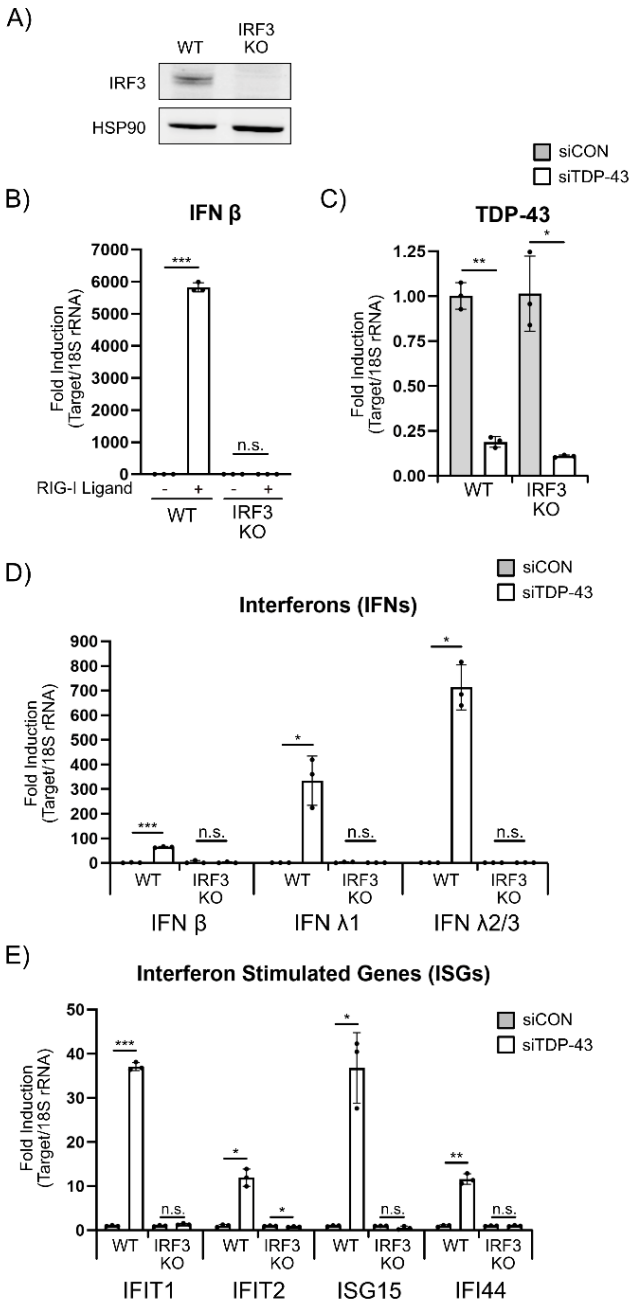

Figure S2.4: IRF3 is responsible for the TDP-43 depletion-induced interferon response in 786-O cells. (A) Western blot analysis of IRF3 knockout cells. **(B)** RT-qPCR analysis of IFN β levels following RIG-I ligand transfection for 6h. **(C, D, E)** RT-qPCR analysis of TDP-43 (C), IFNs (D), and ISGs (E) following siCON/siTDP-43 treatment for 48h. All samples were normalized to 18S rRNA and Mock/siCON levels were set to 1. Student t test was used to determine statistical significance * $p \leq 0.05$; ** $p \leq 0.005$; *** $p \leq 0.0005$; ns: not significant.

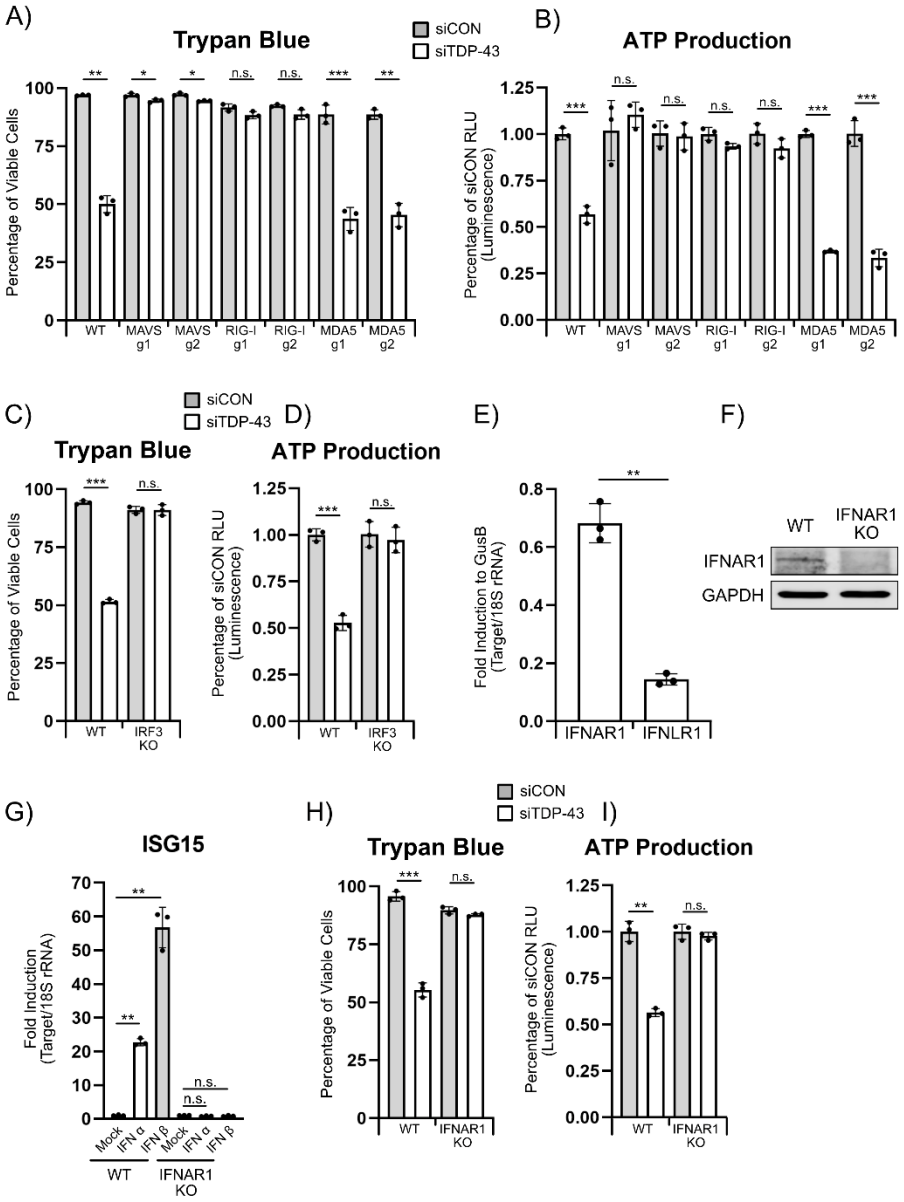

Figure S2.5: TDP-43 depletion-induced cell death requires activation of the RLR signaling pathway and type I interferon signaling in 786-O cells. (A, B) Trypan blue staining (A) and cell titer glo (B) of 786-O KO cells treated with siCON/siTDP-43 for 96h. **(C, D)** Trypan blue staining (C) and cell titer glo (D) of 786-O IRF3 KO cells. **(E)** RT-qPCR analysis of IFNAR1 and IFNLR1 levels from 786-O cells. All samples were normalized to 18S rRNA, followed by the housekeeping gene GusB where GusB levels were set to 1. **(F)** Western blot analysis of IFNAR1 KO 786-O cells. **(G)** RT-qPCR analysis of ISG15 levels from WT and IFNAR1 KO 786-O cells treated with IFN α or β for 8h. Mock levels were set to 1. **(H, I)** Trypan blue staining (H) and cell titer glo (I) of 786-O IFNAR1 KO cells similar to A and B. Student t test was used to determine statistical significance * $p \leq 0.05$; ** $p \leq 0.005$; *** $p \leq 0.0005$; ns: not significant.

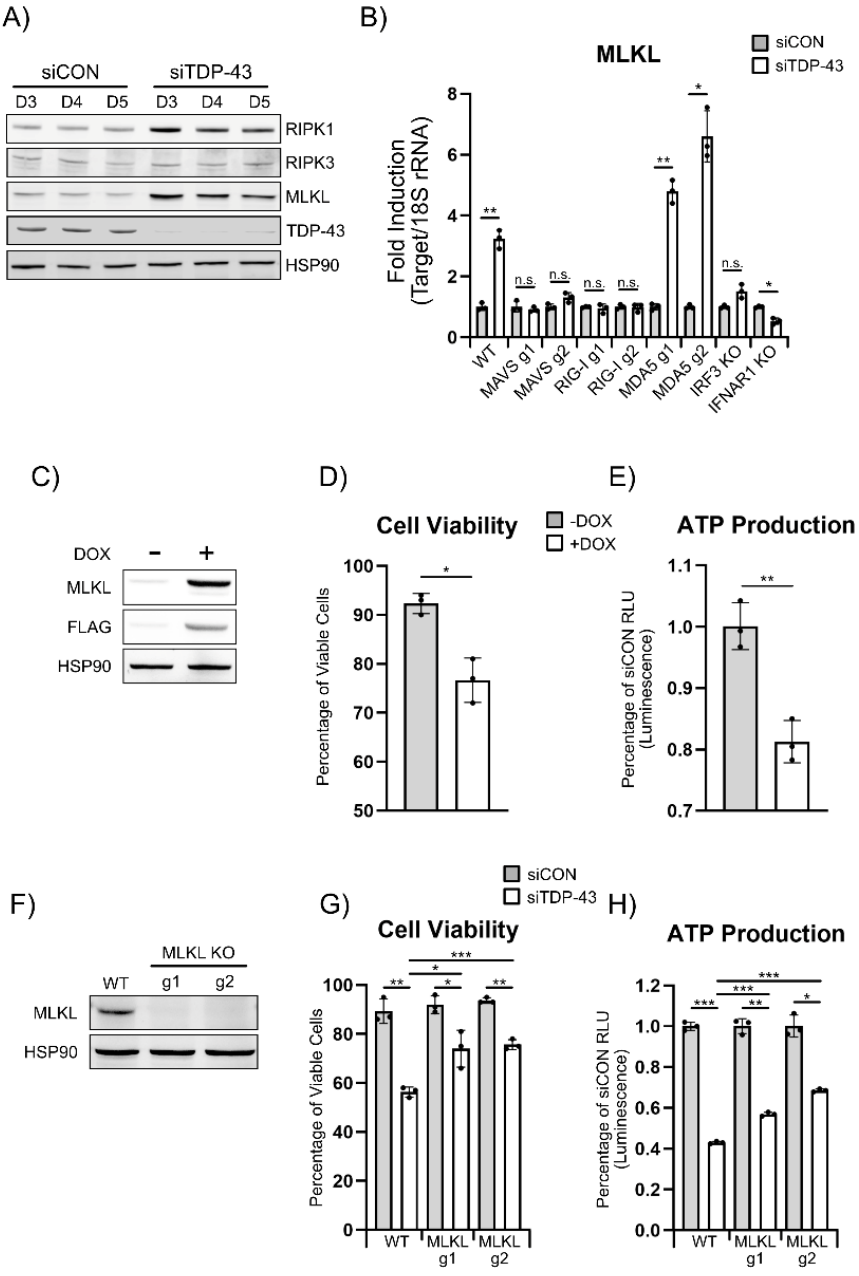

Figure S2.6: TDP-43 knockdown activates interferon-inducible MLKL overexpression induced necroptosis in 786-O cells. (A) Western blot analysis of MLKL levels from 786-O cells treated with siCON/siTDP-43. **(B)** RT-qPCR analysis of MLKL levels from 786-O WT and KO cells treated with siCON/siTDP-43 for 48h. All samples were normalized to 18S rRNA and siCON levels were set to 1. **(C)** Western blot of inducible MLKL 786-O cells where doxycycline was added for 24h. **(D, E)** Trypan blue staining (D) and cell titer glo analysis (E) of cells in D. DOX was added for 48h. **(F)** Western blot of MLKL KO 786-O cells. **(G, H)** Trypan blue staining (G) and cell titer glo analysis (H) of MLKL KO cells treated with siCON/siTDP-43 for 96h. Student t test was used to determine statistical significance * $p \leq 0.05$; ** $p \leq 0.005$; *** $p \leq 0.0005$; ns: not significant.

References:

1. Sehrawat, S.; Kumar, D.; Rouse, B.T. Herpesviruses: Harmonious Pathogens but Relevant Cofactors in Other Diseases? *Front Cell Infect Microbiol* **2018**, *8*, doi:10.3389/fcimb.2018.00177.

2. Weidner-Glunde, M.; Kruminis-Kaszkiel, E.; Savanagouder, M. Herpesviral Latency—Common Themes. *Pathogens* **2020**, *9*, doi:10.3390/pathogens9020125.

3. Grinde, B. Herpesviruses: Latency and Reactivation – Viral Strategies and Host Response. *J Oral Microbiol* **2013**, *5*, doi:10.3402/jom.v5i0.22766.

4. Jung, J.U.; Speck, S.H. Insights into Chronic Gamma-Herpesvirus Infections. *Curr Opin Virol* **2013**, *3*, 225–226, doi:10.1016/j.coviro.2013.05.018.

5. Uldrick, T.S.; Whitby, D. Update on KSHV-Epidemiology, Kaposi Sarcoma Pathogenesis, and Treatment of Kaposi Sarcoma. *Cancer Lett* **2011**, *305*, 150–162, doi:10.1016/j.canlet.2011.02.006.

6. Goncalves, P.H.; Ziegelbauer, J.; Uldrick, T.S.; Yarchoan, R. Kaposi-Sarcoma Herpesvirus Associated Cancers and Related Diseases. *Curr Opin HIV AIDS* **2017**, *12*, 47–56, doi:10.1097/COH.0000000000000330.

7. Okada, S.; Goto, H.; Yotsumoto, M. Current Status of Treatment for Primary Effusion Lymphoma. *Intractable Rare Dis Res* **2014**, *3*, 65–74, doi:10.5582/irdr.2014.01010.

8. Kumar, B.; Chandran, B. KSHV Entry and Trafficking in Target Cells—Hijacking of Cell Signal Pathways, Actin and Membrane Dynamics. *Viruses* **2016**, *8*, doi:10.3390/v8110305.

9. Purushothaman, P.; Dabral, P.; Gupta, N.; Sarkar, R.; Verma, S.C. KSHV Genome Replication and Maintenance. *Front Microbiol* **2016**, *7*, 54, doi:10.3389/fmicb.2016.00054.

10. Aneja, K.K.; Yuan, Y. Reactivation and Lytic Replication of Kaposi's Sarcoma-Associated Herpesvirus: An Update. *Front Microbiol* **2017**, *8*, doi:10.3389/fmicb.2017.00613.

11. Gould, F.; Harrison, S.M.; Hewitt, E.W.; Whitehouse, A. Kaposi's Sarcoma-Associated Herpesvirus RTA Promotes Degradation of the Hey1 Repressor Protein through the Ubiquitin Proteasome Pathway. *Journal of Virology* **2009**, *83*, 6727–6738, doi:10.1128/JVI.00351-09.

12. Yan, L.; Majerciak, V.; Zheng, Z.-M.; Lan, K. Towards Better Understanding of KSHV Life Cycle: From Transcription and Posttranscriptional Regulations to Pathogenesis. *Virol. Sin.* **2019**, *34*, 135–161, doi:10.1007/s12250-019-00114-3.

13. Purushothaman, P.; Uppal, T.; Sarkar, R.; Verma, S.C. KSHV-Mediated Angiogenesis in Tumor Progression. *Viruses* **2016**, *8*, doi:10.3390/v8070198.

14. Choi, U.Y.; Lee, J.J.; Park, A.; Zhu, W.; Lee, H.-R.; Choi, Y.J.; Yoo, J.-S.; Yu, C.; Feng, P.; Gao, S.-J.; et al. Oncogenic Human Herpesvirus Hijacks Proline Metabolism for Tumorigenesis. *PNAS* **2020**, *117*, 8083–8093, doi:10.1073/pnas.1918607117.

15. Macveigh-Fierro, D.; Rodriguez, W.; Miles, J.; Muller, M. Stealing the Show: KSHV Hijacks Host RNA Regulatory Pathways to Promote Infection. *Viruses* **2020**, *12*, doi:10.3390/v12091024.

16. Chen, C.P.; Lyu, Y.; Chuang, F.; Nakano, K.; Izumiya, C.; Jin, D.; Campbell, M.; Izumiya, Y. Kaposi's Sarcoma-Associated Herpesvirus Hijacks RNA Polymerase II To Create a Viral Transcriptional Factory. *J. Virol.* **2017**, *91*, doi:10.1128/JVI.02491-16.

17. Baquero-Perez, B.; Antanaviciute, A.; Yonchev, I.D.; Carr, I.M.; Wilson, S.A.; Whitehouse, A. The Tudor SND1 Protein Is an M6A RNA Reader Essential for Replication of Kaposi's Sarcoma-Associated Herpesvirus. *eLife* **2019**, *8*, e47261, doi:10.7554/eLife.47261.

18. Ye, F.; Chen, E.R.; Nilsen, T.W. Kaposi's Sarcoma-Associated Herpesvirus Utilizes and Manipulates RNA N6-Adenosine Methylation To Promote Lytic Replication. *J Virol* **2017**, *91*, e00466-17, e00466-17, doi:10.1128/JVI.00466-17.

19. Park, A.; Oh, S.; Jung, K.L.; Choi, U.Y.; Lee, H.-R.; Rosenfeld, M.G.; Jung, J.U. Global Epigenomic Analysis of KSHV-Infected Primary Effusion Lymphoma Identifies Functional MYC Superenhancers and Enhancer RNAs. *PNAS* **2020**, *117*, 21618–21627, doi:10.1073/pnas.1922216117.

20. Manzano, M.; Günther, T.; Ju, H.; Nicholas, J.; Bartom, E.T.; Grundhoff, A.; Gottwein, E. Kaposi's Sarcoma-Associated Herpesvirus Drives a Super-Enhancer-Mediated Survival Gene Expression Program in Primary Effusion Lymphoma. *mBio* **2020**, *11*, doi:10.1128/mBio.01457-20.

21. Kerur, N.; Veettil, M.V.; Sharma-Walia, N.; Bottero, V.; Sadagopan, S.; Otageri, P.; Chandran, B. IFI16 Acts as a Nuclear Pathogen Sensor to Induce the Inflammasome in Response to Kaposi Sarcoma Associated Herpesvirus Infection. *Cell Host Microbe* **2011**, *9*, 363–375, doi:10.1016/j.chom.2011.04.008.

22. Ma, Z.; Jacobs, S.R.; West, J.A.; Stopford, C.; Zhang, Z.; Davis, Z.; Barber, G.N.; Glaunsinger, B.A.; Dittmer, D.P.; Damania, B. Modulation of the CGAS-STING DNA Sensing Pathway by Gammaherpesviruses. *PNAS* **2015**, *112*, E4306–E4315, doi:10.1073/pnas.1503831112.

23. Naik, N.G.; Nguyen, T.H.; Roberts, L.; Fischer, L.T.; Glickman, K.; Golas, G.; Papp, B.; Toth, Z. Epigenetic Factor SiRNA Screen during Primary KSHV Infection Identifies Novel Host Restriction Factors for the Lytic Cycle of KSHV. *PLOS Pathogens* **2020**, *16*, e1008268, doi:10.1371/journal.ppat.1008268.

24. Li, D.-J.; Verma, D.; Mosbruger, T.; Swaminathan, S. CTCF and Rad21 Act as Host Cell Restriction Factors for Kaposi's Sarcoma-Associated Herpesvirus (KSHV) Lytic Replication by Modulating Viral Gene Transcription. *PLoS Pathog.* **2014**, *10*, e1003880, doi:10.1371/journal.ppat.1003880.

25. Zhao, Y.; Ye, X.; Shehata, M.; Dunker, W.; Xie, Z.; Karijolich, J. The RNA Quality Control Pathway Nonsense-Mediated MRNA Decay Targets Cellular and Viral RNAs to Restrict KSHV. *Nature Communications* **2020**, *11*, 3345, doi:10.1038/s41467-020-17151-2.

26. Li, D.; Swaminathan, S. Human IFIT Proteins Inhibit Lytic Replication of KSHV: A New Feed-Forward Loop in the Innate Immune System. *PLOS Pathogens* **2019**, *15*, e1007609, doi:10.1371/journal.ppat.1007609.

27. Zhang, Y.; Dittmer, D.P.; Mieczkowski, P.A.; Host, K.M.; Fusco, W.G.; Duncan, J.A.; Damania, B. RIG-I Detects Kaposi's Sarcoma-Associated Herpesvirus Transcripts in a RNA Polymerase III-Independent Manner. *mBio* **2018**, *9*, doi:10.1128/mBio.00823-18.

28. Zhao, Y.; Ye, X.; Dunker, W.; Song, Y.; Karijolich, J. RIG-I like Receptor Sensing of Host RNAs Facilitates the Cell-Intrinsic Immune Response to KSHV Infection. *Nature Communications* **2018**, *9*, 4841, doi:10.1038/s41467-018-07314-7.

29. Tan, A.Y.; Manley, J.L. The TET Family of Proteins: Functions and Roles in Disease. *J Mol Cell Biol* **2009**, *1*, 82–92, doi:10.1093/jmcb/mjp025.

30. Brunet, M.A.; Jacques, J.-F.; Nassari, S.; Tyzack, G.E.; McGoldrick, P.; Zinman, L.; Jean, S.; Robertson, J.; Patani, R.; Roucou, X. FUS Gene Is Dual-Coding with Both Proteins United in FUS-Mediated Toxicity. *bioRxiv* **2020**, 848580, doi:10.1101/848580.

31. Ward, C.L.; Boggio, K.J.; Johnson, B.N.; Boyd, J.B.; Douthwright, S.; Shaffer, S.A.; Landers, J.E.; Glicksman, M.A.; Bosco, D.A. A Loss of FUS/TLS Function Leads to Impaired Cellular Proliferation. *Cell Death & Disease* **2014**, *5*, e1572–e1572, doi:10.1038/cddis.2014.508.

32. Tornin, J.; Hermida-Prado, F.; Padda, R.S.; Gonzalez, M.V.; Alvarez-Fernandez, C.; Rey, V.; Martinez-Cruzado, L.; Estupiñan, O.; Menendez, S.T.; Fernandez-Nevado, L.; et al. FUS-CHOP Promotes Invasion in Myxoid Liposarcoma through a SRC/FAK/RHO/ROCK-Dependent Pathway. *Neoplasia* **2018**, *20*, 44–56, doi:10.1016/j.neo.2017.11.004.

33. Lindén, M.; Thomsen, C.; Grundevik, P.; Jonasson, E.; Andersson, D.; Runnberg, R.; Dolatabadi, S.; Vannas, C.; Luna Santamaría, M.; Fagman, H.; et al. FET Family Fusion Oncoproteins Target the SWI/SNF Chromatin Remodeling Complex. *EMBO Rep* **2019**, *20*, doi:10.15252/embr.201845766.

34. Deng, H.; Gao, K.; Jankovic, J. The Role of FUS Gene Variants in Neurodegenerative Diseases. *Nature Reviews Neurology* **2014**, *10*, 337–348, doi:10.1038/nrneurol.2014.78.

35. Prasad, A.; Bharathi, V.; Sivalingam, V.; Girdhar, A.; Patel, B.K. Molecular Mechanisms of TDP-43 Misfolding and Pathology in Amyotrophic Lateral Sclerosis. *Front. Mol. Neurosci.* **2019**, *12*, doi:10.3389/fnmol.2019.00025.

36. Yu, Y.; Reed, R. FUS Functions in Coupling Transcription to Splicing by Mediating an Interaction between RNAP II and U1 SnRNP. *PNAS* **2015**, *112*, 8608–8613, doi:10.1073/pnas.1506282112.

37. Ishigaki, S.; Masuda, A.; Fujioka, Y.; Iguchi, Y.; Katsuno, M.; Shibata, A.; Urano, F.; Sobue, G.; Ohno, K. Position-Dependent FUS-RNA Interactions Regulate Alternative Splicing Events and Transcriptions. *Sci Rep* **2012**, *2*, doi:10.1038/srep00529.

38. Rogelj, B.; Easton, L.E.; Bogu, G.K.; Stanton, L.W.; Rot, G.; Curk, T.; Zupan, B.; Sugimoto, Y.; Modic, M.; Haberman, N.; et al. Widespread Binding of FUS along Nascent RNA Regulates Alternative Splicing in the Brain. *Scientific Reports* **2012**, *2*, 603, doi:10.1038/srep00603.

39. Yamaguchi, A.; Takanashi, K. FUS Interacts with Nuclear Matrix-Associated Protein SAFB1 as Well as Matrin3 to Regulate Splicing and Ligand-Mediated Transcription. *Scientific Reports* **2016**, *6*, 35195, doi:10.1038/srep35195.

40. Morlando, M.; Dini Modigliani, S.; Torrelli, G.; Rosa, A.; Di Carlo, V.; Caffarelli, E.; Bozzoni, I. FUS Stimulates MicroRNA Biogenesis by Facilitating Co-Transcriptional Drosha Recruitment. *The EMBO Journal* **2012**, *31*, 4502–4510, doi:10.1038/emboj.2012.319.

41. Naumann, M.; Pal, A.; Goswami, A.; Lojewski, X.; Japtok, J.; Vehlow, A.; Naujock, M.; Günther, R.; Jin, M.; Stanslowsky, N.; et al. Impaired DNA Damage Response Signaling by FUS-NLS Mutations Leads to Neurodegeneration and FUS Aggregate Formation. *Nature Communications* **2018**, *9*, 335, doi:10.1038/s41467-017-02299-1.

42. Sama, R.R.K.; Ward, C.L.; Kaushansky, L.J.; Lemay, N.; Ishigaki, S.; Urano, F.; Bosco, D.A. FUS/TLS Assembles into Stress Granules and Is a Prosurvival Factor during Hyperosmolar Stress. *J. Cell. Physiol.* **2013**, *228*, 2222–2231, doi:10.1002/jcp.24395.

43. Shelkovnikova, T.A.; Robinson, H.K.; Troakes, C.; Ninkina, N.; Buchman, V.L. Compromised Paraspeckle Formation as a Pathogenic Factor in FUSopathies. *Hum Mol Genet* **2014**, *23*, 2298–2312, doi:10.1093/hmg/ddt622.

44. Coady, T.H.; Manley, J.L. ALS Mutations in TLS/FUS Disrupt Target Gene Expression. *Genes Dev.* **2015**, *29*, 1696–1706, doi:10.1101/gad.267286.115.

45. Fujii, R.; Takumi, T. TLS Facilitates Transport of MRNA Encoding an Actin-Stabilizing Protein to Dendritic Spines. *Journal of Cell Science* **2005**, *118*, 5755–5765, doi:10.1242/jcs.02692.

46. Yang, L.; Gal, J.; Chen, J.; Zhu, H. Self-Assembled FUS Binds Active Chromatin and Regulates Gene Transcription. *Proc. Natl. Acad. Sci. U.S.A.* **2014**, *111*, 17809–17814, doi:10.1073/pnas.1414004111.

47. Tan, A.Y.; Riley, T.R.; Coady, T.; Bussemaker, H.J.; Manley, J.L. TLS/FUS (Translocated in Liposarcoma/Fused in Sarcoma) Regulates Target Gene Transcription via Single-Stranded DNA Response Elements. *Proc. Natl. Acad. Sci. U.S.A.* **2012**, *109*, 6030–6035, doi:10.1073/pnas.1203028109.

48. Tan, A.Y.; Manley, J.L. TLS Inhibits RNA Polymerase III Transcription. *Mol Cell Biol* **2010**, *30*, 186–196, doi:10.1128/MCB.00884-09.

49. Chen, C.; Ding, X.; Akram, N.; Xue, S.; Luo, S.-Z. Fused in Sarcoma: Properties, Self-Assembly and Correlation with Neurodegenerative Diseases. *Molecules* **2019**, *24*, doi:10.3390/molecules24081622.

50. Schwartz, J.C.; Ebmeier, C.C.; Podell, E.R.; Heimiller, J.; Taatjes, D.J.; Cech, T.R. FUS Binds the CTD of RNA Polymerase II and Regulates Its Phosphorylation at Ser2. *Genes Dev.* **2012**, *26*, 2690–2695, doi:10.1101/gad.204602.112.

51. Peng, L.; Li, E.-M.; Xu, L.-Y. From Start to End: Phase Separation and Transcriptional Regulation. *Biochimica et Biophysica Acta (BBA) - Gene Regulatory Mechanisms* **2020**, *1863*, 194641, doi:10.1016/j.bbagrm.2020.194641.

52. Hicks, G.G.; Singh, N.; Nashabi, A.; Mai, S.; Bozek, G.; Klewes, L.; Arapovic, D.; White, E.K.; Koury, M.J.; Oltz, E.M.; et al. Fus Deficiency in Mice Results in Defective B-Lymphocyte Development and Activation, High Levels of Chromosomal Instability and Perinatal Death. *Nat. Genet.* **2000**, *24*, 175–179, doi:10.1038/72842.

53. Mogensen, T.H. Pathogen Recognition and Inflammatory Signaling in Innate Immune Defenses. *Clin Microbiol Rev* **2009**, *22*, 240–273, doi:10.1128/CMR.00046-08.

54. Takeuchi, O.; Akira, S. Pattern Recognition Receptors and Inflammation. *Cell* **2010**, *140*, 805–820, doi:10.1016/j.cell.2010.01.022.

55. Schlee, M.; Hartmann, G. Discriminating Self from Non-Self in Nucleic Acid Sensing. *Nature Reviews Immunology* **2016**, *16*, 566–580, doi:10.1038/nri.2016.78.

56. Ablasser, A.; Bauernfeind, F.; Hartmann, G.; Latz, E.; Fitzgerald, K.A.; Hornung, V. RIG-I-Dependent Sensing of Poly(DA:DT) through the Induction of an RNA Polymerase III–transcribed RNA Intermediate. *Nature Immunology* **2009**, *10*, 1065–1072, doi:10.1038/ni.1779.

57. Chiu, Y.-H.; MacMillan, J.B.; Chen, Z.J. RNA Polymerase III Detects Cytosolic DNA and Induces Type-I Interferons Through the RIG-I Pathway. *Cell* **2009**, *138*, 576–591, doi:10.1016/j.cell.2009.06.015.

58. Rehwinkel, J.; Gack, M.U. RIG-I-like Receptors: Their Regulation and Roles in RNA Sensing. *Nature Reviews Immunology* **2020**, *20*, 537–551, doi:10.1038/s41577-020-0288-3.

59. Dixit, E.; Boulant, S.; Zhang, Y.; Lee, A.S.Y.; Odendall, C.; Shum, B.; Hacohen, N.; Chen, Z.J.; Whelan, S.P.; Fransen, M.; et al. Peroxisomes Are Signaling Platforms for Antiviral Innate Immunity. *Cell* **2010**, *141*, 668–681, doi:10.1016/j.cell.2010.04.018.

60. Hornung, V.; Ellegast, J.; Kim, S.; Brzózka, K.; Jung, A.; Kato, H.; Poeck, H.; Akira, S.; Conzelmann, K.-K.; Schlee, M.; et al. 5′-Triphosphate RNA Is the Ligand for RIG-I. *Science* **2006**, *314*, 994–997, doi:10.1126/science.1132505.

61. Kato, H.; Takeuchi, O.; Mikamo-Satoh, E.; Hirai, R.; Kawai, T.; Matsushita, K.; Hiiragi, A.; Dermody, T.S.; Fujita, T.; Akira, S. Length-Dependent Recognition of Double-Stranded Ribonucleic Acids by Retinoic Acid–inducible Gene-I and Melanoma Differentiation–associated Gene 5. *J Exp Med* **2008**, *205*, 1601–1610, doi:10.1084/jem.20080091.

62. Pichlmair, A.; Schulz, O.; Tan, C.P.; Näslund, T.I.; Liljeström, P.; Weber, F.; Reis e Sousa, C. RIG-I-Mediated Antiviral Responses to Single-Stranded RNA Bearing 5′-Phosphates. *Science* **2006**, *314*, 997–1001, doi:10.1126/science.1132998.

63. Rehwinkel, J.; Tan, C.P.; Goubau, D.; Schulz, O.; Pichlmair, A.; Bier, K.; Robb, N.; Vreede, F.; Barclay, W.; Fodor, E.; et al. RIG-I Detects Viral Genomic RNA during Negative-Strand RNA Virus Infection. *Cell* **2010**, *140*, 397–408, doi:10.1016/j.cell.2010.01.020.

64. Schlee, M.; Roth, A.; Hornung, V.; Hagmann, C.A.; Wimmenauer, V.; Barchet, W.; Coch, C.; Janke, M.; Mihailovic, A.; Wardle, G.; et al. Recognition of 5′ Triphosphate by RIG-I Helicase Requires Short Blunt Double-Stranded RNA as Contained in Panhandle of Negative-Strand Virus. *Immunity* **2009**, *31*, 25–34, doi:10.1016/j.immuni.2009.05.008.

65. Schmidt, A.; Schwerd, T.; Hamm, W.; Hellmuth, J.C.; Cui, S.; Wenzel, M.; Hoffmann, F.S.; Michallet, M.-C.; Besch, R.; Hopfner, K.-P.; et al. 5′-Triphosphate RNA Requires Base-Paired Structures to Activate Antiviral Signaling via RIG-I. *PNAS* **2009**, *106*, 12067–12072, doi:10.1073/pnas.0900971106.

66. Chen, Y.G.; Kim, M.V.; Chen, X.; Batista, P.J.; Aoyama, S.; Wilusz, J.E.; Iwasaki, A.; Chang, H.Y. Sensing Self and Foreign Circular RNAs by Intron Identity. *Molecular Cell* **2017**, *67*, 228-238.e5, doi:10.1016/j.molcel.2017.05.022.

67. Schuberth-Wagner, C.; Ludwig, J.; Bruder, A.K.; Herzner, A.-M.; Zillinger, T.; Goldeck, M.; Schmidt, T.; Schmid-Burgk, J.L.; Kerber, R.; Wolter, S.; et al. A Conserved Histidine in the RNA Sensor RIG-

I Controls Immune Tolerance to N1-2'O-Methylated Self RNA. *Immunity* **2015**, *43*, 41–51, doi:10.1016/j.immuni.2015.06.015.

68. Kato, H.; Takeuchi, O.; Sato, S.; Yoneyama, M.; Yamamoto, M.; Matsui, K.; Uematsu, S.; Jung, A.; Kawai, T.; Ishii, K.J.; et al. Differential Roles of MDA5 and RIG-I Helicases in the Recognition of RNA Viruses. *Nature* **2006**, *441*, 101–105, doi:10.1038/nature04734.

69. Lazear, H.M.; Schoggins, J.W.; Diamond, M.S. Shared and Distinct Functions of Type I and Type III Interferons. *Immunity* **2019**, *50*, 907–923, doi:10.1016/j.immuni.2019.03.025.

70. Wu, Y.; Zhao, W.; Liu, Y.; Tan, X.; Li, X.; Zou, Q.; Xiao, Z.; Xu, H.; Wang, Y.; Yang, X. Function of HNRNPC in Breast Cancer Cells by Controlling the DsRNA-induced Interferon Response. *The EMBO Journal* **2018**, *37*, e99017, doi:10.15252/embj.201899017.

71. König, J.; Zarnack, K.; Rot, G.; Curk, T.; Kayikci, M.; Zupan, B.; Turner, D.J.; Luscombe, N.M.; Ule, J. ICLIP Reveals the Function of HnRNP Particles in Splicing at Individual Nucleotide Resolution. *Nat. Struct. Mol. Biol.* **2010**, *17*, 909–915, doi:10.1038/nsmb.1838.

72. Zarnack, K.; König, J.; Tajnik, M.; Martincorena, I.; Eustermann, S.; Stévant, I.; Reyes, A.; Anders, S.; Luscombe, N.M.; Ule, J. Direct Competition between HnRNP C and U2AF65 Protects the Transcriptome from the Exonization of Alu Elements. *Cell* **2013**, *152*, 453–466, doi:10.1016/j.cell.2012.12.023.

73. Kim, U.; Wang, Y.; Sanford, T.; Zeng, Y.; Nishikura, K. Molecular Cloning of CDNA for Double-Stranded RNA Adenosine Deaminase, a Candidate Enzyme for Nuclear RNA Editing. *Proc. Natl. Acad. Sci. U.S.A.* **1994**, *91*, 11457–11461, doi:10.1073/pnas.91.24.11457.

74. Liddicoat, B.J.; Piskol, R.; Chalk, A.M.; Ramaswami, G.; Higuchi, M.; Hartner, J.C.; Li, J.B.; Seeburg, P.H.; Walkley, C.R. RNA Editing by ADAR1 Prevents MDA5 Sensing of Endogenous DsRNA as Nonself. *Science* **2015**, *349*, 1115–1120, doi:10.1126/science.aac7049.

75. Mannion, N.M.; Greenwood, S.M.; Young, R.; Cox, S.; Brindle, J.; Read, D.; Nellåker, C.; Vesely, C.; Ponting, C.P.; McLaughlin, P.J.; et al. The RNA-Editing Enzyme ADAR1 Controls Innate Immune Responses to RNA. *Cell Reports* **2014**, *9*, 1482–1494, doi:10.1016/j.celrep.2014.10.041.

76. Melcher, T.; Maas, S.; Herb, A.; Sprengel, R.; Seeburg, P.H.; Higuchi, M. A Mammalian RNA Editing Enzyme. *Nature* **1996**, *379*, 460–464, doi:10.1038/379460a0.

77. Nishikura, K.; Yoo, C.; Kim, U.; Murray, J.M.; Estes, P.A.; Cash, F.E.; Liebhaber, S.A. Substrate Specificity of the DsRNA Unwinding/Modifying Activity. *EMBO J.* **1991**, *10*, 3523–3532.

78. Pestal, K.; Funk, C.C.; Snyder, J.M.; Price, N.D.; Treuting, P.M.; Stetson, D.B. Isoforms of RNA-Editing Enzyme ADAR1 Independently Control Nucleic Acid Sensor MDA5-Driven Autoimmunity and Multi-Organ Development. *Immunity* **2015**, *43*, 933–944, doi:10.1016/j.immuni.2015.11.001.

79. Nabet, B.Y.; Qiu, Y.; Shabason, J.E.; Wu, T.J.; Yoon, T.; Kim, B.C.; Benci, J.L.; DeMichele, A.M.; Tchou, J.; Marcotrigiano, J.; et al. Exosome RNA Unshielding Couples Stromal Activation to Pattern Recognition Receptor Signaling in Cancer. *Cell* **2017**, *170*, 352-366.e13, doi:10.1016/j.cell.2017.06.031.

80. Chiang, J.J.; Sparrer, K.M.J.; van Gent, M.; Lässig, C.; Huang, T.; Osterrieder, N.; Hopfner, K.-P.; Gack, M.U. Viral Unmasking of Cellular 5S RRNA Pseudogene Transcripts Induces RIG-I-Mediated Immunity. *Nature Immunology* **2018**, *19*, 53–62, doi:10.1038/s41590-017-0005-y.

81. Kato, H.; Oh, S.-W.; Fujita, T. RIG-I-Like Receptors and Type I Interferonopathies. *J Interferon Cytokine Res* **2017**, *37*, 207–213, doi:10.1089/jir.2016.0095.

82. Kotredes, K.P.; Gamero, A.M. Interferons as Inducers of Apoptosis in Malignant Cells. *J Interferon Cytokine Res* **2013**, *33*, 162–170, doi:10.1089/jir.2012.0110.

83. Yang, D.; Liang, Y.; Zhao, S.; Ding, Y.; Zhuang, Q.; Shi, Q.; Ai, T.; Wu, S.-Q.; Han, J. ZBP1 Mediates Interferon-Induced Necroptosis. *Cellular & Molecular Immunology* **2020**, *17*, 356–368, doi:10.1038/s41423-019-0237-x.

84. Thapa, R.J.; Nogusa, S.; Chen, P.; Maki, J.L.; Lerro, A.; Andrake, M.; Rall, G.F.; Degterev, A.; Balachandran, S. Interferon-Induced RIP1/RIP3-Mediated Necrosis Requires PKR and Is Licensed by FADD and Caspases. *PNAS* **2013**, *110*, E3109–E3118, doi:10.1073/pnas.1301218110.

85. Malireddi, R.K.S.; Kanneganti, T.-D. Role of Type I Interferons in Inflammasome Activation, Cell Death, and Disease during Microbial Infection. *Front Cell Infect Microbiol* **2013**, *3*, doi:10.3389/fcimb.2013.00077.

86. Bampton, A.; Gittings, L.M.; Fratta, P.; Lashley, T.; Gatt, A. The Role of HnRNPs in Frontotemporal Dementia and Amyotrophic Lateral Sclerosis. *Acta Neuropathol* **2020**, *140*, 599–623, doi:10.1007/s00401-020-02203-0.

87. Broeck, L.V.; Callaerts, P.; Dermaut, B. TDP-43-Mediated Neurodegeneration: Towards a Loss-of-Function Hypothesis? *Trends in Molecular Medicine* **2014**, *20*, 66–71, doi:10.1016/j.molmed.2013.11.003.

88. Kraemer, B.C.; Schuck, T.; Wheeler, J.M.; Robinson, L.C.; Trojanowski, J.Q.; Lee, V.M.Y.; Schellenberg, G.D. Loss of Murine TDP-43 Disrupts Motor Function and Plays an Essential Role in Embryogenesis. *Acta Neuropathol* **2010**, *119*, 409–419, doi:10.1007/s00401-010-0659-0.

89. Schmid, B.; Hruscha, A.; Hogl, S.; Banzhaf-Strathmann, J.; Strecker, K.; van der Zee, J.; Teucke, M.; Eimer, S.; Hegermann, J.; Kittelmann, M.; et al. Loss of ALS-Associated TDP-43 in Zebrafish Causes Muscle Degeneration, Vascular Dysfunction, and Reduced Motor Neuron Axon Outgrowth. *Proc Natl Acad Sci U S A* **2013**, *110*, 4986–4991, doi:10.1073/pnas.1218311110.

90. Barmada, S.J.; Skibinski, G.; Korb, E.; Rao, E.J.; Wu, J.Y.; Finkbeiner, S. Cytoplasmic Mislocalization of TDP-43 Is Toxic to Neurons and Enhanced by a Mutation Associated with Familial Amyotrophic Lateral Sclerosis. *J Neurosci* **2010**, *30*, 639–649, doi:10.1523/JNEUROSCI.4988-09.2010.

91. Weihl, C.C.; Temiz, P.; Miller, S.E.; Watts, G.; Smith, C.; Forman, M.; Hanson, P.I.; Kimonis, V.; Pestronk, A. TDP-43 Accumulation in Inclusion Body Myopathy Muscle Suggests a Common Pathogenic Mechanism with Frontotemporal Dementia. *J. Neurol. Neurosurg. Psychiatry* **2008**, *79*, 1186–1189, doi:10.1136/jnnp.2007.131334.

92. Ke, H.; Zhao, L.; Zhang, H.; Feng, X.; Xu, H.; Hao, J.; Wang, S.; Yang, Q.; Zou, L.; Su, X.; et al. Loss of TDP43 Inhibits Progression of Triple-Negative Breast Cancer in Coordination with SRSF3. *Proc Natl Acad Sci USA* **2018**, *115*, E3426–E3435, doi:10.1073/pnas.1714573115.

93. Mitra, J.; Guerrero, E.N.; Hegde, P.M.; Liachko, N.F.; Wang, H.; Vasquez, V.; Gao, J.; Pandey, A.; Taylor, J.P.; Kraemer, B.C.; et al. Motor Neuron Disease-Associated Loss of Nuclear TDP-43 Is Linked to DNA Double-Strand Break Repair Defects. *PNAS* **2019**, *116*, 4696–4705, doi:10.1073/pnas.1818415116.

94. O'Rourke, J.G.; Bogdanik, L.; Yáñez, A.; Lall, D.; Wolf, A.J.; Muhammad, A.K.M.G.; Ho, R.; Carmona, S.; Vit, J.P.; Zarrow, J.; et al. C9orf72 Is Required for Proper Macrophage and Microglial Function in Mice. *Science* **2016**, *351*, 1324–1329, doi:10.1126/science.aaf1064.

95. WANG, R.; YANG, B.; ZHANG, D. Activation of Interferon Signaling Pathways in Spinal Cord Astrocytes from an ALS Mouse Model. *Glia* **2011**, *59*, 946–958, doi:10.1002/glia.21167.

96. Taylor, J.M.; Minter, M.R.; Newman, A.G.; Zhang, M.; Adlard, P.A.; Crack, P.J. Type-1 Interferon Signaling Mediates Neuro-Inflammatory Events in Models of Alzheimer's Disease. *Neurobiology of Aging* **2014**, *35*, 1012–1023, doi:10.1016/j.neurobiolaging.2013.10.089.

97. Hu, Y.; Cao, C.; Qin, X.-Y.; Yu, Y.; Yuan, J.; Zhao, Y.; Cheng, Y. Increased Peripheral Blood Inflammatory Cytokine Levels in Amyotrophic Lateral Sclerosis: A Meta-Analysis Study. *Sci Rep* **2017**, *7*, 9094, doi:10.1038/s41598-017-09097-1.

98. Yu, C.-H.; Davidson, S.; Harapas, C.R.; Hilton, J.B.; Mlodzianoski, M.J.; Laohamonthonkul, P.; Louis, C.; Low, R.R.J.; Moecking, J.; De Nardo, D.; et al. TDP-43 Triggers Mitochondrial DNA Release via MPTP to Activate CGAS/STING in ALS. *Cell* **2020**, S0092867420311612, doi:10.1016/j.cell.2020.09.020.

99. Lee, S.; Kim, S.; Kang, H.-Y.; Lim, H.R.; Kwon, Y.; Jo, M.; Jeon, Y.-M.; Kim, S.R.; Kim, K.; Ha, C.M.; et al. The Overexpression of TDP-43 in Astrocytes Causes Neurodegeneration via a PTP1B-Mediated Inflammatory Response. *Journal of Neuroinflammation* **2020**, *17*, 299, doi:10.1186/s12974-020-01963-6.

100. Correia, A.S.; Patel, P.; Dutta, K.; Julien, J.-P. Inflammation Induces TDP-43 Mislocalization and Aggregation. *PLoS One* **2015**, *10*, e0140248, doi:10.1371/journal.pone.0140248.

101. Polymenidou, M.; Lagier-Tourenne, C.; Hutt, K.R.; Huelga, S.C.; Moran, J.; Liang, T.Y.; Ling, S.-C.; Sun, E.; Wancewicz, E.; Mazur, C.; et al. Long Pre-MRNA Depletion and RNA Missplicing Contribute to Neuronal Vulnerability from Loss of TDP-43. *Nature Neuroscience* **2011**, *14*, 459–468, doi:10.1038/nn.2779.

102. Tollervey, J.R.; Curk, T.; Rogelj, B.; Briese, M.; Cereda, M.; Kayikci, M.; König, J.; Hortobágyi, T.; Nishimura, A.L.; Župunski, V.; et al. Characterizing the RNA Targets and Position-Dependent Splicing Regulation by TDP-43. *Nature Neuroscience* **2011**, *14*, 452–458, doi:10.1038/nn.2778.

103. Buratti, E.; Baralle, F.E. TDP-43: Gumming up Neurons through Protein–protein and Protein–RNA Interactions. *Trends in Biochemical Sciences* **2012**, *37*, 237–247, doi:10.1016/j.tibs.2012.03.003.

104. Izumikawa, K.; Nobe, Y.; Ishikawa, H.; Yamauchi, Y.; Taoka, M.; Sato, K.; Nakayama, H.; Simpson, R.J.; Isobe, T.; Takahashi, N. TDP-43 Regulates Site-Specific 2'-O-Methylation of U1 and U2 SnRNAs via Controlling the Cajal Body Localization of a Subset of C/D ScaRNAs. *Nucleic Acids Res.* **2019**, *47*, 2487–2505, doi:10.1093/nar/gkz086.

105. Chou, C.-C.; Zhang, Y.; Umoh, M.E.; Vaughan, S.W.; Lorenzini, I.; Liu, F.; Sayegh, M.; Donlin-Asp, P.G.; Chen, Y.H.; Duong, D.M.; et al. TDP-43 Pathology Disrupts Nuclear Pore Complexes and Nucleocytoplasmic Transport in ALS/FTD. *Nature Neuroscience* **2018**, *21*, 228–239, doi:10.1038/s41593-017-0047-3.

106. Alami, N.H.; Smith, R.B.; Carrasco, M.A.; Williams, L.A.; Winborn, C.S.; Han, S.S.W.; Kiskinis, E.; Winborn, B.; Freibaum, B.D.; Kanagaraj, A.; et al. Axonal Transport of TDP-43 MRNA Granules Is Impaired by ALS-Causing Mutations. *Neuron* **2014**, *81*, 536–543, doi:10.1016/j.neuron.2013.12.018.

107. Khalfallah, Y.; Kuta, R.; Grasmuck, C.; Prat, A.; Durham, H.D.; Vande Velde, C. TDP-43 Regulation of Stress Granule Dynamics in Neurodegenerative Disease-Relevant Cell Types. *Scientific Reports* **2018**, *8*, 7551, doi:10.1038/s41598-018-25767-0.

108. Modic, M.; Grosch, M.; Rot, G.; Schirge, S.; Lepko, T.; Yamazaki, T.; Lee, F.C.Y.; Rusha, E.; Shaposhnikov, D.; Palo, M.; et al. Cross-Regulation between TDP-43 and Paraspeckles Promotes Pluripotency-Differentiation Transition. *Mol. Cell* **2019**, doi:10.1016/j.molcel.2019.03.041.

109. Chung, C.-Y.; Berson, A.; Kennerdell, J.R.; Sartoris, A.; Unger, T.; Porta, S.; Kim, H.-J.; Smith, E.R.; Shilatifard, A.; Van Deerlin, V.; et al. Aberrant Activation of Non-Coding RNA Targets of Transcriptional Elongation Complexes Contributes to TDP-43 Toxicity. *Nat Commun* **2018**, *9*, 4406, doi:10.1038/s41467-018-06543-0.

110. Kawahara, Y.; Mieda-Sato, A. TDP-43 Promotes MicroRNA Biogenesis as a Component of the Drosha and Dicer Complexes. *Proceedings of the National Academy of Sciences* **2012**, *109*, 3347–3352, doi:10.1073/pnas.1112427109.

111. Saldi, T.K.; Ash, P.E.; Wilson, G.; Gonzales, P.; Garrido-Lecca, A.; Roberts, C.M.; Dostal, V.; Gendron, T.F.; Stein, L.D.; Blumenthal, T.; et al. TDP-1, the Caenorhabditis Elegans Ortholog of TDP-43, Limits the Accumulation of Double-Stranded RNA. *EMBO J.* **2014**, *33*, 2947–2966, doi:10.15252/embj.201488740.

112. Shelkovnikova, T.A.; Kukharsky, M.S.; An, H.; Dimasi, P.; Alexeeva, S.; Shabir, O.; Heath, P.R.; Buchman, V.L. Protective Paraspeckle Hyper-Assembly Downstream of TDP-43 Loss of Function in Amyotrophic Lateral Sclerosis. *Mol Neurodegener* **2018**, *13*, 30, doi:10.1186/s13024-018-0263-7.

113. Lander, E.S.; Linton, L.M.; Birren, B.; Nusbaum, C.; Zody, M.C.; Baldwin, J.; Devon, K.; Dewar, K.; Doyle, M.; FitzHugh, W.; et al. Initial Sequencing and Analysis of the Human Genome. *Nature* **2001**, *409*, 860–921, doi:10.1038/35057062.

114. Venter, J.C.; Adams, M.D.; Myers, E.W.; Li, P.W.; Mural, R.J.; Sutton, G.G.; Smith, H.O.; Yandell, M.; Evans, C.A.; Holt, R.A.; et al. The Sequence of the Human Genome. *Science* **2001**, *291*, 1304–1351, doi:10.1126/science.1058040.

115. Li, W.; Jin, Y.; Prazak, L.; Hammell, M.; Dubnau, J. Transposable Elements in TDP-43-Mediated Neurodegenerative Disorders. *PLoS One* **2012**, *7*, doi:10.1371/journal.pone.0044099.

116. Morera, A.A.; Ahmed, N.S.; Schwartz, J.C. TDP-43 Regulates Transcription at Protein-Coding Genes and Alu Retrotransposons. *Biochimica et Biophysica Acta (BBA) - Gene Regulatory Mechanisms* **2019**, 194434, doi:10.1016/j.bbagrm.2019.194434.

117. Liu, E.Y.; Russ, J.; Cali, C.P.; Phan, J.M.; Amlie-Wolf, A.; Lee, E.B. Loss of Nuclear TDP-43 Is Associated with Decondensation of LINE Retrotransposons. *Cell Reports* **2019**, *27*, 1409-1421.e6, doi:10.1016/j.celrep.2019.04.003.

118. Chang, Y.; Cesarman, E.; Pessin, M.S.; Lee, F.; Culpepper, J.; Knowles, D.M.; Moore, P.S. Identification of Herpesvirus-like DNA Sequences in AIDS-Associated Kaposi's Sarcoma. *Science* **1994**, *266*, 1865–1869.

119. Kedes, D.H.; Operskalski, E.; Busch, M.; Kohn, R.; Flood, J.; Ganem, D. The Seroepidemiology of Human Herpesvirus 8 (Kaposi's Sarcoma–associated Herpesvirus): Distribution of Infection in KS Risk Groups and Evidence for Sexual Transmission. *Nat Med* **1996**, *2*, 918–924, doi:10.1038/nm0896-918.

120. Moore, P.S.; Chang, Y. Detection of Herpesvirus-like DNA Sequences in Kaposi's Sarcoma in Patients with and Those without HIV Infection. *N. Engl. J. Med.* **1995**, *332*, 1181–1185, doi:10.1056/NEJM199505043321801.

121. Mesri, E.A.; Feitelson, M.A.; Munger, K. Human Viral Oncogenesis: A Cancer Hallmarks Analysis. *Cell Host & Microbe* **2014**, *15*, 266–282, doi:10.1016/j.chom.2014.02.011.

122. Cesarman, E.; Chang, Y.; Moore, P.S.; Said, J.W.; Knowles, D.M. Kaposi's Sarcoma-Associated Herpesvirus-like DNA Sequences in AIDS-Related Body-Cavity-Based Lymphomas. *N. Engl. J. Med.* **1995**, *332*, 1186–1191, doi:10.1056/NEJM199505043321802.

123. Soulier, J.; Grollet, L.; Oksenhendler, E.; Cacoub, P.; Cazals-Hatem, D.; Babinet, P.; d'Agay, M.F.; Clauvel, J.P.; Raphael, M.; Degos, L. Kaposi's Sarcoma-Associated Herpesvirus-like DNA Sequences in Multicentric Castleman's Disease. *Blood* **1995**, *86*, 1276–1280.

124. Purushothaman, P.; Uppal, T.; Verma, S.C. Molecular Biology of KSHV Lytic Reactivation. *Viruses* **2015**, *7*, 116–153, doi:10.3390/v7010116.

125. Aneja, K.K.; Yuan, Y. Reactivation and Lytic Replication of Kaposi's Sarcoma-Associated Herpesvirus: An Update. *Front Microbiol* **2017**, *8*, doi:10.3389/fmicb.2017.00613.

126. Jr, J.F.; Kong, W.; Hottiger, M.O.; Nabel, G.J. P53 Inhibition by the LANA Protein of KSHV Protects against Cell Death. *Nature* **1999**, *402*, 889–894, doi:10.1038/47266.

127. Radkov, S.A.; Kellam, P.; Boshoff, C. The Latent Nuclear Antigen of Kaposi Sarcoma-Associated Herpesvirus Targets the Retinoblastoma–E2F Pathway and with the Oncogene *Hras* Transforms Primary Rat Cells. *Nature Medicine* **2000**, *6*, 1121–1127, doi:10.1038/80459.

128. Guasparri, I.; Keller, S.A.; Cesarman, E. KSHV VFLIP Is Essential for the Survival of Infected Lymphoma Cells. *J Exp Med* **2004**, *199*, 993–1003, doi:10.1084/jem.20031467.

129. Field, N.; Low, W.; Daniels, M.; Howell, S.; Daviet, L.; Boshoff, C.; Collins, M. KSHV VFLIP Binds to IKK-Gamma to Activate IKK. *J. Cell. Sci.* **2003**, *116*, 3721–3728, doi:10.1242/jcs.00691.

130. Liu, L.; Eby, M.T.; Rathore, N.; Sinha, S.K.; Kumar, A.; Chaudhary, P.M. The Human Herpes Virus 8-Encoded Viral FLICE Inhibitory Protein Physically Associates with and Persistently Activates the Ikappa B Kinase Complex. *J. Biol. Chem.* **2002**, *277*, 13745–13751, doi:10.1074/jbc.M110480200.

131. Chaudhary, P.M.; Jasmin, A.; Eby, M.T.; Hood, L. Modulation of the NF-Kappa B Pathway by Virally Encoded Death Effector Domains-Containing Proteins. *Oncogene* **1999**, *18*, 5738–5746, doi:10.1038/sj.onc.1202976.

132. Casper, C.; Nichols, W.G.; Huang, M.-L.; Corey, L.; Wald, A. Remission of HHV-8 and HIV-Associated Multicentric Castleman Disease with Ganciclovir Treatment. *Blood* **2004**, *103*, 1632–1634, doi:10.1182/blood-2003-05-1721.

133. Crum-Cianflone, N.F.; Wallace, M.R.; Looney, D. Successful Secondary Prophylaxis for Primary Effusion Lymphoma with Human Herpesvirus 8 Therapy. *AIDS* **2006**, *20*, 1567–1569, doi:10.1097/01.aids.0000237381.92303.61.

134. Hocqueloux, L.; Agbalika, F.; Oksenhendler, E.; Molina, J.M. Long-Term Remission of an AIDS-Related Primary Effusion Lymphoma with Antiviral Therapy. *AIDS* **2001**, *15*, 280–282.

135. Luppi, M.; Trovato, R.; Barozzi, P.; Vallisa, D.; Rossi, G.; Re, A.; Ravazzini, L.; Potenza, L.; Riva, G.; Morselli, M.; et al. Treatment of Herpesvirus Associated Primary Effusion Lymphoma with Intracavity Cidofovir. *Leukemia* **2005**, *19*, 473–476, doi:10.1038/sj.leu.2403646.

136. Martin, D.F.; Kuppermann, B.D.; Wolitz, R.A.; Palestine, A.G.; Li, H.; Robinson, C.A. Oral Ganciclovir for Patients with Cytomegalovirus Retinitis Treated with a Ganciclovir Implant. Roche Ganciclovir Study Group. *N. Engl. J. Med.* **1999**, *340*, 1063–1070, doi:10.1056/NEJM199904083401402.

137. Bais, C.; Santomasso, B.; Coso, O.; Arvanitakis, L.; Raaka, E.G.; Gutkind, J.S.; Asch, A.S.; Cesarman, E.; Gershengorn, M.C.; Mesri, E.A.; et al. G-Protein-Coupled Receptor of Kaposi's Sarcoma-Associated Herpesvirus Is a Viral Oncogene and Angiogenesis Activator. *Nature* **1998**, *391*, 86–89, doi:10.1038/34193.

138. Staskus, K.A.; Zhong, W.; Gebhard, K.; Herndier, B.; Wang, H.; Renne, R.; Beneke, J.; Pudney, J.; Anderson, D.J.; Ganem, D.; et al. Kaposi's Sarcoma-Associated Herpesvirus Gene Expression in Endothelial (Spindle) Tumor Cells. *J Virol* **1997**, *71*, 715–719.

139. Staudt, M.R.; Kanan, Y.; Jeong, J.H.; Papin, J.F.; Hines-Boykin, R.; Dittmer, D.P. The Tumor Microenvironment Controls Primary Effusion Lymphoma Growth in Vivo. *Cancer Res.* **2004**, *64*, 4790–4799, doi:10.1158/0008-5472.CAN-03-3835.

140. Sun, R.; Lin, S.-F.; Gradoville, L.; Yuan, Y.; Zhu, F.; Miller, G. A Viral Gene That Activates Lytic Cycle Expression of Kaposi's Sarcoma-Associated Herpesvirus. *PNAS* **1998**, *95*, 10866–10871.

141. Lukac, D.M.; Renne, R.; Kirshner, J.R.; Ganem, D. Reactivation of Kaposi's Sarcoma-Associated Herpesvirus Infection from Latency by Expression of the ORF 50 Transactivator, a Homolog of the EBV R Protein. *Virology* **1998**, *252*, 304–312, doi:10.1006/viro.1998.9486.

142. Xu, Y.; AuCoin, D.P.; Huete, A.R.; Cei, S.A.; Hanson, L.J.; Pari, G.S. A Kaposi's Sarcoma-Associated Herpesvirus/Human Herpesvirus 8 ORF50 Deletion Mutant Is Defective for Reactivation of Latent Virus and DNA Replication. *J. Virol.* **2005**, *79*, 3479–3487, doi:10.1128/JVI.79.6.3479-3487.2005.

143. Lukac, D.M.; Garibyan, L.; Kirshner, J.R.; Palmeri, D.; Ganem, D. DNA Binding by Kaposi's Sarcoma-Associated Herpesvirus Lytic Switch Protein Is Necessary for Transcriptional Activation of Two Viral Delayed Early Promoters. *J. Virol.* **2001**, *75*, 6786–6799, doi:10.1128/JVI.75.15.6786-6799.2001.

144. Carroll, K.D.; Khadim, F.; Spadavecchia, S.; Palmeri, D.; Lukac, D.M. Direct Interactions of Kaposi's Sarcoma-Associated Herpesvirus/Human Herpesvirus 8 ORF50/Rta Protein with the Cellular Protein Octamer-1 and DNA Are Critical for Specifying Transactivation of a Delayed-Early Promoter and Stimulating Viral Reactivation. *J. Virol.* **2007**, *81*, 8451–8467, doi:10.1128/JVI.00265-07.

145. Sakakibara, S.; Ueda, K.; Chen, J.; Okuno, T.; Yamanishi, K. Octamer-Binding Sequence Is a Key Element for the Autoregulation of Kaposi's Sarcoma-Associated Herpesvirus ORF50/Lyta Gene Expression. *J. Virol.* **2001**, *75*, 6894–6900, doi:10.1128/JVI.75.15.6894-6900.2001.

146. Liang, Y.; Chang, J.; Lynch, S.J.; Lukac, D.M.; Ganem, D. The Lytic Switch Protein of KSHV Activates Gene Expression via Functional Interaction with RBP-Jκ (CSL), the Target of the Notch Signaling Pathway. *Genes Dev.* **2002**, *16*, 1977–1989, doi:10.1101/gad.996502.

147. Yang, Z.; Wood, C. The Transcriptional Repressor K-RBP Modulates RTA-Mediated Transactivation and Lytic Replication of Kaposi's Sarcoma-Associated Herpesvirus. *J. Virol.* **2007**, *81*, 6294–6306, doi:10.1128/JVI.02648-06.

148. Wang, S.; Liu, S.; Wu, M.-H.; Geng, Y.; Wood, C. Identification of a Cellular Protein That Interacts and Synergizes with the RTA (ORF50) Protein of Kaposi's Sarcoma-Associated Herpesvirus in Transcriptional Activation. *J. Virol.* **2001**, *75*, 11961–11973, doi:10.1128/JVI.75.24.11961-11973.2001.

149. Gwack, Y.; Baek, H.J.; Nakamura, H.; Lee, S.H.; Meisterernst, M.; Roeder, R.G.; Jung, J.U. Principal Role of TRAP/Mediator and SWI/SNF Complexes in Kaposi's Sarcoma-Associated Herpesvirus RTA-Mediated Lytic Reactivation. *Mol. Cell. Biol.* **2003**, *23*, 2055–2067.

150. Gwack, Y.; Nakamura, H.; Lee, S.H.; Souvlis, J.; Yustein, J.T.; Gygi, S.; Kung, H.-J.; Jung, J.U. Poly(ADP-Ribose) Polymerase 1 and Ste20-Like Kinase HKFC Act as Transcriptional Repressors for Gamma-2 Herpesvirus Lytic Replication. *Mol. Cell. Biol.* **2003**, *23*, 8282–8294, doi:10.1128/MCB.23.22.8282-8294.2003.

151. Chang, P.-C.; Fitzgerald, L.D.; Van Geelen, A.; Izumiya, Y.; Ellison, T.J.; Wang, D.-H.; Ann, D.K.; Luciw, P.A.; Kung, H.-J. KRAB Domain-Associated Protein-1 as a Latency Regulator for Kaposi's Sarcoma-Associated Herpesvirus and Its Modulation by the Viral Protein Kinase. *Cancer Res* **2009**, *69*, 5681–5689, doi:10.1158/0008-5472.CAN-08-4570.

152. Schwartz, J.C.; Ebmeier, C.C.; Podell, E.R.; Heimiller, J.; Taatjes, D.J.; Cech, T.R. FUS Binds the CTD of RNA Polymerase II and Regulates Its Phosphorylation at Ser2. *Genes Dev* **2012**, *26*, 2690–2695, doi:10.1101/gad.204602.112.

153. Das, R.; Yu, J.; Zhang, Z.; Gygi, M.P.; Krainer, A.R.; Gygi, S.P.; Reed, R. SR Proteins Function in Coupling RNAP II Transcription to Pre-MRNA Splicing. *Mol. Cell* **2007**, *26*, 867–881, doi:10.1016/j.molcel.2007.05.036.

154. Sama, R.R.K.; Ward, C.L.; Kaushansky, L.J.; Lemay, N.; Ishigaki, S.; Urano, F.; Bosco, D.A. FUS/TLS Assembles into Stress Granules and Is a Prosurvival Factor during Hyperosmolar Stress. *J. Cell. Physiol.* **2013**, *228*, 2222–2231, doi:10.1002/jcp.24395.

155. Myoung, J.; Ganem, D. Generation of a Doxycycline-Inducible KSHV Producer Cell Line of Endothelial Origin: Maintenance of Tight Latency with Efficient Reactivation upon Induction. *J Virol Methods* **2011**, *174*, 12–21, doi:10.1016/j.jviromet.2011.03.012.

156. Brulois, K.F.; Chang, H.; Lee, A.S.-Y.; Ensser, A.; Wong, L.-Y.; Toth, Z.; Lee, S.H.; Lee, H.-R.; Myoung, J.; Ganem, D.; et al. Construction and Manipulation of a New Kaposi's Sarcoma-Associated Herpesvirus Bacterial Artificial Chromosome Clone. *J Virol* **2012**, *86*, 9708–9720, doi:10.1128/JVI.01019-12.

157. Nakamura, H.; Lu, M.; Gwack, Y.; Souvlis, J.; Zeichner, S.L.; Jung, J.U. Global Changes in Kaposi's Sarcoma-Associated Virus Gene Expression Patterns Following Expression of a Tetracycline-Inducible Rta Transactivator. *J Virol* **2003**, *77*, 4205–4220, doi:10.1128/JVI.77.7.4205-4220.2003.

158. Suzuki, K.; Bose, P.; Leong-Quong, R.Y.; Fujita, D.J.; Riabowol, K. REAP: A Two Minute Cell Fractionation Method. *BMC Research Notes* **2010**, *3*, 294, doi:10.1186/1756-0500-3-294.

159. Karijolich, J.; Zhao, Y.; Peterson, B.; Zhou, Q.; Glaunsinger, B. Kaposi's Sarcoma-Associated Herpesvirus ORF45 Mediates Transcriptional Activation of the HIV-1 Long Terminal Repeat via RSK2. *J. Virol.* **2014**, *88*, 7024–7035, doi:10.1128/JVI.00931-14.

160. Hicks, G.G.; Singh, N.; Nashabi, A.; Mai, S.; Bozek, G.; Klewes, L.; Arapovic, D.; White, E.K.; Koury, M.J.; Oltz, E.M.; et al. *Fus* Deficiency in Mice Results in Defective B-Lymphocyte Development and Activation, High Levels of Chromosomal Instability and Perinatal Death. *Nature Genetics* **2000**, *24*, ng0200_175, doi:10.1038/72842.

161. Tan, A.Y.; Riley, T.R.; Coady, T.; Bussemaker, H.J.; Manley, J.L. TLS/FUS (Translocated in Liposarcoma/Fused in Sarcoma) Regulates Target Gene Transcription via Single-Stranded DNA Response Elements. *PNAS* **2012**, *109*, 6030–6035, doi:10.1073/pnas.1203028109.

162. Vieira, J.; O'Hearn, P.M. Use of the Red Fluorescent Protein as a Marker of Kaposi's Sarcoma-Associated Herpesvirus Lytic Gene Expression. *Virology* **2004**, *325*, 225–240, doi:10.1016/j.virol.2004.03.049.

163. Zinszner, H.; Sok, J.; Immanuel, D.; Yin, Y.; Ron, D. TLS (FUS) Binds RNA in Vivo and Engages in Nucleo-Cytoplasmic Shuttling. *J. Cell. Sci.* **1997**, *110 (Pt 15)*, 1741–1750.

164. Phatnani, H.P.; Greenleaf, A.L. Phosphorylation and Functions of the RNA Polymerase II CTD. *Genes Dev.* **2006**, *20*, 2922–2936, doi:10.1101/gad.1477006.

165. Luo, Y.; Blechingberg, J.; Fernandes, A.M.; Li, S.; Fryland, T.; Børglum, A.D.; Bolund, L.; Nielsen, A.L. EWS and FUS Bind a Subset of Transcribed Genes Encoding Proteins Enriched in RNA Regulatory Functions. *BMC Genomics* **2015**, *16*, 929, doi:10.1186/s12864-015-2125-9.

166. Wang, X.; Schwartz, J.C.; Cech, T.R. Nucleic Acid-Binding Specificity of Human FUS Protein. *Nucleic Acids Res* **2015**, *43*, 7535–7543, doi:10.1093/nar/gkv679.

167. Peterlin, B.M.; Price, D.H. Controlling the Elongation Phase of Transcription with P-TEFb. *Molecular Cell* **2006**, *23*, 297–305, doi:10.1016/j.molcel.2006.06.014.

168. Bartkowiak, B.; Liu, P.; Phatnani, H.P.; Fuda, N.J.; Cooper, J.J.; Price, D.H.; Adelman, K.; Lis, J.T.; Greenleaf, A.L. CDK12 Is a Transcription Elongation-Associated CTD Kinase, the Metazoan Ortholog of Yeast Ctk1. *Genes Dev.* **2010**, *24*, 2303–2316, doi:10.1101/gad.1968210.

169. Di Vona, C.; Bezdan, D.; Islam, A.B.M.M.K.; Salichs, E.; López-Bigas, N.; Ossowski, S.; de la Luna, S. Chromatin-Wide Profiling of DYRK1A Reveals a Role as a Gene-Specific RNA Polymerase II CTD Kinase. *Molecular Cell* **2015**, *57*, 506–520, doi:10.1016/j.molcel.2014.12.026.

170. Toth, Z.; Brulois, K.F.; Wong, L.-Y.; Lee, H.-R.; Chung, B.; Jung, J.U. Negative Elongation Factor-Mediated Suppression of RNA Polymerase II Elongation of Kaposi's Sarcoma-Associated Herpesvirus Lytic Gene Expression. *J. Virol.* **2012**, *86*, 9696–9707, doi:10.1128/JVI.01012-12.

171. Tsai, W.-H.; Wang, P.-W.; Lin, S.-Y.; Wu, I.-L.; Ko, Y.-C.; Chen, Y.-L.; Li, M.; Lin, S.-F. Ser-634 and Ser-636 of Kaposi's Sarcoma-Associated Herpesvirus RTA Are Involved in Transactivation and Are Potential Cdk9 Phosphorylation Sites. *Front Microbiol* **2012**, *3*, doi:10.3389/fmicb.2012.00060.

172. Dormann, D.; Rodde, R.; Edbauer, D.; Bentmann, E.; Fischer, I.; Hruscha, A.; Than, M.E.; Mackenzie, I.R.A.; Capell, A.; Schmid, B.; et al. ALS-Associated Fused in Sarcoma (FUS) Mutations Disrupt Transportin-Mediated Nuclear Import. *EMBO J.* **2010**, *29*, 2841–2857, doi:10.1038/emboj.2010.143.

173. Bou-Nader, C.; Gordon, J.M.; Henderson, F.E.; Zhang, J. The Search for a PKR Code—differential Regulation of Protein Kinase R Activity by Diverse RNA and Protein Regulators. *RNA* **2019**, *25*, 539–556, doi:10.1261/rna.070169.118.

174. Choi, U.Y.; Kang, J.-S.; Hwang, Y.S.; Kim, Y.-J. Oligoadenylate Synthase-like (OASL) Proteins: Dual Functions and Associations with Diseases. *Exp Mol Med* **2015**, *47*, e144–e144, doi:10.1038/emm.2014.110.

175. Kawasaki, T.; Kawai, T. Toll-Like Receptor Signaling Pathways. *Front Immunol* **2014**, *5*, doi:10.3389/fimmu.2014.00461.

176. Loo, Y.-M.; Gale, M. Immune Signaling by RIG-I-like Receptors. *Immunity* **2011**, *34*, 680–692, doi:10.1016/j.immuni.2011.05.003.

177. Reikine, S.; Nguyen, J.B.; Modis, Y. Pattern Recognition and Signaling Mechanisms of RIG-I and MDA5. *Front Immunol* **2014**, *5*, doi:10.3389/fimmu.2014.00342.

178. Lalmansingh, A.S.; Urekar, C.J.; Reddi, P.P. TDP-43 Is a Transcriptional Repressor. *J Biol Chem* **2011**, *286*, 10970–10982, doi:10.1074/jbc.M110.166587.

179. Brulois, K.F.; Chang, H.; Lee, A.S.-Y.; Ensser, A.; Wong, L.-Y.; Toth, Z.; Lee, S.H.; Lee, H.-R.; Myoung, J.; Ganem, D.; et al. Construction and Manipulation of a New Kaposi's Sarcoma-Associated Herpesvirus Bacterial Artificial Chromosome Clone. *J. Virol.* **2012**, *86*, 9708–9720, doi:10.1128/JVI.01019-12.

180. Suzuki, K.; Bose, P.; Leong-Quong, R.Y.; Fujita, D.J.; Riabowol, K. REAP: A Two Minute Cell Fractionation Method. *BMC Res Notes* **2010**, *3*, 294, doi:10.1186/1756-0500-3-294.

181. Petrie, E.J.; Sandow, J.J.; Jacobsen, A.V.; Smith, B.J.; Griffin, M.D.W.; Lucet, I.S.; Dai, W.; Young, S.N.; Tanzer, M.C.; Wardak, A.; et al. Conformational Switching of the Pseudokinase Domain Promotes

Human MLKL Tetramerization and Cell Death by Necroptosis. *Nature Communications* **2018**, *9*, 2422, doi:10.1038/s41467-018-04714-7.

182. Freibaum, B.D.; Chitta, R.K.; High, A.A.; Taylor, J.P. Global Analysis of TDP-43 Interacting Proteins Reveals Strong Association with RNA Splicing and Translation Machinery. *Journal of Proteome Research* **2010**, *9*, 1104–1120, doi:10.1021/pr901076y.

183. Weber, F.; Wagner, V.; Rasmussen, S.B.; Hartmann, R.; Paludan, S.R. Double-Stranded RNA Is Produced by Positive-Strand RNA Viruses and DNA Viruses but Not in Detectable Amounts by Negative-Strand RNA Viruses. *Journal of Virology* **2006**, *80*, 5059–5064, doi:10.1128/JVI.80.10.5059-5064.2006.

184. Biacchesi, S.; LeBerre, M.; Lamoureux, A.; Louise, Y.; Lauret, E.; Boudinot, P.; Brémont, M. Mitochondrial Antiviral Signaling Protein Plays a Major Role in Induction of the Fish Innate Immune Response against RNA and DNA Viruses. *Journal of Virology* **2009**, *83*, 7815–7827, doi:10.1128/JVI.00404-09.

185. Hou, F.; Sun, L.; Zheng, H.; Skaug, B.; Jiang, Q.-X.; Chen, Z.J. MAVS Forms Functional Prion-like Aggregates to Activate and Propagate Antiviral Innate Immune Response. *Cell* **2011**, *146*, 448–461, doi:10.1016/j.cell.2011.06.041.

186. Giffin, L.; Damania, B. KSHV: Pathways to Tumorigenesis and Persistent Infection. *Adv Virus Res* **2014**, *88*, 111–159, doi:10.1016/B978-0-12-800098-4.00002-7.

187. White, R.J. Transcription by RNA Polymerase III: More Complex than We Thought. *Nature Reviews Genetics* **2011**, *12*, 459–463, doi:10.1038/nrg3001.

188. Burke, J.M.; Kincaid, R.P.; Nottingham, R.M.; Lambowitz, A.M.; Sullivan, C.S. DUSP11 Activity on Triphosphorylated Transcripts Promotes Argonaute Association with Noncanonical Viral MicroRNAs and Regulates Steady-State Levels of Cellular Noncoding RNAs. *Genes Dev.* **2016**, *30*, 2076–2092, doi:10.1101/gad.282616.116.

189. Burke, J.M.; Sullivan, C.S. DUSP11 – An RNA Phosphatase That Regulates Host and Viral Non-Coding RNAs in Mammalian Cells. *RNA Biology* **2017**, *14*, 1457–1465, doi:10.1080/15476286.2017.1306169.

190. Bose, J.K.; Huang, C.-C.; Shen, C.-K.J. Regulation of Autophagy by Neuropathological Protein TDP-43. *J. Biol. Chem.* **2011**, *286*, 44441–44448, doi:10.1074/jbc.M111.237115.

191. Mitra, J.; Guerrero, E.N.; Hegde, P.M.; Liachko, N.F.; Wang, H.; Vasquez, V.; Gao, J.; Pandey, A.; Taylor, J.P.; Kraemer, B.C.; et al. Motor Neuron Disease-Associated Loss of Nuclear TDP-43 Is Linked to DNA Double-Strand Break Repair Defects. *Proceedings of the National Academy of Sciences* **2019**, *116*, 4696–4705, doi:10.1073/pnas.1818415116.

192. Iguchi, Y.; Katsuno, M.; Niwa, J.; Yamada, S.; Sone, J.; Waza, M.; Adachi, H.; Tanaka, F.; Nagata, K.; Arimura, N.; et al. TDP-43 Depletion Induces Neuronal Cell Damage through Dysregulation of Rho Family GTPases. *J Biol Chem* **2009**, *284*, 22059–22066, doi:10.1074/jbc.M109.012195.

193. Sarhan, J.; Liu, B.C.; Muendlein, H.I.; Weindel, C.G.; Smirnova, I.; Tang, A.Y.; Ilyukha, V.; Sorokin, M.; Buzdin, A.; Fitzgerald, K.A.; et al. Constitutive Interferon Signaling Maintains Critical Threshold of

MLKL Expression to License Necroptosis. *Cell Death & Differentiation* **2019**, *26*, 332–347, doi:10.1038/s41418-018-0122-7.

194. Knuth, A.-K.; Rösler, S.; Schenk, B.; Kowald, L.; van Wijk, S.J.L.; Fulda, S. Interferons Transcriptionally Up-Regulate MLKL Expression in Cancer Cells. *Neoplasia* **2019**, *21*, 74–81, doi:10.1016/j.neo.2018.11.002.

195. Arnež, K.H.; Kindlova, M.; Bokil, N.J.; Murphy, J.M.; Sweet, M.J.; Gunčar, G. Analysis of the N-Terminal Region of Human MLKL, as Well as Two Distinct MLKL Isoforms, Reveals New Insights into Necroptotic Cell Death. *Biosci Rep* **2016**, *36*, doi:10.1042/BSR20150246.

196. Hildebrand, J.M.; Tanzer, M.C.; Lucet, I.S.; Young, S.N.; Spall, S.K.; Sharma, P.; Pierotti, C.; Garnier, J.-M.; Dobson, R.C.J.; Webb, A.I.; et al. Activation of the Pseudokinase MLKL Unleashes the Four-Helix Bundle Domain to Induce Membrane Localization and Necroptotic Cell Death. *PNAS* **2014**, *111*, 15072–15077, doi:10.1073/pnas.1408987111.

197. Jiang, X.; Muthusamy, V.; Fedorova, O.; Kong, Y.; Kim, D.J.; Bosenberg, M.; Pyle, A.M.; Iwasaki, A. Intratumoral Delivery of RIG-I Agonist SLR14 Induces Robust Antitumor Responses. *J Exp Med* **2019**, *216*, 2854–2868, doi:10.1084/jem.20190801.

198. Heidegger, S.; Wintges, A.; Stritzke, F.; Bek, S.; Steiger, K.; Koenig, P.-A.; Göttert, S.; Engleitner, T.; Öllinger, R.; Nedelko, T.; et al. RIG-I Activation Is Critical for Responsiveness to Checkpoint Blockade. *Science Immunology* **2019**, *4*, eaau8943, doi:10.1126/sciimmunol.aau8943.

199. Mackenzie, I.R.A.; Rademakers, R. The Role of TDP-43 in Amyotrophic Lateral Sclerosis and Frontotemporal Dementia. *Curr Opin Neurol* **2008**, *21*, 693–700, doi:10.1097/WCO.0b013e3283168d1d.

200. Tank, E.M.; Figueroa-Romero, C.; Hinder, L.M.; Bedi, K.; Archbold, H.C.; Li, X.; Weskamp, K.; Safren, N.; Paez-Colasante, X.; Pacut, C.; et al. Abnormal RNA Stability in Amyotrophic Lateral Sclerosis. *Nature Communications* **2018**, *9*, 2845, doi:10.1038/s41467-018-05049-z.

201. Chu, J.-F.; Majumder, P.; Chatterjee, B.; Huang, S.-L.; Shen, C.-K.J. TDP-43 Regulates Coupled Dendritic MRNA Transport-Translation Processes in Co-Operation with FMRP and Staufen1. *Cell Rep* **2019**, *29*, 3118-3133.e6, doi:10.1016/j.celrep.2019.10.061.

202. Woerner, A.C.; Frottin, F.; Hornburg, D.; Feng, L.R.; Meissner, F.; Patra, M.; Tatzelt, J.; Mann, M.; Winklhofer, K.F.; Hartl, F.U.; et al. Cytoplasmic Protein Aggregates Interfere with Nucleocytoplasmic Transport of Protein and RNA. *Science* **2016**, *351*, 173–176, doi:10.1126/science.aad2033.